Università degli Studi di Padova

Istituto Zooprofilattico Sperimentale di Venezie, Dipartimento di Scienze Biomediche Comparate

Dipartimento di Biomedicina Comparata e Alimentazione

SCUOLA DI DOTTORATO DI RICERCA IN SCIENZE VETERINARIE

INDIRIZZO EPIDEMIOLOGIA VETERINARIA, IGIENE E SALUTA PUBBLICA

CICLO XXVII

ONCOLYTIC ACTIVITY OF AVIAN INFLUENZA VIRUS IN HUMAN PANCREATIC DUCTAL ADENOCARCINOMA CELL LINES

Direttore della Scuola: Ch.mo Prof. Gianfranco Gabai

Coordinatore d'indirizzo: Ch.mo Prof. Gianfranco Gabai

Supervisore: Ch.mo Prof. Ilaria Capua

Dottorando: Samantha Beth Kasloff

Acknowledgements

The following work would not have been possible without the support and collaboration of numerous individuals. First and foremost, I would like to express my gratitude to my Supervisor Dr. Ilaria Capua for providing me with the opportunity to work on this project. I would also like to extend a tremendous thank-you to all of my colleagues at the IZSVe who have contributed directly to this work or who have helped me at the many phases along the way. A tremendous portion of this work was carried out at the Istituto Oncologico Veneto, and I believe that this collaboration was key to bringing the research to the next level. Thank you to Dr. Ciminale and especially Dr. Silic-Benussi for the support and guidance you have shown me in these last few years and to all of the IOV staff for making me feel like a colleague rather than a guest. A series of experiments characterizing virus binding were performed over a two month period at the Virology Institute at the University of Marburg, and I am truly grateful to Dr. Matrosovich and his lab members for having welcomed me into their laboratory and for their patience and guidance in helping me learn new techniques. I would also like to thank the Staff at the Glycobiology Core at the Imperial College of London, particularly Dr. Paola Grassi and Dr. Poh-Choo Pang, for all of their help during my stay in London and all of the post-visit support with my data interpretation. I would also like to thank the Fondazione CARIPARO, the PREDEMICS Program and the Department of Comparative Biomedicine at the University of Padova for the various financial support over the last three years.

Finally, to my friends and family near and far, thank you for your support – always.

Table of Contents

RIASSUNTO

L’adenocarcinoma duttale pancreatico (PDA) è la forma più aggressiva e comune di tumore al pancreas. Terapie efficaci nei confronti di altri tipi di tumore hanno mostrato scarsi risultati nel trattamento del PDA; pertanto la necessità di tecniche alternativeè di cruciale importanza. Viroterapia e un trattamento che impiega virus ingegnerizzati geneticamente al fine di infettare ed uccidere selettivamente le cellule tumorali, e negli ultimi sta crescendo molto come campo scientifici. L’osservazione di un tropismo pancreatico del virus influenzale ha guidato il nostro gruppo a testarne l’impiego come agente oncolitico nei confronti dell’adenocarcinoma duttale del pancreas. Sebbene studiato per le influenze stagionali e le pandemie ad esso associate, il virus influenzale non è stato altrettanto investigato per il suo potenziale impiego come agente oncolitico. Lo scopo di questo studio era di testare l'efficacia di IAV come virus oncolitico contro le linee cellulari PDA umane.

Diverse linee cellulari di adenocarcinoma pancreatico sono state caratterizzate dal punto di vista recettoriale per valutare la presenza sulla loro superficie di recettori sialici alpha-2,3 o alpha-2,6 in grado di legare i virus influenzale aviari (alpha2-3) o di mammifero (alpha 2-6), e la presenza di tutti e due tipi di ricettori e stato confermato sulla superfice di tutte le linee.

Coerentemente con questo risultato, esperimenti pilota hanno dimostrato che linee cellulari PDA erano sensibili alle infezioni da IAV umana e aviaria isolati. Esperimenti di cinetica di crescita hanno mostrato che vari cicli di replicazione del virus sono stati raggiunti da virus altamente patogeni, ma non a bassa patogenicità (LP) virus. Questo è stato attribuito alla sensibilità eccessiva queste cellule hanno mostrato per la tripsina esogeno richiesto da questi virus per più cicli di infezione in vitro, come le analisi di virus in momenti iniziali dopo l'infezione ha mostrato RNA replica di alto livello. Per determinare quantitativamente la morte cellulare indotta dai diversi isolati virali in cellule PDA seguenti infezione, saggi MTT state eseguite e dimostrato una significativa induzione di morte cellulare a 24 ore dopo l'infezione, e questo era particolarmente grave nel caso di un isolato H7N3. Le analisi di induzione dell'apoptosi usando il mercatore annessina V hanno messo in luce come tutti i ceppi virali testati diano livelli di apoptosi più alti rispetto al controllo (Gem+Cisp) in tutte le linee cellulari tumorali impiegate nello studio. In particolare in BXPC-3 (la linea più sensibile tra quelle testate) il ceppo H7N3 A/tukey/Italy/2962/03 ha indotto livelli più alti. In HPDE6, invece si registra una maggiore morte cellulare derivata dal trattamento con i chemoterapici rispetto a quelle portata dall’infezione virale. Il virus influenzale, quindi, mostrava una abilità innata nel causare morte cellulare

più efficacemente in linee tumorali rispetto alle cellule sane. Per scoprire il meccanismo tramite cui il cepo H7N3 ha eserito il suo effeto apototico sulle cellule BxPC-3, una valutazione dei citochini indotti dal virus H7N3 ha rivelato che nella linea cellulare BxPC-3 PDA, l'apoptosi veniva indotto dal via mitocondriale intrinseca.

Per determinare se i ceppi IAV sperimentali avevano una maggiore affinità intrinsica verso i glicani frequentemente associati con il fenotipo tumorale, le affinità di legame dei tre virus LP che hanno mostrato una buona capacità di indurre la morte delle cellule di PDA sono stati valutati mediante un solid phase binding assay. Due dei virus, H7N3 e H7N7, hanno mostrato una forte preferenza vincolante per gli antigeni tumorali associate Slex e Slea, anche se questa affinità non è assoluto e non è probabilmente un meccanismo adeguato per limitare tropismo tissutale.

Sulla base della sua capacità nell'indurre apoptosi il virus H7N3 A/tukey/Italy/2962/03 è stato scelto per vedere la sua capacita antitumorale usando un modello di xenotrapianto di crescita cellulare PDA in topi SCID. Dopo una serie di iniezioni intratumorali, il gruppo trattato con il virus ha avuto una crescita tumorale molto ridotta rispetto al gruppo controllo. Presi insieme, questi risultati suggeriscono che i virus influenzali di bassa patogenicita possono rivelarsi efficaci per viroterapia oncolytic di PDA, e giustificano ulteriori studi per lo sviluppo di virus specifici e modificati, con l'obiettivo di testare la loro efficacia in contesti clinici.

SUMMARY

Pancreatic Ductal Adenocarcinoma (PDA), the most common form of pancreatic cancer, is among the most lethal forms of cancer due to diagnoses being made at late stages when tumours are no longer resectable and the disease has often metastasized. Chemotherapy and radiation therapy are employed as part of the management of most patients, however in the absence of surgery these treatments are considered only life prolonging rather than life saving. As a result, the 5-year survival rates for PDA are less than 5% and the need for alternative therapies is critical. Oncolytic virotherapy is a branch of cancer therapy that has grown vastly in recent years in terms of scientific advances. This form of cancer therapy uses modified viruses that are specifically targeted to the malignant phenotype yet leave healthy bystander cells largely unharmed. Influenza A viruses have been largely overlooked as agents of oncolytic virotherapy, with only a small number of publications produced over the last two decades. Building on the observation that avian influenza A viruses (IAVs) have a tropism for the pancreas *in vivo*, the present study was aimed at testing the efficacy of IAV as oncolytic agents to kill human PDA cell lines.

To determine whether human PDA cells could be susceptible to Receptor characterization of the pancreatic cell lines included confirmed the expression of both alpha-2,3 and alpha-2,6-linked glycan receptors required for virus attachment by avian and human-tropic influenza viruses, respectively. Consistent with this finding, pilot experiments demonstrated that PDA cell lines were sensitive to infection by human and avian IAV isolates. Growth kinetic experiments showed that multiple rounds of virus replication were achieved by highly pathogenic viruses but not low pathogenic (LP) viruses. This was attributed to the excessive sensitivity these cells showed for the exogenous trypsin required by these viruses for multiple rounds of infection *in vitro*, as analyses of viruses at early time points post-infection showed high level RNA replication. To quantitatively determine cell death induced by the different virus isolates in PDA cells following infection, MTT assays were performed and demonstrated a significant induction of cell death at 24 hours post infection, and this was particularly severe in the case of an H7N3 isolate. Analyses of apoptosis induction by Annexin V staining further confirmed these results, and interestingly showed that infection with LP IAVs at early time points post treatment caused higher levels of apoptosis in PDA cells compared to gemcitabine and cisplatin, which are the cornerstone of current therapies for PDA. Even more, IAVs did not induce apoptosis in the non-transformed pancreatic ductal HPDE6 cells at near comparable levels to those

observed in the PDA cell lines. A closer examination of the mechanisms through which these high levels of apoptosis were induced by the H7N3 virus revealed that in the BxPC-3 PDA cell line, apoptosis resulted from the engagement of the intrinsic mitochondrial pathway.

To determine whether any experimental isolates showed an enhanced affinity towards glycans frequently associated with the cancerous phenotype, the binding affinities of three LP viruses that showed good ability to induce PDA cell death were assessed by solid-phase binding assay. Two of the viruses, H7N3 and H7N7, showed strong binding preference for cancer-associated antigens SLeX and SLeA, though this affinity is not absolute and is not likely a suitable mechanism to limit tissue tropism.

Finally, using a xenograft model of PDA cell growth in SCID mice, the H7N3 virus was shown to significantly inhibit BxPC-3 tumour growth following a series of intratumoural injection. Taken together, these results suggest that low pathogenic IAVs may prove to be effective for oncolytic virotherapy of PDA, and provide grounds for further studies to develop specific and targeted viruses with the aim of testing their efficacy in clinical contexts.

INTRODUCTION

1. PANCREATIC CANCER

1.1 Overview: Statistics, Signs, Symptoms, Diagnosis

Of all the human malignancies described, pancreatic cancer ranks among the deadliest. With the majority of patients diagnosed at late stage disease, with median survival of 3-6 months and a dismal 5-year survival rate of 5%. Surgical resection remains the only possible curative therapy, and of the 20% of patients eligible presenting local resectable or borderline resectable tumours, median survival lies at only 20 months (Abbas, 2013; Vincent *et al.*, 2011).

A major factor in the lethality of pancreatic cancer lies in the fact that the disease is largely asymptomatic, with late-stage diagnosis often resulting from a seemingly unrelated illness. Some of the symptoms associated with PDA include unexpected weight loss, indigestion, vomiting, abdominal pain, backache, jaundice, nausea and clay-colored stools. Patients often show signs and symptoms of chronic pancreatitis or new onset of diabetes mellitus, and interestingly a number of patients are diagnosed with depression prior to diagnosis, suggesting that PDA may induce depression (Mendieta Zerón *et al.*, 2009; Wolfgang *et al.*, 2014).

As such, the greatest hope at present lies in early detection of PDA. Current screening methods for persons considered high-risk based on family history and genetic factors rely on a combination of scans including endoscopic ultrasound, computed tomography and magnetic resonance imaging to look for early pancreatic lesions (Wolfgang *et al.*, 2014). While these approaches have brought success in detecting early, curable disease, they also bring the risk of overtreatment (Vincent *et al.*, 2011). A comprehensive risk prediction tool called PancPRO, which provides risk assessments for the likelihood that a person carries a genetic predisposition as well as their likelihood of developing pancreatic cancer based on family history information, was released in 2007. The tool has been proven quite accurate in its risk assessments, and may assist physicians in deciding whom to include in screening programs and at what age they should begin, but clearly works together with medical screening in order to improve detection (Wolfgang *et al.*, 2014).

Considering limitations in imaging-based screening methods in detecting microscopic pancreatic lesions as well as the invasive nature of endoscopic ultrasounds, the development of alternative, less invasive testing based on the presence of genetic markers in serum or pancreatic fluid will be will be key in early detection and increased success in treatment of PDA.

1.2 Risk factors (Environmental and genetic)

Several risk factors, both inherited and environmental, are associated with an increased risk in development of pancreatic cancer. Of all environmental factors, cigarette smoking has the highest associated risk and is associated with approximately 25% of pancreatic cancers. Further lifestyle-associated factors suggested to increase the risk include heavy alcohol consumption, a high body mass index, chronic pancreatitis and long-standing type 2 diabetes (Vincent *et al.*, 2011; Wolfgang *et al.*, 2014). In addition to behavior-associated considerations, a number of inherited genetic factors lead to a higher probability of developing PDA, and those with a family history of this malignancy have a 1.9 to 13-fold increased risk, particularly in the case of a first-degree relative (Klein, 2013). Germline mutations in the *BRCA2* gene, further to their role in breast and ovarian cancer, are strongly associated with increased risk for PDA, while the influence of mutated *BRCA1* is not as clear. Genetic mutations in *PALB2*, the partner and localizer of *BRCA2*, have also been consistently associated with increased risk for PDA. Mutations in additional genes such as *CDKN2A/p16* are also strongly associated with enhanced probability of developing pancreatic cancer, and in PDA tumour cells this gene is among the most frequently mutated (Deer *et al.*, 2010; Wolfgang *et al.*, 2014). A number of hereditary syndromes, including Lynch Syndrome, hereditary pancreatitis, and Peutz-Jeghers Syndrome, also increase one's likelihood of developing pancreatic cancer in a lifetime.

1.3 Biology

Solid tumours of the pancreas are by far the most commonly encountered in the clinical setting, and of these pancreatic ductal adenocarcinomas are the most frequently described. Tumours containing invasive branches of neoplastic cells into surrounding tissues have the capacity to invade and spread along nerves, lymphatic spaces, and small veins, and commonly metastasize to the liver. The tumour microenvironment is also highly desmoplastic, and the presence of extensive fibrous tissues combined with the high interstitial pressure makes these malignancies extremely resistant to treatment.

The development of pancreatic ductal adenocarcinoma is considered a multi-staged process associated with the gradual accumulation of somatic mutations in regulatory and tumor suppressor genes. These mutations also generally correspond with the histological grading of the lesion, where the transformation from normal pancreatic duct to cancer is divided into three stages of pancreatic intraepithelial neoplasia (PanIN) before transformation into malignant tumours (Deramaudt & Rustgi, 2005; Makohon-Moore *et al.*, 2013). Pancreatic cancers may also arise from intraductal papillary mucinous neoplasms, mucinous cystic neoplasms, though PDAs are by far the most common.

The first step in carcinogenesis is the alteration of a normal ductal epithelial cell progenitor to provide it with a replicative advantage, and this is most frequently associated with an activating *KRAS* mutation, causing constitutive activation of downstream effectors of receptor tyrosine kinases. Cells in these low-grade precursor lesions termed PanIN-1 also show architectural changes, represented as columnar epithelial cells rather than the typical cuboidal epithelia of the pancreatic duct. The progression of PanIN-1 to PanIN-2 typically involves inactivation of the *CDKN2A/p16* gene, resulting in the loss of cell cycle control at the G1-S phase and subsequently uncontrolled proliferation. Morphologically these lesions are characterized by pseudostratified cells with nuclear atypia, loss of polarization and papillary formations. High-grade PanIN-3 stage cells present a complete loss of polarization, high nuclear to cytoplasmic ratio and pseudopapillary formation. At this stage in nearly 50% of patients cells accumulate further mutations, including inactivation of the tumor suppressor genes *TP53*and *SMAD4* (Deramaudt & Rustgi, 2005; Makohon-Moore *et al.*, 2013; Wolfgang *et al.*, 2014).

Numerous detailed studies have been published describing various genetic alterations observed in PDA. In a recent study Jones and colleagues (Jones *et al.*, 2008) performed a comprehensive sequencing analysis of 24 advanced pancreatic cancers to determine the most frequently encountered mutations. Their results showed that on average these cancers contained 63 genetic alterations. In line with information presented above, the most frequent genetic alterations in pancreatic cancers are in *KRAS, CDKN2A/p16, TP53* and *SMAD4,* though numerous others have been found in PDA patients including *MAP4K3, MYC, SOX3, CASP10 and ADAM11* (Hong *et al.*, 2011; Jones *et al.*, 2008). However, given the great heterogeneity observed between patients with respect to additional genetic modifications and combinations thereof, it is of greater practicality to focus on the downstream pathways rather than each individual gene. In light of this, Jones and colleagues inferred from their findings that 12 core signaling pathways were highly affected in pancreatic cancers. Most notably, 100% of cancers screened contained at least one modified gene in regulatory processes or pathways regarding apoptosis, regulation of G1/S phase transition, as well as hedgehog, KRAS, TGF-β, and Wnt/Notch signaling. Additional pathways and processes highly affected included DNA damage control, homophilic cell adhesion, regulation of invasion, and other non *KRAS*-mediated small GTPase-dependent signaling (Jones *et al.*, 2008). Increasing scientific understanding of these pathways combined with genetic testing of tumours on an individual patient basis will likely be key in targeted patient-based therapy in years to come.

1.4 Treatment

Treatment strategies for PDA patients are based largely on the stage of disease at diagnosis. Surgery is still considered the only curative treatment for PDA, however even then up to 85% of patients experience a recurrence of the cancer within two postoperative years (Zakharova *et al.*, 2012). Stage I and II patients with local resectable tumours that have no vessel involvement are often treated by a combination of surgical resection and post-operative adjuvant chemotherapy or chemoradiotherapy starting 1-2 months later in an attempt to reduce the likelihood or recurrence. The selection of patients for surgery, however, goes beyond the staging of the malignancy and considers both their overall health and their particular tumour biology, though the lack of available validated biomarkers makes this highly subjective for each physician or medical center. The benefit of neoadjuvant therapy in candidate patients remains debatable, however the implementation of a pre-operative chemotherapy or radiation regimen may increase likelihood of successful resection by shrinking tumours and creating better defined borders for surgery. In stage III patients with borderline resectable tumours, neoadjuvant therapy is recommended before surgical resection. The precise surgical procedure required depends on the location of the tumour, with those located in the head of the pancreas requiring the Whipple procedure (pancreaticoduodenectomy), while tumours in the tail are resected by distal pancreatectomy and accompanying splenectomy. Malignant lesions located in the body of the pancreas may sometimes require a complete pancreatectomy.

With the majority of patients classified as non-resectable, systemic therapies including chemotherapy and radiation are central to almost every treatment regime. Since 1997, the standard treatment for advanced pancreatic cancer is monotherapy with gemcitabine, a deoxycytidine analogue, via standard 30-minute infusion at a rate of 10 mg/m2/h. Though generally better tolerated and causing fewer complications that the previous treatment regime of bolus 5-fluorouracil, response rates are poor to gemcitabine alone and life-saving results are rarely achieved (Rivera *et al.*, 2009; Vincent *et al.*, 2011; Wolfgang *et al.*, 2014). Numerous clinical trials were undertaken to assess the benefits of employing a dual therapy strategy of gemcitabine with other drugs including platinums (cisplatin, oxaliplatin), monoclonal antibodies (bevacizumab, cetuximab), and matrix metalloproteinase inhibitors (marimasmat) , yet none proved more effective than gemcitabine alone (Rivera *et al.*, 2009). As an alternative, a new combination regimen termed FOLFIRINOX (oxaliplatin 85 mg/m^2, leucovorin 400 mg/m^2, irinotecan 180 mg/m^2, 5-FU bolus 400 mg/m^2 plus continuous infusion of 5-FU (2400 mg/m2) for 46 hours) gave a better overall survival rate compared to gemcitabine in a randomized trial, though some additional toxicity was reported.

Radiation therapy is also frequently used to treat various stages of pancreatic cancer and patients typically receive a total of 45-60 in a period of 6 weeks plus the addition of a radiosensitizing drug (Vincent *et al.*, 2011). Rather than being used as a single therapy, radiation is most often given as chemoradiaotherapy in combination with drugs such as gemcitabine. In this scenario, and of particular importance for patients with advanced disease, the order in which the two are administered can have a great effect on outcome. If administered first, radiation-associated toxicities may cause patients to feel too unwell to fully comply with subsequent chemotherapy, and in fact treatment in this order may result in increased number of metastases (Wolfgang *et al.*, 2014). The increased use of more modern 3D platforms to allow better tumour targeting with radiation, combined with better radiosensitizers and the use of rigorous chemotherapy beforehand will likely contribute to improved responses, though additional innovative therapies are required for curative treatment of PDA.

2. ONCOLYTIC VIROTHERAPY

2.1 History of Oncolytic Virotherapy

Cancer therapy in its beginnings was completely reliant on surgical removal of the malignancy. By the early twentieth century the use of chemotherapy and radiation offered additional strategies in the treatment of various cancers, however early recognition of the inherent limitations of these therapies led to the search for alternative measures (Kelly & Russell, 2007). The notion that viruses could be used to treat cancer patients originated from clinical observations of tumour regression following acute viral illness such as influenza and chickenpox or after rabies vaccination (Ferguson *et al.*, 2012; Kelly & Russell, 2007; Mullen & Tanabe, 2002). As early as 1949, the first significant clinical trial was conducted using viral hepatitis to treat patients with Hodgkin's Disease, followed by trials using West Nile Virus against a range of advanced cancers and Adenovirus in cervical cancer patients in the decade that followed. Though all of these trials had a certain degree of success, with transient tumour regression observed in some patients, unwanted side effects were also reported and tumours generally grew back, with most patients eventually dying from the primary disease.

Though an array of human pathogens were included in early investigations for oncolytic activity, problems with unexpected virulence and/or immune clearance by pre-existing antibodies prompted investigations into the use of animal pathogens for oncolytic virotherapy, and the establishment of tissue culture and animal models in the 1950s allowed for significant advances in this area. With interest in the field varying over the decades, the establishment of recombinant DNA technology to allow for genetic manipulation of the viral genome caused a resurgence in oncolytic

virus (OV) research, allowing for numerous targeting strategies to improve safety and increase specificity to cells with the malignant phenotype. In 1996, the first FDA-approved clinical trial was launched using the modified adenovirus ONYX-15® to treat advanced head and neck cancers (Ganly *et al.*, 2000) and in 2005 a nearly identical virus, H101®, was licensed for use in China (Kelly & Russell, 2007). OVs have been proposed as single agent therapy but also in combination therapy with chemotherapeutic drugs and/or radiation, with excellent pre-clinical results and a number of clinical trials underway.

A number of advances in the field of oncolytic virotherapy have been made in recent years, not only in terms of virus design but also in delivery methods. In addition to successful results following intratumoural injections, advances have been made to allow for systemic delivery following intravenous injections of OVs, though further research to enhance its efficacy in the clinical setting are warranted. At the time of writing, there are over 35 actively recruiting clinical trials in the United States alone (Clinicaltrials.gov, 2015).

2.2 Mechanisms of cytotoxicity and Strategies to improve specificity

OVs exhibit their cancer cell-killing abilities through a number of different mechanisms, and effective tumour destruction can involve their combined effects. At the most basic level, the infection and replication of a virus inside the cancerous cell leads to cell lysis, and this process can be continued by the infection of neighboring cells. In this scenario, viruses provide a unique advantage over conventional therapeutics in that the initial dose can be continually maintained inside the tumour environment(Mullen & Tanabe, 2002; Parato *et al.*, 2005). In addition to their direct actions, viral infection of tumours can lead to significant down-stream killing of cancer cells by stimulating the immune system, whereby recognizing viral epitopes on infected cells allows for concurrent recognition of tumour antigens, leading to immune-mediated destruction of tumour cells (Auer & Bell, 2012; Mullen & Tanabe, 2002; Pol *et al.*, 2011).This concept has been taken even further, with the design of viruses engineered to express cytokines and immune modulating co-stimulatory molecules (Kaur *et al.*, 2009; Pol *et al.*, 2007). At the level of viral proteins, certain gene products have been shown to induce cell death even in the absence of productive replication, whereas other act to increase cell sensitivity to either chemotherapy or radiation (Mullen & Tanabe, 2002; Pol *et al.*, 2007). Though all of these means can contribute to efficient cancer cell killing, they do not address the issue of specificity.

Several classes of viruses display preferential tropism to cancerous cells, due to the fact that they offer an environment for immune evasion and are typically resistant to apoptosis, the natural

altruistic mechanism by which cells induce their own death following infection to safeguard uninfected neighboring cells(Russell *et al.*, 2012). However, given that the ultimate scope of oncolytic virotherapy is to use an agent which is targeted to cancerous cells with limited ability to infect healthy bystanders, several strategies have been proposed to increase specificity towards the malignant phenotype at the pre-infection, post-transcriptional and post-translational levels.

2.2.1 Enhancing affinity for tumour-specific surface markers.

The genesis of a cancerous cell from its untransformed progenitor involves the continuous acquisition of genetic anomalies, including under- or overexpression of particular molecules and pathways. Among these, the expression of surface molecules is highly dysregulated in tumour cells that may display high quantities of "tumour antigens". Given the first step in the viral life cycle involves specific recognition and attachment to host receptors, modification of the viral receptor-binding proteins to recognize molecules present on cancer cells acts to limit infection of bystander cells and restrict infection to the malignant targets (Cattaneo *et al.*, 2008; Parato *et al.*, 2005). This strategy has been employed with adenovirus, specifically by decreasing the interaction of its hexon protein with coagulation factor X to diminish infection of liver cells and increasing its affinity carcinoma cell-associated $\alpha_v\beta_6$integrins(Hernández-Alcoceba, 2011; Mathis *et al.*, 2005). Similarly, the insertion of a specific coding sequence for a single chain antibody into the herpes simplex virus type 1 (HSV-1) glycoprotein not only detargeted it from its natural receptor molecule, heparan sulfate, but caused specific binding to EGFR-vIII, a mutated form of the EGF receptor that is highly expressed on tumour cells (Grandi *et al.*, 2004, 2010).

2.2.2 Targeting to tumour-associated proteases

In order for a tumour to metastasize, it must first penetrate the basement membrane, enter the nearby vasculature to circulate, migrate out of the vasculature at a distant site and invade a new area of tissue (Fuster & Esko, 2005; Koblinski *et al.*, 2000). Among the many factors that contribute to these processes the expression of extracellular proteases by cancer cells is considered essential, and the role of matrix metalloproteinases has been extensively described (Vartak & Gemeinhart, 2007). In addition to specific receptor recognition, many viruses require post-translational cleavage of their surface glycoproteins for activity, and the particular sequence at the cleavage site dictates their protease susceptibility. Modifications of these cleavage sites to express motifs specific for cancer-associated proteases has become increasingly utilized as a method to limit OV activity to the tumour environment

(Cattaneo *et al.*, 2008). Using various strategies from directly modifying the glycoprotein cleavage site to be MMP-dependent, or by the addition of MMP-cleavable linkers into their terminal regions, successful results have been observed both *in vitro* and *in vivo* with measles virus (Mühlebach *et al.*, 2010; Springfeld *et al.*, 2006) sendai virus (Kinoh *et al.*, 2004), and adenovirus (José *et al.*, 2014)as well as with retroviruses for gene therapy (Hartl *et al.*, 2005). Though this strategy is most relevant for enveloped viruses, modification of capsid proteins on non-enveloped viruses to be dependent on activation by cancer-associated proteases remains a possibility for future investigations (Cattaneo *et al.*, 2008).

2.2.3 microRNA targeting

A relatively novel strategy to limit the spread of OVs to healthy tissues involves the insertion of specific target sequences into the viral genome for detection and elimination by non-target host cells. MicroRNAs (miRNAs) are small 22nt-long fragments of RNA endogenously expressed in a host-, tissue-, and cell type-specific manner. These regulatory elements influence numerous processes at a post transcriptional level, interacting with complementary mRNA fragments and contributing to either their translational repression or catalytic degradation (Bartel, 2004; Kelly & Russell, 2009). Accordingly, viruses engineered to express tissue-specific miRNA target sequences are not detargeted from a particular physiological site, but are destroyed once their replication cycle commences. Preclinical models of engineered adenoviruses using liver-specific miRNA 122-targeting demonstrated suppressed replication in hepatic cells without affecting its ability to replicate in a liver metastasis originating from colon cancer (Ylösmäki *et al.*, 2013a). With Semliki forest virus, the insertion of the neuron-specific mir124 target sequence attenuated neurovirulence associated with the wild-type strain (Ylösmäki *et al.*, 2013b), and similarly the insertion of several miRNA target sequences into the Sindbis viral genome successfully depressed its natural tropism for macrophages, liver, and muscle cells (Kueberuwa *et al.*, 2014). Work with measles virus, vesicular stomatitis virus, polio virus and others have all confirmed the proof-of-principle that miRNA targeting is an excellent strategy for limiting infection in unwanted sites (Edge *et al.*, 2008; Kelly & Russell, 2009; Leber *et al.*, 2011). In fact, this strategy has been similarly explored for enhancing safety of live virus vaccines (Barnes *et al.*, 2008), and has been proven effective in the species-specific attenuation of influenza virus in the context of vaccine production (Perez *et al.*, 2009).

2.2.4 Removal of Interferon Antagonists

In their quest for immortality, cancer cells are often dysregulated in a number of regulatory pathways. Type I interferons are a family of proteins that play regulatory roles in innate antiviral defense, regulation of cell growth and activation of the immune response (Doly *et al.*, 1998). Interferons are stimulate by a number of factors considered exogenous from normal cell products including double-stranded RNA, a critical component in the replication cycle of RNA viruses. In order to evade this immune-mediated detection, many viruses encode for proteins that can antagonize the interferon response to allow for their continued replication in the host cell, though such proteins are not required for productive replication in an interferon incompetent host (Russell, 2002). Due to the fact that interferons also contribute to immune-mediated detection of malignant cells by enhancing antigen presentation, many cancers acquire genetic alterations contributing to the loss of interferon production and/or the ability to respond to it (Cattaneo *et al.*, 2008; Parato *et al.*, 2005). As a result, genetically engineered OVs with defective IFN-antagonistic gene products are able to productively replicate in IFN-deficient malignant cells yet are attenuated in healthy cells with an intact IFN pathway. This strategy has been extensively utilized in the design of multiple OVs, including VSV, measles virus, adenovirus, and influenza virus (Cattaneo *et al.*, 2008; Parato *et al.*, 2005; Russell, 2002)Likewise, myxoma virus exhibits an inherent interferon sensitivity, and has proven capable of infecting cancerous cells with minimal toxicity in preclinical immune-competent models (Lun *et al.*, 2010).

2.2.5 Removal of anti-apoptotic factors

The loss of tissue homeostasis mediated by apoptosis is the quintessential hallmark of cancer. Apoptosis is a highly regulated intrinsic cell death program launched in response to particular physiological or pathological stimuli. By entering into this suicidal state, abnormal or infected cells shut down their metabolism, preventing the production of altered or foreign gene products and similarly blocking the replication cycle of intracellular pathogens(Fulda & Debatin, 2006; Westphal & Kalthoff, 2003). By acquiring mutations at various stages in the apoptotic pathway, highly metabolic cancer cells producing vast quantities of abnormal gene products can undergo continued replication. This provides a highly favourable environment for viruses, which under normal circumstances must produce anti-apoptotic factors to counteract the host response (Auer & Bell, 2012; Le Bœuf & Bell, 2010).One of the most well studied OVs is the adenovirus ONYX-015, designed to lack expression of its E1B-55K gene product that normally serves to interact with p53, an important mediator of apoptotic induction that is defective in more than half of cancers (Mathis *et al.*, 2005; Parato *et al.*, 2005).

2.2.6 Controlling Gene Expression with Tumour-Specific Promoters

As an alternative to complete removal or truncation of viral gene products, OVs are modified so that gene expression is under the specific control of promoters that are generally absent from healthy somatic cells but highly expressed in the tumour environment (Russell *et al.*, 2012). In fact, this was among the earliest methods of engineering tumour specificity into OVs as demonstrated with herpes virus in 1997 (Miyatake *et al.*, 1997). This strategy of transcriptional has been used for numerous viruses, including oncolytic adenoviruses, herpesvirus, and (Goldufsky *et al.*, 2013), and as genetic profiling of cancer cells continues, additional regulatory elements will be revealed to restrict OV gene expression to particular cancer cell targets.

3. ONCOLYTIC VIROTHERAPY FOR PANCREATIC CANCER

The high rate or recurrence in resectable tumours combined with the limited success of chemotherapy and radiation treatment regimens has led researchers to investigate alternative methods in the battle against pancreatic cancer. Recent advances into the understanding of its genetic and molecular mechanisms are creating better opportunities for the design and use of specifically targeted therapeutics, making oncolytic virotherapy an increasingly promising strategy (Ady JW, Heffner J, Klein E, 2014; Wennier *et al.*, 2011). An effective OV to treat pancreatic cancer should be tailored to selectively replicate in cells with PDA-associated genetic markers, be able to survive in the highly hypoxic tumour microenvironment, and ideally induce some level of tumour immunity (Ady JW, Heffner J, Klein E, 2014).

A number of virus families have been proposed as oncolytic agents for pancreatic cancer, some still in early stages of laboratory investigation while others have been tested as far as Phase III clinical trials. Generally speaking, conditionally-replicating adenoviruses (CRAds) are the most highly characterized oncolytic agents for cancer treatment, and similarly have been heavily investigated for the treatment of PDA (Ady JW, Heffner J, Klein E, 2014; Wennier *et al.*, 2011; Xu *et al.*, 2013). With the coxsackie-adenovirus receptor lacking on most pancreatic cancer cells, PDA-specific serotype 5 CRAds have been generated by generating chimeric viruses expressing capsid proteins from diverse serotypes (Chu *et al.*, 2012) or protein sequences generated from screening libraries (Yamamoto *et al.*, 2014) to increase binding to their targets. ONYX-015, harboring the E1B deletion, has been tested in Phase I and II clinical trials and though tolerance has been quite good, limited results in patients have been observed even in combination with gemcitabine (Khan *et al.*, 2014). Improvements to oncolytic adenovirus design have included removal of additional virulence factors such as antiapoptotitc proteins

and the *E1B* gene, which is normally involved in cell cycle dysregulation. Arming of CRADs with antiangiogenic factors, somatostatin receptor 2 (*SSTR2*) to restore normal expression in pancreatic cancer cells, and IL-24 has also proven effective in the pre-clinical setting, and tumour targeting has been increased by placing viral genes under the control of tumour-specific promoters (Armstrong *et al.*, 2012). At the time of writing, a Phase-I dose-escalation study in patients with advanced pancreatic cancer using a CRAD armed with hyaluronidase with or without gemcitabine is actively recruiting.

Herpesviruses have also been widely investigated for their oncolytic properties against pancreatic cancer, using different platforms containing deletions of genes essential for viral replication such as *UL39*, regulation of the PKR pathways such as *γ34.5*, or placement of key viral genes under control of cancer cell promoters. Numerous preclinical studies have been undertaken and have shown promising results in xenograft models treated with combinations of oncolytic HSV-1 and either gemcitabine or glancovir, though specific synergy was not always obtained and highlighted the importance of using the correct combination therapies with regard to mechanisms of action. T-VEC, formerly known as OncoVex-GM-CSF, is a GM-CSF-armed HSV-1 vector that has been extensively studied for use in melanoma patients, but has also been investigated in a Phase I clinical trial against pancreatic cancer, with official results yet to be published (Hughes *et al.*, 2014).

A variety of other viruses have been studied for their oncolytic properties against PDA in *in vitro* and pre-clinical models, including vesicular stomatitis virus (Blackham *et al.*, 2014; Murphy *et al.*, 2012), rodent parvoviruses (Angelova *et al.*, 2014; Nüesch *et al.*, 2012), myxoma virus (Wennier *et al.*, 2012), measles virus and reovirus (Ady JW, Heffner J, Klein E, 2014; Khan *et al.*, 2014; Wennier *et al.*, 2011), with some in Phase I and II clinical testing. Overall, similar to observations with OVs against other forms of cancer, promising results at the pre-clinical stage do not always translate to significant results in the clinic due to major differences in laboratory animal models and actual patients. Mechanisms though which OVs exert their anti-tumour effects are not always clearly understood, and this can greatly influence the ability to correctly choose a chemotherapeutic drug to act synergistically with the virus. Additional factors to help viruses spread within the highly stromal tumour microenvironment as well as those to increase the development of antitumour responses are all areas with many outstanding questions to be answered. However, the great diversity of genetic alterations in pancreatic cancers suggests that a single modified oncolytic agent will not likely be appropriate for all patients, and further investigations into other virus families specifically targeted to additional genetic signatures or combinations thereof will therefore be key in offering patients a personalized, legitimate treatment option with the hope for recovery.

4. INFLUENZA VIRUS

4.1 Classification and Structure

Of the five genera in the *Orthomyxoviridae* family, Influenza A viruses are the most widely characterized. Orthomyxoviruses, also including influenza B, influenza C, *Isavirus*and *Thogotovirus*, are characterized as enveloped viruses with a negative sense, linear single-stranded, segmented RNA genome, with the number of segments varying depending on the genus. Influenza viruses primarily cause disease if the mucosal systems, and accordingly the name *Orthomyxoviridae* comes from the Greek words *orthos*and *myxa*, meaning "correct" and "mucus". Within the genus, influenza A viruses are further classified based on the antigenicity of their two major surface glycoproteins, with eighteen HA subtypes and eleven NA subtypes described thus far. The HA and NA subtypes have been found in nature in a great variety of combinations with the exception of H17N10 and H18N11 viruses that have only recently been described in bats (Cox *et al.*, 2010; Tong *et al.*, 2013). A standard nomenclature system for these viruses is used, starting with the specific genus and followed by species of isolation, geographical location, isolate number, and year of isolation. The antigenic description of the HA and NA subtypes follows in parentheses. An example of this is A/turkey/Italy/2962/2003 (H7N3), indicating the isolate is an influenza A virus isolated from a turkey in Italy that was assigned the isolate number 2962 by the laboratory where it was characterized 2003 and is of the H7 hemagglutinin type and N3 neuraminidase type. The naming system for most human influenza viruses follows the same format but the species of isolation is not included, though early influenza isolates such as A/Wilson-Smith/33 (H1N1) include the names of the scientists involved rather than the place of isolation (Cox *et al.*, 2010).

The influenza A virus genome consist of eight gene segments of viral RNA packaged as ribonucleoprotein complexes (RNPs), each consisting of the negative sense RNA strand encapsidated by several copies of the viral nucleoprotein (NP) and associated polymerase complex, containing the three virus-encoded polymerase proteins. These gene segments are numbered 1 through 8, going from largest to smallest, and have been found to encode for at least seventeen gene products depending on the particular isolates (Cheung & Poon, 2007; Vasin *et al.*, 2014). A full list of viral segments, their associated proteins, and putative major functions is found in **Table 1**.

Virions are pleiomorphic, found predominantly as spherical or ovoid shaped particles measuring 100-300 nm in diameter observed in following *in vitro* passage, while filamentous particles up to 30 μm are typical of primary or low-passage isolates (Seladi-Schulman *et al.*, 2013). The influenza A virus has a complex structure of cellular and viral components. The surface of the virus

Table 1. Influenza A virus gene segments, their relative sizes, encoded proteins and associated functions.

Gene Segment	Relative Size (nucleotides)	Gene Products	Polypeptide Length (amino acids)	Associated Function [b]
1 - PB2	2341	PB2	759	Part of polymerase complex, involved in cap-snatching of host pre-mRNAs for viral transcription. Associated with host range restriction
2 - PB1	2341	PB1	757	Part of polymerase complex, RNA-dependent RNA Polymerase involved in elongation of nascent RNA strands during transcription and replication
		PB1-N40	718	
		PB1-F2	90 (or truncated)	Maintain balance between PB1 and PB1-F2 expression. Induction of mitochondrial-associated apoptosis.
3 - PA	2233	PA	716	Part of polymerase complex, RNA endonuclease activity.
		PA-X	252	Modulation of host immune response.
		PA-N155	568	Unknown
		PA-N182	535	Unknown
4 - HA	1778	HA	566	Dominant surface glycoprotein responsible for receptor-mediated recognition of host cells and fusion of viral and endosomal membranes.
5 - NP	1565	NP	498	Viral RNA encapsidation, protection of nascent RNA strands during replication, and nuclear import of RNPS.
6 - NA	1413	NA	454	Sialidase activity – cleaves sialic acid from HA and NA molecules during budding process, prevents virion aggregation.
7 - M	1027	M1	252	Major structural determinant of virion, role in nuclear export of RNPs, primary mediator of virus assembly.
		M2	97	Ion channel protein, allows proton influx from acidified endosomes leading to uncoating process.
		M42	99	Homologous activity to M2 protein in M2-null viruses.
8 - NS	890	NS1	230	Non-structural protein found only in infected cells, interferon antagonist, regulates host and viral gene expression.
		NS2 (NEP)	121	Structural protein involved in nuclear export of nascent RNP complexes to the cytoplasm.
		NS3	174	Potentially associated with adaptation of human viruses to mice.
		NEG8	216	Unknown.

[b] Based on information from (Cheung & Poon, 2007; Cox *et al.*, 2010; Vasin *et al.*, 2014; Wright *et al.*, 2006)

particle is heavily decorated by two viral glycoproteins, the hemagglutinin (HA) and neuraminidase (NA), which protrude like spikes from the viral envelope at a ratio of approximately 500 HA: 100 NA molecules (Cox *et al.*, 2010). A third viral protein, M2, is embedded in the envelope and creates a channel between the virus interior and the external environment. The outer membrane, in addition to its three viral protein components, also contains a number of host cell-derived factors as it is formed by budding out of the host cell membrane. Immediately below the envelope lies the M1 layer, composed of the viral matrix protein (M1), which interacts with cytoplasmic tails of the envelope glycoproteins as well as the NS2 protein and RNP complexes on the interior. The packaging of the eight RNP complexes appears highly organized, with inter-RNP interactions maintaining a particular "7+1" structure of seven RNP segments organized in a ring around a central RNP (Zheng & Tao, 2013).

4.2 Replication Cycle

4.2.1. Attachment, Entry and Uncoating

The infectious cycle of IAV consists of several phases, beginning with viral entry into the host cell and release of its genetic material within the cytoplasm. This process begins with receptor recognition and binding by the viral hemagglutinin (HA). Attachment is mediated by an interaction between the receptor binding site of the HA molecule and sialic acid (SA)-containing glycoconjugates, on target cells. The nature of the SA linkage to its underlying galactose is considered the first major determinant for successful infection, as avian-tropic viruses preferentially recognize and bind to SAs with an alpha-2,3 linkage to galactose while human-tropic viruses generally bind SAs with alpha-2,6 linkages. Following receptor binding, the virus is internalized into endosomes, either through clathrin-coated pits or a micropinocytosis, depending on virion size and cell types (Hutchinson & Fodor, 2013; Zheng & Tao, 2013). The uncoating process occurs at the late endosome stage, where the viral membrane protein M2 acts as an ion channel, allowing protons to enter the virion from the endosomal interior. This process leads to virion acidification, which causes two major consequences: first, RNP complexes dissociate from the M1 protein layer and second, conformational changes in the HA result exposure of a fusion peptide that anchors with the endosomal membrane. Given that several HA glycoproteins undergo this process simultaneously, a pore is eventually created in the endosomal membrane through which the viral RNP complexes are released into the cytoplasm, completing the uncoating process. In fact, it is these RNP complexes, consisting of a single segment of viral RNA associated with the trimeric polymerase complex and encapsidated with nucleoprotein, that act as the

functional unit for influenza virus, orchestrating the entire replication process within the infected cell (Cox *et al.*, 2010; Hutchinson & Fodor, 2013).

4.2.2. The RNP

The influenza virus virion as a whole plays a large role in the attachment and entry into host cells as well as release of newly formed viral particles. However, the intracellular replication process depends entirely on the viral RNP complexes, which are the functional units for influenza virus. Each of the eight segments of IAV RNA is introduced into the host cell in the form of the RNP, consisting of the full length coding sequence for that particular segment with 12 conserved nucleotides at the 3' end and 13 conserved nucleotides at the 5' end. The partial complementarity of the termini allows base pairing between them, causing the RNA segment to fold back on itself and adopt a double helix conformation similar to that of DNA (Zheng & Tao, 2013). This structure is then encapsidated with nucleoprotein at a ratio of approximately one NP per 24 nucleotides, and finally is bound to the three viral RNA-dependent RNA polymerase proteins at a distal end (Fodor, 2013). After release into the host cell cytoplasm, the RNP complexes must enter the nucleus to begin the replication process. This is achieved through the utilization of nuclear localization signals (NLS) found on the nucleoprotein (NP) as well as the three associated polymerase proteins, which interact with host importins that deliver the RNP through nuclear pore complexes (Hutchinson & Fodor, 2013). Unlike most RNA viruses, orthomyxoviruses are unique in that they undergo transcription and replication within the nucleus.

4.2.3 Transcription

Transcription of the viral RNA is the first step in the replication process of influenza A virus and relies *cis*-acting viral polymerases as well as host factors for its initiation. The synthesis of viral transcripts is greatest at 2-6 hours post-infection, after which there is a great decline. This process requires the presence of a 5' cap obtained from host cell pre-mRNA. The "cap-snatching" activity of the influenza A virus polymerase is largely attributed to the polymerase basic 2 (PB2) subunit, which seeks out and binds to host cell pre-mRNA (m^7GpppX^m-containing) transcripts produced by cellular RNA polymerase II. These transcripts are then cleaved by the PA subunit typically 10-13 nucleotides from its 5' end. The presence of a C residue in the penultimate position of the viral RNA at the 3' end directs the addition of a guanine residue to the 3' end of the capped primer, initiating the process of transcription (Fodor, 2013). Elongation of the newly synthesized mRNA continues as the vRNA is threaded through the polymerase complex, but the 5' end remains bound to the PB1 subunit and causes

the polymerase to stutter on a stretch of 5-7 uridines found 15-22 nucleotides from the 5' end of the vRNA. As such, the 3' end of the nascent mRNA transcript is polyadenylated and this terminates the process of transcription (Cheung & Poon, 2007; Fodor, 2013; Palese & Shaw, 2007).

4.2.4 Protein Synthesis

Similar to the exploitation of host cell nascent mRNA primers for the synthesis of viral mRNA transcripts, influenza viruses profit from additional cellular proteins that promote the maturation and nuclear export of cellular mRNAs (York & Fodor, 2013). Translation of NP, the viral three polymerase proteins, NS gene products and M1 occur in the cytoplasm, however their presence in the nucleus is required for further steps in the replication cycle. The NP and polymerase proteins migrate back into the nucleus due to the presence of nuclear localization signals, as does the M1 protein at later time points. The nuclear export protein (NS2/NEP) also enters the nucleus following translation where it binds to M1 proteins that have associated with newly formed viral RNPs allowing for their eventual nuclear export (Hutchinson & Fodor, 2013; Palese & Shaw, 2007). Upon commencement of vRNA replication, transcripts of the HA, NA and M segments predominate. Synthesis of the HA and NA, and M2 glycoproteins occurs on membrane-bound ribosomes, from where they enter the endoplasmic reticulum and are transported through the trans-Golgi network. The M1 polypeptide has an inhibitory role on transcription and is also involved in nuclear export of RNPs, and therefore its expression must be delayed until later times post-infection. The increase in transcription of structural genes at later times also indicates that RNA synthesis has reached a critical level and that morphogenesis and assembly can begin (Palese & Shaw, 2007).

4.2.5 Regulation of Transcription and Genome Replication

Influenza A virus releases its negative-sense RNA into the host cell nucleus, which serves as a template not only for transcription of viral mRNA but for the synthesis of cRNA required for genome replication. In order to avoid an innate antiviral response, nascent viral RNA must be encapsidated by NP prior to nuclear export. As such, transcription predominates over RNA replication at early stages of infection in order to synthesize NP and other viral gene products that are critical for the subsequent steps in the virus replication cycle. The regulation of transcription and RNA replication has also recently been attributed to the source of the polymerase proteins. The polymerase complex associated transcription operates in *cis,* transcribing its associated RNA segment following nuclear import of the RNP complex. Replication of viral RNA, however, is thought to occur in *trans*, requiring the activity of

newly synthesized polymerase proteins that have entered the nucleus from the cytoplasm (Hutchinson & Fodor, 2013). Though transcription continues throughout the replication cycle of the virus, the balance shifts towards genome replication later in infection, which becomes the predominant process.

4.2.6 vRNA Replication and Nuclear Export of RNPs

Unlike transcription, replication is a primer independent process that results in a full-length duplication of the vRNA. Prior to binding the trans-acting polymerase, the 3´ end of the vRNA template dissociates from its vRNP-associated polymerase. The trans-acting polymerase then binds to GTP and the synthesis of the positive-sense complementary strand begins. The full length cRNA is complementary to the viral RNA, including the conserved nucleotides at the 5' and 3'ends, distinguishing it from mRNA that contains a capped structure at its 5' end and a poly-A tail. Although it exists only as a replicative intermediate, the cRNA is encapsidated by NP in the same manner as vRNA. This interaction is thought to stabilize the strands of RNA and is especially important for allowing the polymerase to read through the entire segment and preventing the formation of a poly-A tail (Fodor, 2013). Once the trans-acting polymerase synthesizes a nascent vRNA strand from the cRNA template, this newly synthesized RNP complex must exit the nucleus for packaging into newly forming virions. Nuclear export relies several viral gene products, including M1 and NEP, which enter the nucleus following synthesis in the cytoplasm. NEP contains a nuclear export signal and interacts with cellular nuclear export factor Crm1 as well as many nucleoporins, and the current model suggests NEP interacts with the M1 protein, which is thought to bind NP, and the entire NEP-M1-vRNP complex is exported together (Cox *et al.*, 2010; Fodor, 2013; Hutchinson & Fodor, 2013).

4.2.7 Assembly, Budding and Release

The majority of viral proteins are translated by host cell machinery in the cytoplasm, from which point they migrate to carry out their various functions. The three envelope proteins (HA, NA, and M2), however, are synthesized on membrane-associated ribosomes and are transported through the trans-Golgi network where they undergo post-translational processing and are delivered to cell membrane. HA and NA contain strong apical sorting signals and accordingly are delivered to the apical surfaces of polarized cells where they accumulate on lipid rafts. The M1 protein accumulates below these rafts and can interact with the cytoplasmic tails of the three surface glycoproteins as well as the directly with the lipid envelope. The M2 ion channel protein is found between raft domains, and

consequently is found at lower concentrations in virus particles compared to the surface of infected cells (Rossman & Lamb, 2011).

Nuclear export of RNPs leads to their initial accumulation in the perinuclear cytoplasm at the microtubule organizing center. From here, they are believed to interact with recycling endosomes where they associate and form complexes and are transported to the apical plasma membrane along a microtubule network. Since the genome is segmented, all eight segments must be packaged into progeny virions for them to be infectious. Influenza viruses contain highly conserved non-coding regions at their 3' and 5' termini, and these are thought to direct packaging (Muramoto *et al.*, 2006). Despite its original designation as a non-structural protein (NS2), NEP retains its interaction with the RNP complexes and is incorporated into new virions. Interaction of the M1 proteins with the newly transported RNPs may cause a conformational change that initiates the process of bud formation, which terminates with M2-mediated membrane abscission (Rossman & Lamb, 2011). When the virion pinches off from the host cell membrane, it often remains attached to the cell through HA-sialic acid receptor interactions, and therefore the sialidase activity of the viral neuraminidase is required for efficient virion release (Cox *et al.*, 2010).

4.3. Influenza in Humans

4.3.1. Disease – Organ and Cell Tropism

Influenza virus causes annual epidemics of influenza disease in humans, characterized by a range of common symptoms that may include sneezing, cough, nasal congestion, fever, malaise, sore throat, chills, anorexia, myalgia and headache. The severity of illness correlates with levels of virus shedding, both peaking at approximately 48 hours post-disease onset and declining until the seventh day, at which time little shed virus is detectable. Influenza viruses are transmitted primarily via aerosol droplets of approximately 2 microns in size or smaller, which are generated by coughing and sneezing (Wright *et al.*, 2006). In humans, the virus replicates exclusively in the respiratory tract where α-2,6-linked sialic acid receptors are found on epithelial cells of the nasal mucosa, paranasal sinuses, pharynx, trachea and bronchi. Deep within the lung the virus can also infect ciliated alveolar epithelial cells in addition to alveolar macrophages and dendritic cells (Shinya *et al.*, 2006).

4.3.2. Innate barriers to Respiratory Infection

The primary site of human influenza virus infection is the respiratory tract, which is equipped with several lines of defense to prevent infections from occurring. Mucus within the respiratory tract acts as a physical barrier to infection, trapping virus particles before they reach their host cell targets. A particular component of mucus are the mucins, a family of glycoproteins with a high content of alpha-2,3 SA-containing glycans. These molecules not only prevent human infection by avian IAVs, whose HA preferentially bind to these glycans, but also act as decoys for human influenza viruses by binding with NA, which has an inherent preference for the alpha-2,3 linkages. The presence of carbohydrate-binding lectins in the respiratory tract also provide a first line of defense, either acting as receptor decoys or by directly binding to glycosylation sites on the HA and NA of influenza viruses (Nicholls, 2013). Additional extracellular barriers include circulating protease inhibitors and the act of ciliary beating, preventing proteolytic activation of HA and successful attachment to epithelial cells, respectively (Wright *et al.*, 2006).

The lungs are also home to a plethora of circulating leukocytes, including macrophages, neutrophils and natural killer cells, that as a first line of defense to eliminate virus-infected cells in an attempt to break the cycle of infection and influence the adaptive immune response. At an intracellular level, the detection of influenza A virus by pattern recognition receptors including RIG-I and toll-like receptors leads to the production of key modulators of the innate immune response (Cox *et al.*, 2010; Nicholls, 2013). Interferons are found at high levels in nasal and pulmonary secretions following infection with influenza and correlate with peak viral titers and symptom scores in experimentally infected humans. IFN-α and IFN-β play an integral role in inhibiting virus spread, acting as warning signals to nearby uninfected cells to produce enzymes that block viral replication. Additionally, they affect the adaptive immune response; enhancing cytotoxic T lymphocyte (CTL)-mediated killing by promoting class I major histocompatibility complex (MHC) expression on the surface of infected cells (Abbas & Lichtman, 2003).

4.3.3 Adaptive Immune Response

While the innate immune response plays a substantial role in limiting viral infection, complete recovery from influenza A virus infection relies on the individual and coordinated actions of B and T lymphocytes. Anti-influenza antibodies produced by B cells play a critical role in protection from re-

infection, while cellular-mediated responses are largely responsible for clearing an active infection by targeted killing of infected cells (Wright *et al.*, 2006).

Influenza virus infection results in the production of antibodies against HA, NA, NP and M viral proteins, with anti-HA antibodies providing the majority of virus-neutralizing activity. Antibody-mediated protection can last for decades, and a recent study of 1918 pandemic survivors found functional, circulating memory B cells that produced neutralizing antibodies against the virus *in vitro* (Yu *et al.*, 2008). However, as seen in the case of vaccination-induced antibodies, the continual accumulation of antigenic changes on the HA of circulating viruses from year to year allows for infection in previously vaccinated individuals, indicating antibody-mediated protection is incomplete (Thomas *et al.*, 1998; Wright *et al.*, 2006). In addition to the humoral response, cell-mediated immunity plays a major role in recovery from influenza virus infection and is mediated by a CD8+, Type 1-helper T cell (T_H1) dominated response (Fernandez-Sesma *et al.*, 2006). Virus-specific CTLs, responding to a variety of viral epitopes including surface and internal virus gene products, begin proliferating in the regional lymph nodes by 3-4 days post-infection and migrate to the lungs shortly thereafter. CD4+ T cells are also involved in the immune response, with T_H1 cells secreting IFN-γ to aid in CTL-mediated killing, and T_H2-mediated responses directing B cells to produce antibodies (Fernandez-Sesma *et al.*, 2006; Wright *et al.*, 2006).

4.3.4 Vaccines and Antivirals

An annual influenza vaccination campaign is coordinated by the WHO, which makes recommendations on particular antigens to include every year based on data collected by collaborating centres describing the predominant strains in circulation. The standard vaccination strategy used for the last several decades is the use of a trivalent inactivated vaccine containing two influenza A subtypes, an H3N2 and H1N1, and one influenza B virus (CDC, 2009). However, due to the variation in circulating viruses, the vaccine must be reformulated each year in order to provide efficient protection against strains predicted to circulate in the upcoming influenza season, and predictions are not always correct. Intranasally-administered live virus vaccines are also available and appear to be more effective, but is only approved for those aged 2-49 years, and is not safe for people in certain risk groups such as asthmatics and other immunocompromised individuals (Harris *et al.*, 2014; Katz *et al.*, 2006).

In addition to vaccines aimed at preventing disease, two major classes of compounds are approved for use as prophylactic and therapeutic agents in North America, each presenting a blockade at different points in the infectious cycle. The first group of compounds, including amantadine

hydrochloride and rimantadine, prevent the uncoating process by blocking the M2 ion channel. The second class of anti-influenza therapeutics are the neuraminidase inhibitors, Zanamivir and Oseltamivir(Tamiflu®), which compete for the neuraminidase active site, preventing sialidase activity and inhibiting release of virions from infected cells. The use of M2 inhibitors has been limited in recent years due to resistance, whereas only low level clinical resistance has been observed for the neuraminidase inhibitors, making them the current line of defense against epidemic and pandemic influenza (Wright *et al.*, 2006).

4.3.5 Antigenic Shift and Drift: Escape from Antibody-Mediated Detection

The success of influenza virus as a pathogen that causes seasonal disease lies greatly in its ability to evolve and avoid neutralization by pre-existing antibodies in the exposed population. Antigenic variation of the HA and NA surface glycoproteins occurs through two diverse mechanisms. The first, known as antigenic drift, refers to the gradual accumulation of amino acid mutations at the any of the five antigenic sites on the HA or the four sites on the NA leading to the inability to be recognized by pre-existing antibodies. Antigenic drift is caused by spontaneous mutations resulting from a lack of proof-reading by the influenza virus polymerase, and variations are thought to occur at a rate of less than 1% each year. However, after a few years of continued accumulation a new variant strain will become predominant and cause the next rounds of seasonal epidemics.

Unlike antigenic drift, Influenza A viruses can undergo a rapid and significant change in its antigenicity, known as antigenic shift. This phenomenon results from the segmented nature of the genome, where simultaneous infection with two influenza viruses can result in genetic reassortment producing progeny virions with a combination of genes from the two parent viruses. When an isolate emerges with different HA subtype than the currently circulating strain, a pandemic can result since the population is immunologically naïve (Cox *et al.*, 2010).

4.3.6 History and Pandemics

Over the last century influenza A viruses have caused four major pandemics, though descriptions of influenza-like disease causing human outbreaks date back more than 2000 years.

In the spring of 1918a devastating influenza pandemic struck the globe that cause an estimated 20-50 million deaths. The causative agent was an H1N1 subtype virus likely introduced directly into the human population from an avian host. Combining the fact that the population was immunologically naïve, the particular pathogenic nature of this virus and the lack of antibiotics to combat secondary

bacterial infections led to the unprecedented severity of the disease. H1N1 remained the dominant subtype causing seasonal epidemics until the start of the second pandemic. The "Asian flu", caused by a human-avian reassortant virus containing H2 and N2 surface glycoproteins as well as the PB1 gene of an avian virus, spanned from 1957-1958 and caused approximately 1 million excess deaths worldwide. From that point the H2N2 virus became the dominant circulating subtype until the start of the "Hong Kong flu" in 1968. This virus resulted from genetic reassortant with an avian H3 virus from which it obtained it's HA glycoprotein as well as a new PB1 gene, whereas all other genes from the circulating descendants of the 1957 virus were retained. The retention of the N2 segment from the circulating human viruses led to some degree of immunological protection from the new virus and mortality rates were therefore much lower than in previous pandemics. The Hong Kong H3N2 virus completely replaced the previous H2N2 human virus, and its descendants continue to circulate and cause annual influenza epidemics (Cox *et al.*, 2010). In 1977, the H1N1 virus was re-introduced into the human population but did not cause a full-fledged pandemic. Nonetheless, it became established and has circulated alongside H3N2 viruses since.

The most recent pandemic of 2009 had several characteristics not observed with the previous pandemics. First, the causative agent was an H1N1 virus, and therefore did not involve the introduction of a novel subtype into the human population. Second, the genetic signatures of the virus indicated that it was a triple reassortant avian-swine virus that had likely been spread from pigs to humans. Though case fatality rates were low, there was a high associated morbidity and this new H1N1 variant became dominant, replacing the previously circulating descendants of the 1977 virus(Neumann & Kawaoka, 2011; Webster & Govorkova, 2014) (http://www.cdc.gov/flu/pastseasons/1314season.htm).

4.4. Ecology and Epidemiology

4.4.1 Avian Influenza

Of the five genera of *Orthomyxoviridae*, influenza A virus is the only genus to infect avian species. Waterfowl of the orders *Anseriformes, Passeriformes*, and *Charadriiformes* are considered the primary reservoirs of all influenza A viruses, and isolates of all known subtypes have been found in these populations (Alexander, 2007). Though not classified among the natural reservoirs, poultry and other gallinaceous birds such as turkeys and quail can be infected by viruses transmitted from wild birds. In the wild, viruses are transmitted from bird to bird via the fecal oral route in contaminated water basins. Conversely, the respiratory route appears to be responsible for transmission of influenza

in land birds such as domestic poultry where direct contact with wild birds or their fecal material leads to the primary introduction of viruses into the flocks (Capua & Alexander, 2008; Webster, 2006).

Avian influenza viruses can be classified into two groups based on their resulting clinical disease. Viruses of all 16 HA and 9 NA subtypes cause low pathogenic avian influenza (LPAI), resulting in mild or asymptomatic gastrointestinal infection in birds, whereas some viruses of the H5 and H7 subtypes cause severe disease known as highly pathogenic avian influenza (HPAI). HPAI is characterized by systemic infection and rapid mortality, resulting in up to 100% mortality in infected poultry flocks within 48 hours of infection. The molecular determinants of this pathogenicity lies in the sequence at the HA0 cleavage site, which depends on host proteases for cleavage into its HA1 and HA2 subunits for functionality. LPAI viruses contain a single arginine at the cleavage site, limiting cleavage to a small number of extracellular host proteases and thereby restricting tissue tropism to anatomical sites where such proteases are found. Conversely, highly pathogenic viruses contain multiple basic amino acids at the HA0 cleavage site, permitting cleavage by ubiquitous intracellular proteases and ultimately allowing for systemic spread of the virus (Capua & Alexander, 2008; Taubenberger, 1998).

HPAI isolates generally emerge after their low pathogenic precursors are introduced into from wild birds into domestic poultry flocks. In these new host populations, viruses acquire the highly pathogenic cleavage site by either by stuttering of the polymerase during replication or rarely via non-homologous recombination with other viral gene segments (Webster, 2006).

4.4.2. Receptor Specificity and Interspecies Transmission

In order for a virus to successfully cross the species barrier it must overcome several constraints at the virus and host levels. As a result, the introduction of a virus from its reservoir species into a new host often results in unproductive infection. Even if infection does occur, the ability of the virus to spread to from the primary spillover event to another susceptible individual depends on several determinants. A major factor that restricts influenza A virus infection to a particular species lies in the first step of viral infection - recognition and specific binding with host cell receptors. Avian and human-tropic influenza viruses differ in their specificity for sialic acid-containing receptors based on the type of linkage between sialic acid and its underlying galactose (Cox *et al.,* 2010). The avian GI tract is predominated by α-2,3-linked sialic acid species, while the human respiratory tract contains mostly α-2,6-linked sialic acids, though α-2,3-linked sialic acid species are found on some ciliated cells in the lower respiratory tract. Accordingly, mammalian viruses are specific for α-2,6-linked SA

residues while avian viruses are specific for α-2,3-linkages. Even though avian viruses can infect cells deep within the human respiratory tract, a change in affinity of their HA towards the mammalian receptor conformation is required for the virus to successfully transmit from human-to-human, since influenza viruses are transmitted via droplets and aerosols released from the upper respiratory tract. Additionally, NA must be able to interact with the receptor to cleave SA residues from nascent HA molecules during the budding process. Therefore, both the HA and NA glycoproteins must shift their affinities from the avian to mammalian receptor for efficient transmission in the human population (Neumann & Kawaoka, 2006).

4.4.3 PB2 and Interspecies Transmission

While the viral glycoproteins are key determinants of host range of influenza viruses, the internal proteins must also function in the new host environment in order for efficient genome transcription and replication to occur. Another major limitation to interspecies transmission of IAVs lies at the level of the virus polymerase. The IAV polymerase complex, comprised of PB1, PB2 and PA proteins, together with the nucleoprotein (NP), carry out viral mRNA synthesis and genome replication (Mänz *et al.*, 2013). PB2 in particular is implicated in host range restriction as it was shown to restrict limit the growth of certain avian viruses in mammalian cells, and two theories have been proposed for the mechanism of host range restriction. The first suggests that it directly interacts with host cell factors required for RNA transcription and replication, and differences between factors from avian and mammalian species require a specific amino acid for optimal interaction (Tarendeau *et al.*, 2008). The second explanation is that PB2 is unable to function at temperatures outside its natural host (Massin *et al.*, 2001; Subbarao *et al.*, 1993). A single amino acid (AA) residue, PB2-627, has been implicated as the major determinant of temperature sensitivity, where avian viruses possess glutamic acid (E) while mammalian viruses possess lysine (K) at this position, conferring optimal RNA polymerase activity at the temperature of the natural host. As such, PB2-627E allows optimal replication at 41^{o}C, typical of the avian GI tract, while PB2-627K allows for optimal/favours replication at 33^{o}C and 37^{o}C, temperatures of the upper and lower human respiratory tracts (Bradel-Tretheway *et al.*, 2008; Massin *et al.*, 2001). Though several exceptions to this theory have been observed, and additional amino acid residues are thought to play a role in host adaptation, the role of the viral polymerase in host adaptation and the temperature level clearly plays a part in the complex process involving factors at both the viral and host level.

5. INFLUENZA VIRUS – POTENTIAL AS AN ONCOLYTIC VIRUS AGAINST PDA?

5.1 Influenza virus as an oncolytic agent

While much attention has been paid to DNA viruses, the potential of RNA viruses as agents of oncolytic virotherapy has been highlighted in recent years. The first potential case of antitumor activity of influenza virus was reported in 1904 when a leukemia patient underwent a dramatic regression following presumed influenza virus infection. However the lack of virus isolation techniques at the time cannot rule out the infection was cause by another agent and no similar cases have been reported since (Russell, 2002). Laboratory investigations using influenza virus to treat mouse-derived tumors including Erlich Ascites were carried out by a small number of groups in the 1950's however long-term tumour reduction was not observed, there was no decrease in mortality and the viruses capable of tumour replication were often associated with neurotropism (Cassel, 1957; Kelly & Russell, 2007; Wagner, 1954).

The advent of a reverse genetics system for the rescue of genetically engineered viruses (Fodor et al., 1999; Neumann et al., 1999) allowed for the oncolytic capabilities of influenza A virus to be revisited, permitting the modification of virulence factors to limit viral replication in healthy cells. In 2001, the first report of an influenza A virus with *ras*-dependent oncolytic targeting (Bergmann *et al.*, 2001) demonstrated that an engineered virus with a deletion in its NS1 gene (delNS1) replicated in PKR-deficient melanoma cell line but not normal cells and importantly repressed tumour growth in mice with subcutaneously implanted tumours. Subsequent work demonstrated that affinity towards the malignant phenotype in the case of this virus was attributed to the cell's inherent interferon resistance (Muster *et al.*, 2004), a trait commonly observed in numerous cancers including PDA. Further work with delNS1 viruses demonstrated that influenza A virus has immune boosting activity in its contest as an OV, with exposure of both natural killer cells and CD8+ T cells to delNS1-infected prostate cancer cells greatly enhancing recognition and lysis of the same cell type even in the absence of infection (Efferson *et al.*, 2006; Ogbomo *et al.*, 2010). Taking reverse genetics to the next step, a recent publication by van Rikxoort and colleagues describe an influenza A virus expressing the IL-15 coding sequence in its NS gene segment that replicated efficiently and produced biologically active IL-15 in infected melanoma cell lines that was able to stimulate NK-mediated cytotoxicity against uninfected tumour cells (van Rikxoort *et al.*, 2012). Taken together, though the number of studies on the oncolytic activities of influenza virus have been limited to only a few types of cancer cells, further investigations into its oncolytic capabilities are warranted as numerous viral factors can be modified to specifically target them to the malignant phenotype.

5.2 Influenza A Virus and Pancreatic Tropism

Avian influenza viruses replicate primarily in the respiratory and intestinal tracts of their natural hosts. However, observational studies and pathological findings in animals both naturally and experimentally infected with influenza viruses have also indicated a specific tropism for the pancreas. In both domesticated avian species and migratory waterfowl this has been observed with both highly pathogenic and low pathogenic avian influenza viruses (Brojer *et al.*, 2009; Clavijo *et al.*, 2001; Keawcharoen *et al.*, 2008; Kwon *et al.*, 2010; Pantin-Jackwood & Swayne, 2009; Shinya *et al.*, 1995). Necrosis of the pancreatic ductal epithelium was observed in ferrets intragastrically infected with HP H5N1 virus (Lipatov *et al.*, 2009),and pancreatic post-mortem lesions ranging from inflammation to necrosis have also been observed in HPAI-infected domestic cats as well as a stone marten (Reperant *et al.*, 2009).In addition to these observations, pancreatic tropism of influenza A virus has additionally been described in humans. The H1N1 2009 influenza pandemic was associated with a small number of case reports of acute pancreatitis (Baran *et al.*, 2012; Blum *et al.*, 2010), and pathological examinations of human fatalities also revealed pancreatic lesions in two of six post-mortem examinations (Calore *et al.*, 2011).Additional studies by our laboratory using *in vitro* and *ex vivo* models demonstrated that human cells originating from the exocrine pancreas were infected and killed by LPAI viruses (Capua *et al.*, 2013). Therefore, although the pancreas is not considered a typical site of replication following the standard route of infection, influenza virus seems to have a capacity to infect and damage pancreatic cells in severe infections.

5.3 Potential Targeting Strategies for Restricted Replication in the Tumour Microenvironment.

5.3.1 Removal of Virulence Factors: NS1 and PB1-F2

Influenza A viruses are employ several strategies to evade immune detection. At the innate immune level, the virus synthesizes proteins that specifically counteract these responses. The first and best characterized of these is the non-structural protein NS1 encoded by gene segment 8, produced at very high levels early in infection. In interferon competent hosts, NS1 functions as an interferon antagonist. NS1 counteracts the host interferon response at both pre-and post-transcriptional levels (Cox *et al.*, 2010; Hale *et al.*, 2008). The original model held that NS1 sequesters viral double-stranded RNA, preventing dsRNA-mediated activation of transcription factors of the innate immune response, however these viral dsRNA species have yet to be detected. Recently it has been shown that NS1 forms a complex with RIG-I, blocking IFN−β production pre-transcriptionally. At the post-transcriptional

level, NS1 blocks nuclear export of cellular mRNAs, preventing the synthesis of host antiviral proteins. As such, it interferes with the cell's ability to enter into an antiviral state and permits continued viral replication (Cox *et al.*, 2010; Hale *et al.*, 2008). In infected bone marrow-derived dendritic cells (DCs), expression of NS1 is also associated with suboptimal DC maturation and a decrease in production of the chemokines required to prime a T_H1-mediated immune response. In this way NS1 not only suppresses the innate immune response, but can also down regulate adaptive immunity (Fernandez-Sesma *et al.*, 2006). Given the lack of an intact interferon response in the majority of PDA cells, the generation of a modified influenza A virus with a truncated or deleted NS1 gene would not impede virus replication in the tumour microenvironment, however replication in interferon-competent bystander cells would be halted.

In 2001 a new protein encoded by an alternate reading frame within the PB1 gene segment was discovered and has been implicated in pathogenicity, though it is not produced by all isolates. The PB1-F2 protein is the smallest gene product encoded by influenza A viruses and has both pro-apoptotic and interferon antagonistic properties (Cox *et al.*, 2010; Varga & Palese, 2011). Following its synthesis this protein localizes to the mitochondria where it interacts with the mitochondrial antiviral signaling protein (MAVS), preventing it from initiating its signaling cascade for downstream activation of interferon transcription. In addition to blocking the antiviral response, PB1-F2 is best known for its pro-apoptotic activity. Apoptosis mediated by the intrinsic pathway initiates at the mitochondria, and PB1-F2 is thought to induce this pathway either by self-oligomerizing and creating pores in the mitochondrial membrane, or by interacting with inner and outer mitochondrial membrane proteins and inducing the formation of a pore complex, both of which leading to cytochrome c release and subsequent downstream caspase activation (Varga & Palese, 2011). Similar to NS1, by generating a PB1-F2-modified virus with decreased ability to prevent MAVS-mediated interferon transcription as well as one with a moderate phenotype regarding induction of apoptosis it would create an added safeguard to restrict viral replication malignant, IFN-deficient cells.

5.3.2 Host Cell Retargeting – Hemagglutinin

The hemagglutinin (HA) is the most abundant surface glycoprotein on the influenza virion, accounting for roughly 25% of viral protein produced. Given its abundance in the influenza virus particle, the HA is responsible for two key processes in thee infectious cycle. First it mediates receptor binding by attachment to SA-containing host cell glycoconjugates, and second, it is responsible for fusion with host cell endosomal membranes leading to the uncoating process. At the functional level,

HAs are expressed as homotrimers of three identical monomers that extend 14 nm out from the viral membrane. The HA is synthesized as a monomer, HA0, that is post-translationally cleaved by intracellular or extracellular proteases into its functionally active form of two polypeptides (HA1 and HA2) that remain linked by a disulfide bond. Each monomer has two structurally distinct domains, including a globular head composed entirely of HA1 residues and a fibrous stalk that contains residues of both HA1 and HA2. The cleavage of HA0 into its two subunits is particularly essential for the fusion of the viral and endosomal membranes as uncleaved HAs are unable to utilize their 19 amino acid-long fusion protein, leading to non-productive infection (Cheung & Poon, 2007; Cox *et al.*, 2010; Nayak *et al.*, 2004).

More recently it has been shown that the degree of receptor affinity is far more complex, with oligosaccharide length, sulfation, fucosylation, and specific subterminal residues of the Sia-containing glycoconjugate all affecting the interaction at the HA binding site (Nicholls *et al.*, 2008). In their 2006 publication, Stevens and colleagues compared the binding affinities of several influenza viruses of mostly human origin to 200 different glycoconjugates and were able to correlate differences in HA amino acid sequences with differential binding to various glycans. This work pointed out a number of key residues in the receptor binding site of human H1 viruses that affect binding to sulfated or fucosylated moieties in addition to those which affect overall preference to alpha-2,3 and alpha-2,6-linked receptors (Stevens *et al.*, 2006). In another study, a solid phase binding assay was used to examine binding affinities of nearly 50 viruses of human, swine, equine, wild aquatic bird and domestic poultry origins to nine different glycoconjugates, which demonstrated that viruses belonging to specific hemagglutinin subtypes generally displayed similar binding preferences (Gambaryan *et al.*, 2008).

Sialic acid is transferred to the terminal carbohydrates of glycolipids and glycoproteins by intracellular golgi membrane-associated sialyltransferases, grouped according the type of linkage they catalyze. In humans, eight alpha-2,6-sialyltransferases, four alpha-2,8-sialyltransferases, and six alpha-2,3-sialyltransferases have been identified and are responsible for creating specific forms of alpha-2,6-, alpha-2,8-, and alpha-2,3-linkages, respectively. The expression of various sialyltransferases is known to change in many types or tumours, including colon, breast, cervical, gastric, renal and bladder cancers, and increased expression of these genes are associated with increased tumour aggression. The over-expression of the alpha-2,3 sialyltransferase ST3 Gal III in pancreatic adenocarcinoma cell lines was recently shown to increase cancer cell motility, and binding to E-selectin. Additionally, the increased expression of ST3 Gal III led to increased surface expression of Sialyl Lewis X (SLe^X), a fucosylated alpha-2,3-linked glycoconjugate (Neu5Acα2-3Galβ1-4(Fucα1-3)GlcNAcβ). *In vivo*

experiments have also demonstrated that ST3 Gal III overexpression lead to increased tumour establishment in mice (Pérez-Garay *et al.*, 2010).

In humans, immunohistochemical studies comparing pancreatic tissues from normal pancreas, patients with chronic pancreatitis, and pancreatic adenocarcinoma demonstrated SLe^X-related antigens were found in the majority of pancreatic cancer tissues while absent from normal tissues, and were particularly highly expressed on cells of highly differentiated tumours (Kim *et al.*, 1988a; Mas *et al.*, 1998). Similarly, in the clinical setting, increased levels of SLe^X on pancreatic tumours cells are correlated with poor patient prognosis (Pérez-Garay *et al.*, 2010). Modifying the receptor binding site of the viral hemagglutinin to have increased binding affinity towards PDA-associated receptors, such as ST3 Gal III-synthesized sialic acid-containing glycans such as SLe^X, may present a promising retargeting strategy to limit viral attachment to the cancerous cells of interest.

6. GAPS IN KNOWLEDGE & RESEARCH OBJECTIVES

Pancreatic cancer remains a grave condition for which no effective treatments are available. The field of oncolytic virotherapy has gained major ground in recent decades and though a number of viruses have been tried in the laboratory and clinical setting, much work remains in searching for an effective oncolytic agent against PDA. Given that influenza virus has a documented predilection for the pancreas, and given that the virus presents numerous possibilities for specific targeting to the malignant phenotype, the research presented in this thesis aims to address important initial questions regarding the oncolytic capacity of influenza A virus in human PDA cells. Given the lack of circulating antibodies in the human population and the poor ability for these viruses to cause respiratory infection in humans, this research focuses in particular on the use of low pathogenic influenza A viruses of avian origin.

The following questions were proposed:

1. Do human PDA cell line express receptors permitting the recognition and attachment by avian influenza virus isolates?

2. Do human PDA cell lines express particular receptor glycoforms previously reported in literature against which an IAV could be potentially re-targeted?

3. Do receptor binding properties of the experimental isolates indicate any viruses with an innate preference for cancer-associated glycans?

4. Are avian influenza viruses able to replicate in PDA cells under normal physiological conditions?

5. Does influenza virus infection cause PDA cell death, and are certain isolates more cytopathic than others?

6. Can influenza virus induce apoptosis in PDA cells, and if so what is the mechanism employed?

MATERIALS AND METHODS

1. Cells. Madin-Darby Canine Kidney (MDCK) cells were maintained in Alpha's Modified Eagle Medium (MEM, Sigma), supplemented with 10% Foetal Bovine Serum (FBS) (Euroclone), 1% 200mM L-glutamine (Sigma) and a 1% antibiotic solution of Penicillin-Streptomycin-nystatin (10,000U/ml, 10,000 μg/ml, 10,000 U/ml, Gibco & Sigma). The non-tumoural human pancreatic ductal cell line HPDE6, PDA lines BxPC-3 and AsPC-1, and murine PDA PANC-02 cells were maintained in RPMI, PANC-1 and MIA paca2 cells were maintained in DMEM and CFPAC-1 cells were maintained in Iscove's modified Dulbecco's medium. All media were supplemented with FBS, L-glutamine and antibiotics as for the MEM, and all cell lines were maintained in a humidified incubator at 37ºC with 5% CO_2 and sub cultured twice weekly.

2. Viruses. A panel of IAVs from multiple host species, including high and low pathogenicity isolates, were examined for their ability to infect the pancreatic cells. Viral strains used in this study included A/turkey/Italy/2962/2003 (H7N3), A/turkey/Italy/4580/99 (H7N1 HP), A/cockatoo/England/72 (H4N8), A/macaw/England/626/80 (H7N7), A/mallard/Italy/3401/05 (H5N1), A/chicken/ Egypt/1701/6 (H5N1 HP), A/PuertoRico/8/34 (H1N1) and A/canine/Florida/43/2004 (H3N8). Virus stocks were grown in 9-10 day old SPF embryonated chicken eggs (Charles River), and harvested allantoic fluid was clarified by centrifugation and tested for bacterial contamination prior to use.

3. Plaque Assay. All viruses were titrated by standard plaque assay procedure. Semiconfluent cultures of MDCK cells were trypsinized, counted, and seeded at a density of 85,000 cells/cm2 on six-well plates the day prior to use. The following day, plates were examined under a light microscope to confirm confluency of monolayers. Wells were washed once with Ca^{++} and Mg^{++}-free PBS, once with serum-free MEM, and then inoculated with 500 μl per well of serially diluted virus stocks prepared in serum-free MEM. Inoculum was removed after one hour of incubation and replaced with 3 mL of a 0.8% agarose overlay with a final concentration of 1X DMEM, 1% antibiotics, 1% L-glutamine, and TPCK-Trypsin (Sigma) at a concentrations ranging from 0-2 μg/ml, depending on the virus isolate. Plaques were visualized and counted at three days post-infection after fixation with 10% formalin and staining with 0.5% crystal violet.

4. Sialic Acid Receptor Characterization. The presence of alpha-2,3- and alpha-2,6-linked sialic acid residues was determined by flow cytometry for each PDA cell line included in the study. Following trypsinization, $1x10^6$ cells were aliquoted into microfuge tubes and washed twice by centrifugation with 500 µl of PBS-10 mM HEPES (PBS-HEPES. To control for endogenous biotins or avidin binding sites, an Avidin/Biotin blocking kit (Vector Laboratories, USA) was employed prior to staining. Reagents were prepared as per manufacturer's instructions and cells were incubated with 100 µl of each solution for 15 minutes, with two PBS-HEPES washes after each treatment. Alpha-2,3 and alpha-2,6 sialic acid linkages, respectively, were detected by incubating cells for 30 minutes with 100 µl of biotinylated *Maackia amurensis* lectin II (Vector Laboratories) (5 µg/ml) followed by 100 µl of PE-Streptavidin (BD Biosciences) (10 µg/ml) for 30 minutes at 4ºC in the dark, or with 100 µl of Fluorescein conjugated lectin (Vector Laboratories) (5 µg/ml). Cells were washed twice with PBS-HEPES between staining and resuspended in PBS with 1% formalin prior to flow cytometric analyses. To confirm specificity of lectins, cells were pre-treated with 1U per mL of neuraminidase from *Clostridium perfringens* (Sigma) for one hour prior to the avidin/biotin blocking step. For each cell line characterized, five samples were included for analysis: 1. Unstained negative control; 2. Cells stained only for presence of α-2,3-linked receptors using primary and secondary reagents; 3. Cells stained with only the secondary PE-Avidin D; 4. Cells stained only for presence of α-2,6-linked receptors; 5. Double stained cells for detection of α-2,3 and α-2,6-linked receptors. Samples were analyzed on a BD Facscalibur or the BD LSR II (BD Biosciences) and a minimum of 5,000 events were recorded.

5. Sensitivity of PDA cells to influenza virus infection. To determine whether pancreatic cell lines were susceptible to infection by IAV, a pilot experiment was conducted where cells seeded on 96-well plates were infected with 10-fold serial dilutions of virus stocks and incubated at 37ºC. A minimum of four wells were infected per dilution of virus, and infections were performed in the presence of 0.05 µg/ml of TPCK-Trypsin, to the maximum concentration tolerated by the pancreatic cells without toxicity. At 72 HPI the highest dilution of inoculum where CPE was noted was recorded, and supernatants from each virus dilution were *harvested*, pooled, and directly passaged onto 96-well plates of MDCKs for virus isolation where TPCK-trypsin was used at a concentration of 1 µg/mL for all viruses except highly pathogenic isolates.

6. Virus Replication Kinetics in Pancreatic Cell Lines. The ability of selected viruses to replicate in select cell lines was monitored over a 72 hour time-course. BxPC-3, PANC-02, HPDE6, and MDCK cells were seeded on 24-well plates one day prior to infection in order to achieve a confluent monolayer. On the day of infection cells were washed once with pre-warmed PBS and then once with serum-free media. Cells were then infected with 200 μL of inoculum per well at an MOI of 0.001 PFU/cell, and following one hour of incubation inoculum was removed and replaced with 1ml of serum-free media containing 0.05 μg/ml L-1-Tosylamide-2-phenylethyl chloromethyl ketone (TPCK)-Trypsin. Mock-infected control wells were included in all experiments. At 1, 24, 48 and 72 HPI, supernatants from three infected wells were harvested and viral titres were determined via the 50% tissue culture infectious dose ($TCID_{50}$) assay on MDCK cells.

7. $TCID_{50}$ assay for Endpoint Titration of Experimental Supernatants. Confluent monolayers of MDCK cells on 96-well plates (Corning) were infected with serial ten-fold dilutions of harvested supernatants, using eight replicate wells per dilution. Fifty microlitres of inoculum, prepared in serum-free MEM, were added to each well and plates were incubated at 37ºC with 5% CO_2. After one hour of incubation, the volume in each well was topped up to 100 ml by the addition of 50 μl of MEM containing 2 μg/ml of TPCK treated-trypsin and plates were incubated for 3 days at 37ºC with 5% CO_2. Cytopathic effect was visualized first by examination under a light microscope and additionally after cells were fixed for 20 minutes with 10% buffered formalin (Fisher) and stained with a 0.5% crystal violet solution prepared in deionized water. Virus titre was calculated using the method of Reed and Muench (Reed & Muench, 1938).

8. Replication Kinetics at 33ºC, 37ºC, and 41ºC. To ensure that the lack of virion production by low pathogenicity IAVs observed in time course experiments was not attributed to temperature sensitivity of avian viruses in the human cells, BxPC-3 and MDCKs were infected with a selection of viruses in parallel at MOI=0.001 as above, and plates were incubated simultaneously at three physiologically relevant temperatures to human and avian conditions, namely 33ºC, 37ºC and 41ºC. Three infected samples were harvested at 24, 48 and 72 HPI and viral titres were determined by $TCID_{50}$ assay.

9. Viral RNA replication in PDA cell lines. To assess active viral genome replication, AsPC-1, BxPC-3, CFPAC-1, MIA paca 2, and PANC-1, HPDE6 and MDCK cells (positive control) were infected with

the panel of viruses excluding HPAI viruses at an MOI of 0.1. Monolayers were washed once with PBS after inoculum removal and overlaid with serum-free medium containing 0.05 μg/mL TPCK-Trypsin. At 1, 16, and 24 HPI supernatants and trypsinized cell pellets from infected wells were collectively harvested and stored at -80C for RNA extraction. Total RNA from infected cells and supernatants was obtained by automated extraction (Hamilton Robotics, Switzerland) using the Magmax 96 AI/ND Viral RNA Isolation Kit (Ambion, AM1835) according to manufacturer's instructions.

10. One step rRT-PCR. Real Time (r)RT-PCR targeting the conserved Matrix (M) gene of influenza A virus was performed isolated RNA using the published primers and probes previously described (40). The amplification reaction was performed using five microliters of extracted RNA in a final volume of 25 μL using the QuantiTect Multiplex RT-PCR kit (Qiagen, Hilden, Germany). Each reaction contained 300 nM of forward and reverse primers (M25F and M124-R, respectively) and 100 nM fluorescently labelled probe (M+64). The PCR was carried out under the following parameters: 50°C for 20 mins, 95°C for 15 mins, followed by 40 cycles of 94°C for 45 seconds and 60°C for 45 seconds.

11. Detection of Virus-induced Apoptosis by Flow Cytometry. Cells seeded in 24 well plates were infected at MOI = 1, and after one hour of absorption the inoculum was removed and replaced with 1 ml of serum-free media. Gemcitabine (2000 μM) and Cisplatin (0.8 μM), two common chemotherapeutic agents used for PDA treatment (36,5), were included in combination as a positive control. One hour prior to harvesting, FBS was added to each well for a final concentration of 10% to ensure cell membrane integrity for the labelling process. At 16 and 24 HPI, cells were harvested from two infected and one control well and incubated with Alexa Fluor® 647 Annexin V conjugate (Invitrogen) (1 μL per 375,000 cells) and propidium iodide (PI, 0.5 μl per 375,000 cells) in a volume of 300 μL of media with 10% FBS for 10 minutes in the dark. Samples were then fixed for 15 minutes in 3.6% paraformaldehyde, centrifuged, resuspended in 300 μL of PBS-FBS and read on a BD FACSCalibur. A minimum of 5,000 events were recorded. Virus-induced apoptosis, denoted as specific cell death, was determined by subtracting the percentage of Annexin V-positive controls from infected cells.

12. Detection of Virus-induction of Caspase Activity by Immunocytochemistry. BXPC-3 and HPDE6 cells were seeded on sterile glass chamber slides (BD) and high-binding slides, respectively, at seeding densities of 190,000 cells/cm^2 for the former and 100,000 cells/cm^2 for the latter. The

following day, semi-confluent monolayers were infected at MOI = 1, with inoculums removed following 1 hr of absorption and replaced with serum-free RPMI. At 16 and 24 HPI supernatants were removed, slides were air-dried under the biosafety cabinet, fixed in ice-cold acetone for 20 minutes, and then stored at -20ºC until analysis. Uninfected cells and those treated with Gemcitabine and Cisplatin served as negative and positive controls, respectively. Prior to staining, frozen slides were thawed and washed 3 times for five minutes with deionized water to remove residual acetone, blocked with 3% H_2O_2 for eight minutes at RT to remove endogenous peroxidases, washed 3X with deionized water and once with PBS-tween. Slides were then blocked for 30 minutes with 1% BSA, washed with PBS-Tween and permeabilized with 0.1% Triton X-100 for 10 minutes. Anti-active/cleaved caspase-8 (1:50, Imgenex), anti-active-caspase-9 (1:10, BioVision), and anti-active-caspase-3 (1:30, Cambridge, UK) primary antibodies were applied for 1 hour in a humidified chamber at room temperature. Immunoreactivity was revealed by the avidin–biotin method (LSAB+/System-HRP, DakoCytomation Glostrup) using aminoetile-carbazole substrate (AEC + Substrate-Chromogen Ready-to-use, DakoCytomation). Carazzi's haematoxylin was used as a counterstain and Faramount Mounting Medium (DakoCytomation) was used to mount coverslips on slides. Ten histological counts of 500 cells each were performed per cell line/treatment/time point using Nis Elements BR software (Nikon) to determine the percentage of caspase-positive cells.

13. Cell Proliferation Assay. Cells were seeded in 96-well plates at densities of 30,000 cells per well and infected with a panel of influenza A viruses the following day using an MOI of 1. Cell proliferation and subsequently cell viability was determined based on tetrazolium reduction at 24 HPI using the standard MTT assay. Briefly, 10 μL of MTT reagent (Sigma M2128) freshly prepared in PBS was added directly to culture medium producing a final concentration of 0.5 mg/mL. Following 4 hours of incubation at 37°C, 100 μL of solubilisation solution (10% SDS in 0.01M HCL) was added to each well for overnight incubation at 37°C. Absorbance was read at 570 nm with correction at 690 nm, and results from infected cells were normalized to uninfected controls.

14. Solid-Phase Receptor-Binding Assays.

14.1. Preparation of Fetuin-Coated Plates. A 1:5000 dilution of fetuin (Sigma, Cat. No. F3004) was prepared in 50 mL of PBS, and 50 μl of this solution was added to the bottom of all wells of flat-bottom 96-well plates (costar). Plates were incubated overnight in a humidified container at 4ºC,

washed 3X with tap water the following day and inverted to dry on absorbent paper. Dried plates were stored at room temperature until further use.

14.2. Preparation of Virus Stocks. Four virus isolates were utilized for receptor binding experiments, including experimental isolates H4N8, H7N3 and H7N7 as well as a previously characterized control isolate, A/Mallard/Alberta/119/98 (H1N1). Stocks of infectious virus were prepared by inoculation of embrionated hen's eggs as described above. The hemagglutination titre of all virus stocks was determined, and those with HA values of less than 256 HAU were pelleted by high-speed centrifugation at 120,000 x g for 1 hour. Virus pellets were thoroughly resuspended in a volume of approximately 500 μl by pipetting up and down a minimum of 100 x, and all final virus stocks were stored in small aliquots at -80^{o}C.

14.3 Hemagglutination Assays. The titre of virus stocks was determined using a standard hemagglutinaion (HA) assay. Briefly, fifty microlitres of PBS was added across an entire row of wells of a 96-well, V-bottom assay plate (Sigma, Cat No. CLS3894). Fifty microlitres of harvested allantoic fluid or concentrated virus was then added to the first well of the row and serially diluted two-fold across the row by transferring 50 μl from the first well into the second well and so on until. A row of PBS only was included on each assay plate to act as a negative control. Fifty microlitres of 0.5% chicken erythrocytes (prepared in sterile PBS) were then added to each well; plates were gently tapped to mix, and incubated for 25 minutes on ice to control for possible endogenous neuraminidase activity. The HA titre was determined as the reciprocal of the highest dilution of sample where hemagglutination was observed.

14.4. Titration of Virus Stocks and Fetuin preparations for Binding Assays. The binding affinity of experimental isolates towards various sialic acid-containing glycans was determined by both direct and indirect binding assays. In direct binding assays, the binding association of each virus with avian or human associated glycan receptors was assessed using monospecific Neu5Acα2-3Gal- and Neu5Acα2-6Gal-containing HRP-labelled fetuin preparations, herein referred to as 3-Fet-HRP and 6-Fet-HRP, respectively (Matrosovich & Gambaryan, 2012). For both types of assays, the first steps involved titration of the Fetuin solution followed by the virus dilution in order to select appropriate concentrations to generate results with a range of absorbencies and avoid saturation of the curve by

using unnecessarily high concentrations of either virus or Fetuin. Fifty microlitres of virus solutions at a single concentration selected on the basis of initial HA titres were added to Fetuin-coated plates (Matrosovich & Gambaryan, 2012), with two full columns dedicated to each given virus dilution and the first and last columns reserved as PBS controls. Plates were covered and incubated overnight in a humidified container at 4ºC, and virus solution was aspirated using a vacuum manifold. Wells were then blocked with PBS containing 0.05% desialylated BSA (Matrosovich & Gambaryan, 2012), covered and incubated at 4ºC for 3-4 hours. Towards the end of incubation time, eight serial two-fold dilutions of each Fet-HRP solution were prepared in reaction buffer (PBS with 0.02% Tween, 0.1% desialylated BSA, 1 μm Neuraminidase inhibitor) from 1:200 up to 1:25,600. Blocking solution was removed by suction with a vacuum manifold and 50 μl of prepared fetuin solutions were added in descending order to each well of a given column, with the highest concentration added to the top well and the lowest concentration added to the bottom. Plates were covered and incubated at 4ºC for exactly 1 hour, then washed 5X in ice-cold wash buffer (PBS 0.01% Tween) employing the following scheme for the volume of wash buffer utilized per washing step: 100μl, 200μl, 300μl, 200μl, 100μl. Fetuin solution and wash buffer was removed by aspiration using a vacuum manifold between all wash steps and plates were kept on ice throughout the process. After the final wash, 100 μl of substrate solution (0.01% tetramethylbenzidine (TMB), 1:1000 H_20_2 (from a 30% stock) in 0.05 M Sodium Acetate (pH 5.5)) was added to all wells and plates were incubated for 30 mins at room temperature. Reactions were stopped by the addition of 50 μl of 3% H_2SO_4 to the wells and absorbance was recorded at 450 nm on a standard plate reader. As an alternative to TMB, HRP was detected using ABTS (2,2'-Azinobis [3-ethylbenzothiazoline-6-sulfonic acid]-diammonium salt) reconstituted in 1 mL H_2O and diluted 1:1000 in sodium acetate substrate solution. ABTS-colourized plates were read at 405 and 416 nm after 15 and/or 30 minutes incubation. Results were imported to Microsoft Excel for analysis and background values based on mean absorbance readings of virus-free negative control (PBS) wells with each Fet-HRP dilution. Calculations of absorbance/Fet-HRP concentration (C), using 1000 arbitrary units as concentration for stock solutions, were made for each virus-coated well, and Scatchard plots of absorbance/C vs. absorbance were constructed. A best-fit-line to determine maximum absorbency (A_{max}) and Y-intercept (Y_o) was generated, and Fet-HRP dilutions resulting in a range of absorbencies from 0.1 to the beginning of the plateau were selected for use in subsequent direct binding assays. This was followed by virus titration experiments, where plates were coated with serial dilutions of stock virus that were subsequently incubated with a single Fet-HRP solution. Plots of background-corrected

absorbance versus virus dilution were generated, and the optimal virus dilution was determined as the maximal dilution of virus at the end of the absorbency plateau. With optimum Fet-HRP dilution range and virus concentration determined, assays were repeated and results of virus binding with both 3-Fet-HRP and 6-Fet-HRP were reported as affinity constants, or K_{aff}. This value was determined based on information from the scatchard plots by taking the ratio of Y_o/A_{max} for the particular sialylated Fetuin or SGP considered. The higher the K_{aff}, the stronger the binding.

14.5. Direct Binding Assays for Determination of Fine Differences in Receptor Specificity. The specificity of virus binding to receptor molecules with fine structural differences was characterized by assessing their binding to biotinylated soluble synthetic poly-N-(2-hydroxy- ethyl)acrylamide-based sialylglycopolymers (SGPs) (Lectinity Holding, Inc., Moscow, Russia), which contain 20 mol% of the specific sialyloligosaccharide linked to a 30-kDa carrier. The structures and designations of the glycan moieties of the eight SGPs utilized were as follows:

Structure	Designation
Neu5Acα2-3Galβ1-4GlcNAcβ	3'SLN
Neu5Acα2-3Galβ1-3GalNAcα	STF
Neu5Acα2-3Galβ1-4(6-O-HSO3)GlcNAcβ	6'Su-3'SLN
Neu5Acα2-3Galβ1-4(Fucα1-3)GlcNAcβ	SLe^x
Neu5Acα2-3Galβ1-4(Fucα1-3)(6-O-HSO3)GlcNAcβ	Su-SLe^x
Neu5Acα2-3Galβ1-3GlcNAcβ	SLe^c
Neu5Acα2-3Galβ1-3(Fucα1-4)GlcNAcβ	SLe^a
Neu5Acα2-6Galβ1-4GlcNAcβ	6'SLN

Two sets of the above SGPs, consisting of high molecular weight (1,500 kDa) and low molecular weight polymers (30kDa), were included for experimental purposes to accurately characterize viruses with higher or lower overall binding affinities. Experimental protocols, including incubation, washing, and developing steps, were as described for direct binding assays with HRP-labeled monosialylated fetuin preparation, with an important additional step. Here, following removal of SGPs and wash steps, 50 μl of Streptavidin-HRP prepared at a 1:400 dilution in reaction buffer was added to each well and incubated for one hour at 4°C. This was followed by the typical 5-step wash and subsequent addition of HRP substrate. Binding affinity constants, K_{aff}, were determined as described above.

14.6. Determination of Fetuin-HRP dilutions for Fetuin binding inhibition (FBI) assay. As an alternative to direct binding assays, the receptor binding affinity of viruses for glycans with fine structural differences was determined in a competitive assay by simultaneous incubation with non-labeled SGPs and Fetuin-HRP preparations. Titrations of two Fetuin-HRP preparations, designated as "2.2" (standard) and "39" (high avidity), were performed via direct binding assay with all virus isolates to determine optimal working concentration for use prior to initiation of binding inhibition assays. Procedures followed those described for Fet-HRP titrations for direct binding assays, and Scatchard Plots of results were generated. For each Fet-HRP dilution tested, the parameter α was then determined, representing the proportion of free binding sites remaining on the viral HA tested at each particular Fet-HRP concentration.

Alpha was calculated as follws: $\alpha = (A_{max} / A_{405}) / A_{max}$,

where A_{max} was determined from the trendline and A_{405} was the corrected absorbance value for the specific Fet-HRP dilution examined. By comparing alpha values and corresponding Fet-HRP dilutions for each of the experimental isolates, the dilution of Fet-HRP resulting in an alpha value close to 0.5 for the majority of viruses was selected as the appropriate dilution for use in FBI assays.

14.7. Fetuin Binding Inhibition (FBI) Assay. The experimental methods, including coating of plates, use of negative control wells, incubation steps and buffers utilized were as described for the direct binding assay, with important differences lying in the step where SGPs were used. For the FBI assay, serial two-fold dilutions of high or low molecular weight non-biotinylated SGPs were prepared in reaction buffer containing a constant concentration of Fetuin-HRP previously determined in titration experiments. SGPs utilized for FBI assays were identical in structure to those described for direct binding assays, with the distinction of being non-labeled. Negative (PBS-coated) and positive control (virus-coated) columns of Fetuin-HRP without SGPs were included to account for non-specific binding and maximum binding, respectively. Results were recorded and analyzed in Excel as described previously. Association constants for viruses with various SGPs in the FBI assay were determined as follows. First, the mean absorbency value in positive control wells (virus coated + Fet-HRP without SGP inhibitors) was determined, and denoted A_0. Using A_0 as a measure of 100% binding, the percentage of Fet-HRP binding (B) in wells containing SGP inhibitors was then determined for each well and SGP dilution: $B_i = 100 \times A_i / A_0$.

For wells with binding (B_i) values between 20% and 80%, the value of their affinity constant with the SGPs was calculated as follows: $K_{aff} = (100\text{-}B_i)/\alpha * B_i * C_i$,
where B_i reflects virus binding to Fet-HRP and a given SGP inhibitor concentration (C_i), and alpha represents the proportion of free receptor binding sites on the virus when incubated with the concentration of Fet-HRP used. Affinity constants for each of the SGPs resulting in 20-80% binding inhibition were averaged to determine a mean affinity constant, followed by determination and graphical representation of association constants Kass, where $K_{ass} = 1/K_{aff.}$

15. Analysis of Cell Surface Receptors by Mass Spectrometry.

15.1. Glycan Analysis of PDA cell lines. The glycan expression pattern on the surface of all experimental cell lines was determined via Matrix-assisted Laser Desorption/Ionization-Time of Flight (MALDI-TOF). Paramount to obtaining optimal results and avoiding contaminating carbohydrates, the use of plastic laboratory equipment was reduced to a minimum, with disposable Pyrex culture tubes containing Teflon inserts, sterile Pasteur pipettes and sterile glass micropipettes replacing traditional plastic ware. Additionally, all glassware was thoroughly cleaned with running water before use and dried in a 90°C oven. No detergents were used for cleaning of metal or glassware, powder-free gloves were worn at all times, and aluminum foil rather than paper towel was used to surface-dry instruments such as spatulas when necessary. A detailed description of solutions used and their preparation are found in Appendix 1.

15.2. Preparation of Cell Lysates. Confluent flasks of pancreatic cell lines, including AsPC-1, BxPC-3, CFPAC-1, MIA paca2, PANC-1 and HPDE6, were washed 5x with serum-free culture medium followed by PBS and then harvested by cell scraping in a small volume of PBS. Harvested cells were gently pelleted by centrifugation, flash-frozen in liquid nitrogen, and stored at 80°C until further analysis. Microfuge tubes containing frozen pancreatic cell line pellets were weighed and transferred to 15 mL falcon tubes. Assuming 80% of sample weight was water, an additional 4 volumes of ice-cold water was added to the tube, and samples were sonicated on ice in continuous mode for 10 seconds at 40 Amps followed by a 15 second pause on ice, and this procedure was repeated three more times. Based on the total sample volume, including the added volume of water plus 80% of the initial pellet weight, 2.67 volumes of methanol were added and samples were vigorously vortexed. Once samples reached room temperature 1.33 volumes of chloroform was added (based on original calculation, excluding the added methanol), tubes were vigorously mixed and then centrifuged to pellet the proteins

at 3000 RPM for 10 minutes. Supernatants were aspirated at a small amount of TRIS Buffer was added to the pellet. Tubes were transferred to the chemical fume hood and placed under a gentle stream of nitrogen for approximately 20 seconds to evaporate residual chloroform, stopping the process before the sample was completely dry.

15.3. Cleavage and blocking of disulphide bridges. To enhance glycoprotein cleavage by trypsin at a later step, disulphide bridges were split by reduction and blocked by carboxymethylation. Samples were dissolved in 500 µL of a 2 mg/ml DTT (Sigma, Cat. No. D-5545) solution, incubated for 60 minutes in a 37°C heating bath, and centrifuged. Five hundred microliters of a 12 mg/mL iodoacetic acid (Sigma, Cat. No. I-4386) solution were added to the sample and incubated for 90 mins at room temperature in the dark. Samples were then cleaned by dialysis by transferring homogenates into high quality Snakeskin® pleated dialysis tubing (Pierce, Cat. No. 68700) and dialysing for 24 hours in a cold room at 4°C. Dialysis buffer was changed with fresh buffer several times, most frequently in the first few hours. Samples were transferred into glass tubes, dialysis tubes were rinsed with deionized water and added to the tube, and the total volume was reduced to approximately 1 mL in a SpeedVac. The resulting volume was then transferred to clean screw capped glass culture tubes (Corning, Cat. No. 9949-13) covered with perforated parafilm and lyophilized overnight.

15.4. Cleavage into Glycopeptides. Lyophilized, carboxymethylated glycoproteins were cleaved into a mixture of peptides and glycoproteins via trypsin digestion to permit efficient release of N-glycans without the use of detergents in subsequent steps. A TPCK-Trypsin solution (Sigma, Cat. No. T-1426) was prepared in ammonium bicarbonate (Ambic) buffer at a concentration of 1 µg/mL and added to samples at a ratio of 50 µg trypsin per million cells in the original sample. Tubes were incubated for 14 hours at 37°C, briefly centrifuged, and the reaction was terminated by placing samples at 100°C for 5 minutes. The resulting glycopeptides were purified by reverse phase chromatography utilizing a conditioned Oasis® HLB Plus cartridge with step-wise elution using 5% acetic acid (20 mL), 20% isopropanol solution (4 mL), 40% isopropanol solution (4 mL) and 100% isopropanol (4 mL). The final three fractions collected and sample volume was reduced with a SpeedVac® and subsequently lyophilized in a clean screw-capped glass tube covered with perforated Parafilm.

15.5. Cleavage of N-glycans from glycopeptides. The separation of *N*-glycans from cleaved glycopeptides was achived via *N*-glycodase F digestion. The purified, lyophilized samples were dissolved in 150 µl of 50 mM Ambic buffer and incubated with 5U of *N*-Glycodase F (Roche, Cat. No.1365117) at 37°C for 20-24 hours. Samples were subsequently frozen, lyophilized, resuspended in 200 µl of acetic acid and purified using a Sep-Pak® C_{18} cartridge (Waters). Samples were eluted as described above, however only 5 mL acetic acid was utilized in the first elution step and all fractions were collected separately. Sample volumes were reduced by SpeedVac followed by lyophilization.

15.6. NaOH Permethylation. The purified *N*-glycans, contained in the acetic acid fraction, were permethylated prior to MALDI-TOF MS profiling. Briefly, 3 NaOH pellets per sample (Sigma, Cat. No. 221065) were placed in a dry mortar and ground with a pestle to form a powdery paste, and approximately 3 mL of Hi Dry™ anhydrous DMSO (Romil, Cat. No. D4281) was quickly added to the DMSO to form a slurry, mixing with a glass pipette. Between 0.5-1 mL of the resultant slurry was added to each lyophilized sample, followed by 0.5 mL of methyl iodide (Lancaster, Cat. No. 0347). Tubes were vigorously vortexed to mix, placed on an automated shaker for 20 minutes at room temperature, and reactions were quenched by slow drop-wise addition of ultra-pure H_2O with constant shaking until the exothermic reaction (fizzing) ceased. The volume was then topped to 5 mL with ultrapure H_2O, 2 mL of chloroform was added, and tubes were vortexed and then centrifuged to separate the mixture into two layers. The upper, DMSO-containing aqueous layer was removed and discarded, and the lower chloroform layer was washed several times with ultrapure H_2O. Following the final wash, the chloroform layer was dried under a gentle stream of nitrogen and lyophilized. Samples were then dissolved in a 1:1 mixture of methanol: ultrapure H_2O and purified through a conditioned Sep-Pak C_{18} cartridge through stepwise elution with ultrapure H_2O (5 mL) and then 3 mL each of 15%, 35%, 50% and 75% aqueous acetonitrile (Romil, Cat. No. H050). The 35%, 50% and 75% acetonitrile fractions were all collected in separate glass tubes, reduced in volume by SpeedVac and lyophilized.

15.7. Mass Spectrometric Analysis. Derivatized *N*-glycans were prepared for Mass Spectrometry as follows. Samples were dissolved in 10 µl methanol, and 1 µl of the sample suspension was then mixed with an equal volume of 2,5-dihydrobenzoic acid (DHB) (Sigma, Cat. No. G5254) prepared at a concentration of 20 mg/mL in 3 parts ultrapure H_2O:7 parts methanol. One microlitre of this mixture was spotted onto a clean stainless steel target on the MALDI-TOF plate and allowed to dry under vacuum. Mass Spectrometry was performed using MALDI-TOF technology and data were acquired on

a Voyager-DE STR mass spectrometer (PerSeptive Biosystems, Framingham, MA). All three acetonitrile fractions were analyzed for each sample.

15.8. Data Analysis and Interpretation. Analysis and annotation of MS data was performed with assistance from the GlycoWorkbench software suite (Ceroni *et al.*, 2008), with manual interpretation of data based on known masses of permethylated monosaccharides combined with likelihood of potential modifications being present on human-derived tissues.

16. Oncolytic effects of LP IAV *in vivo*. Twelve six-week-old female SCID mice were subcutaneously injected with 5 x 10^6 BxPC-3 cells in a volume of 100 µl into the right flank. Palpable tumours developed after eight days and mice were then randomly divided into two groups (n=6 per group), one group receiving an intratumoural inoculation of 2.4 x 10^4 pfu of H7N3 in a volume of 100 µL, and the other receiving 100 µL of PBS. The procedure was subsequently repeated 3, 5, and 7 days later for a total of four intratumoural inoculations per treatment group. The overall physical condition and behavior of the mice were monitored daily, and measurements of tumour size were performed on day 8, 15, 19 and 25 following initial injection. Caliper measurements of tumour sizes were taken at regular intervals throughout the experiment and the length (L) and width (W) were recorded to determine tumour volume using the formula: $V = L \times W^2 \times (\pi/6)$. At 25 days post-infection, mice were sacrificed and tumours were snap frozen for RNA extraction and IAV-specific rRT-PCR as described above. All experimental protocols employed were previously approved by the Italian Ministry of Health (130/2011).

17. Statistical Analyses. GraphPad PRISM® Version6 statistical analysis software was used for the analyses of experimental data. Results from *in vitro* growth curves, Annexin V expression, and caspase induction experiments were analyzed using a one-way ANOVA followed by Tukey's HSD post-hoc test for multiple comparisons, whereas MTT assay results were analyzed using a one-way ANOVA followed by Dunnett's post-hoc test. Data from experiments examining effects of different growth temperatures as well as *in vivo* experiments were analyzed using a two-way ANOVA plus Bonferroni post-test. *P*-values of ≤ 0.05 were considered statistically significant.

RESULTS

1. Expression of Alpha-2,3- and Alpha-2,6-linked sialic acid receptors on human PDA cell lines. To determine whether human PDA cell lines expressed receptors specific for avian IAVs, sialic acid-specific lectin staining was performed. Flow cytometry results demonstrated the presence of receptors for both human and avian influenza A viruses on the PDA cell lines examined, as well as the non-transformed pancreatic ductal line HPDE6 **(Figure 1)**. MDCK cells, included as a positive control for both receptors glycoforms, confirmed functionality of lectins used in the assay. The PANC-1 cells contained high levels of the alpha-2,3 receptors (specific for avian IAVs) but expressed a bimodal distribution of alpha-2,6 receptors (specific for human IAVs). Interestingly, AsPC-1 cells showed higher expression of alpha-2,3 receptors compared to alpha-2,6.

2. Sensitivity of Cell Lines to Influenza Virus Infection. To determine whether the PDA cell lines were susceptible to infection by IAV and could support viral replication, cells were infected with serial dilutions of a panel of highly pathogenic (HP) and low pathogenic (LP) viruses and monitored for cytopathic effect (CPE) over a period of 72 hours. Inoculum for all initial infections was supplemented with 0.05 μg/mL TPCK-trypsin, the maximum concentration tolerated by PDA cells without associated cytotoxicity. CPE was observed in all cell lines following infection with HP or LP isolates, though not all cells displayed CPE with all virus strains (**Table 2**). Due to their unusual growth characteristics CPE was difficult to discern in AsPC-1, MIA paca2 and PANC-1 cells. In all cases, however, virus re-isolation on MDCKs confirmed the presence of live virus in the supernatants, often at several logs above the endpoint dilution where CPE was originally observed.

3. IAV Replication Kinetics in Pancreatic cells. The replication kinetics of the virus panel over an extended period was examined in three cell lines; BxPC-3, HPDE6, and MDCK. BxPC-3 was chosen as the representative human PDA cell line based on results from the virus sensitivity experiments and compared with the non-tumoural HPDE6 cells to test whether IAVs showed an intrinsic tropism for cancer cells. PANC-02 cells were also included due to their murine origin and possible utility in future xenograft experiments. Using an MOI of 0.001 and a TPCK-trypsin concentration of 0.05 μg/mL, BxPC-3 infection led to successful virion production in the case of PR/8, H5N1 LP, and HP H5N1 and H7N1 isolates (**Figure 2**), however three other LP viruses (H7N3, H4N8, H7N7) were never re-

isolated over the 72 hour time course. These results closely mirrored the CPE observed, as infection with HP IAVs led to progressive destruction of the monolayer whereas LP IAVs did not cause any

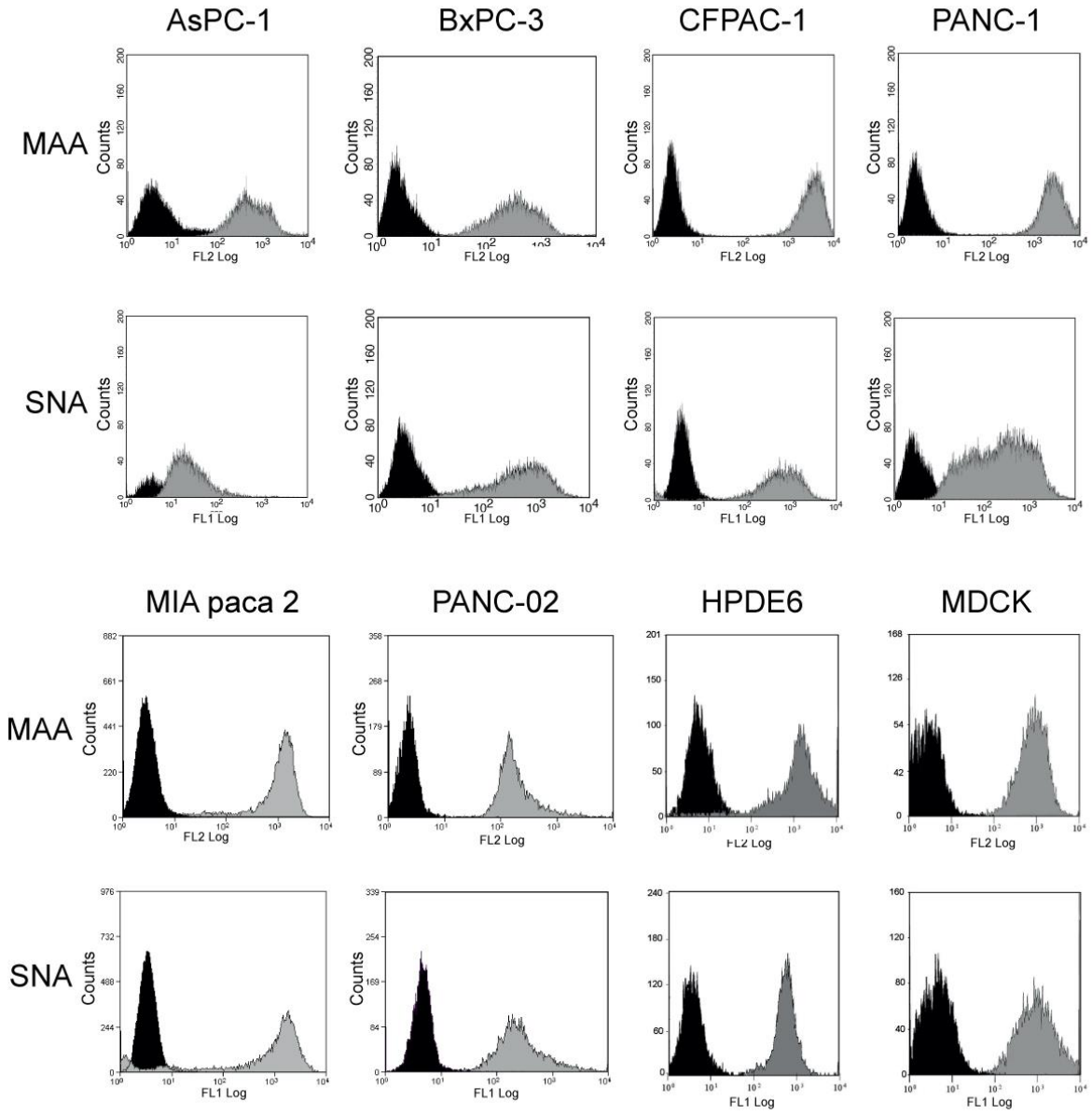

Figure 1. Expression of alpha-2,3 and alpha-2,6-linked SA receptors on pancreatic cell lines. Human PDA cell lines AsPC-1, BxPC-3, CFPAC-1, PANC-1 and MIA paca2, murine PDA line PANC-02 and human pancreatic ductal cell line HPDE6 were incubated with either fluorescein isothiocyanate-labeled Sambucus nigra (SNA) lectin or biotinilated Maackia amurensis (MAA) lectin II lectin followed by phycoerythrin-streptavidin to detect α-2,6 and α-2,3 SA, respectively. MDCK cells were included as positive controls. Samples were read on a BD FACScalibur with a minimum of 5,000 events recorded. Profiles in black, negative control (no lectin added); grey profiles, binding of indicated lectin.

Table 2. Cytopathic effect and virus isolation following infection of various PDA cell lines with highly and low pathogenic avian and human influenza viruses. Cells were infected in quadruplicate wells with 10-fold serial dilutions of stock virus and isolations on pooled supernatants performed on MDCK cells. Results indicate highest dilution at which CPE was observed either on initial infection at 72 HPI or following re-isolation in MDCKs. nd – no definitive cytopathic effect.

Virus Isolate	MDCK		BxPC-3		CFPAC-1		AsPC-1		PANC-1		PANC 02		MIA PACA-2		HPDE6	
	CPE	Isolation	CPE	Isolation	CPE	Isolation	CPE	Isolation	CPE	Isolation	CPE	Isolation	CPE	Isolation	CPE	Isolation
A/chicken/Egypt/1701/6 (H5N1 HP)	10^{-9}	10^{-9}	10^{-7}	10^{-7}	10^{-3}	10^{-4}	10^{-5}	10^{-6}	10^{-3}	10^{-3}	10^{-6}	10^{-6}	10^{-3}	10^{-8}	10^{-4}	10^{-6}
A/turkey/Italy/4580/99 (H7N1 HP)	10^{-6}	10^{-8}	10^{-5}	10^{-5}	10^{-5}	10^{-5}	10^{-5}	10^{-5}	10^{-3}	10^{-5}	10^{-3}	10^{-3}	10^{-3}	10^{-7}	10^{-4}	10^{-5}
A/mallard/Italy/3401/05 (H5N1)	10^{-6}	10^{-6}	10^{-4}	10^{-4}	10^{-3}	10^{-6}	10^{-2}	10^{-4}	nd	10^{-3}	10^{-2}	10^{-2}	10^{-2}	10^{-4}	10^{-2}	10^{-4}
A/turkey/Italy/2962/V03 (H7N3)	10^{-8}	10^{-8}	10^{-3}	10^{-4}	10^{-5}	10^{-6}	10^{-3}	10^{-6}	10^{-3}	10^{-4}	10^{-3}	10^{-3}	10^{-3}	10^{-5}	10^{-4}	10^{-5}
A/Puerto Rico/8/34(H1N1)	10^{-6}	10^{-6}	10^{-2}	10^{-5}	nd[c]	10^{-3}	10^{-3}	10^{-5}	nd	10^{-2}	10^{-2}	10^{-2}	nd	10^{-4}	nd	10^{-5}
A/canine/Florida/2004 (H3N8)	10^{-4}	10^{-4}	nd	10^{-2}	nd	10^{-2}	nd	10^{-2}	nd	10^{-1}	10^{-1}	10^{-1}	nd	10^{-3}	nd	10^{-3}
A/cockatoo/England/72 (H4N8)	10^{-6}	10^{-6}	10^{-2}	10^{-5}	10^{-2}	10^{-4}	10^{-4}	10^{-5}	10^{-2}	10^{-4}	-[a]	-	10^{-3}	10^{-3}	10^{-2}	10^{-3}
A/macaw/England/626/80 (H7N7)	10^{-7}	10^{-7}	10^{-4}	10^{-5}	10^{-2}	10^{-6}	10^{-4}	10^{-6}	10^{-3}	10^{-5}	-	-	10^{-2}	10^{-4}	10^{-2}	10^{-6}

a - not performed

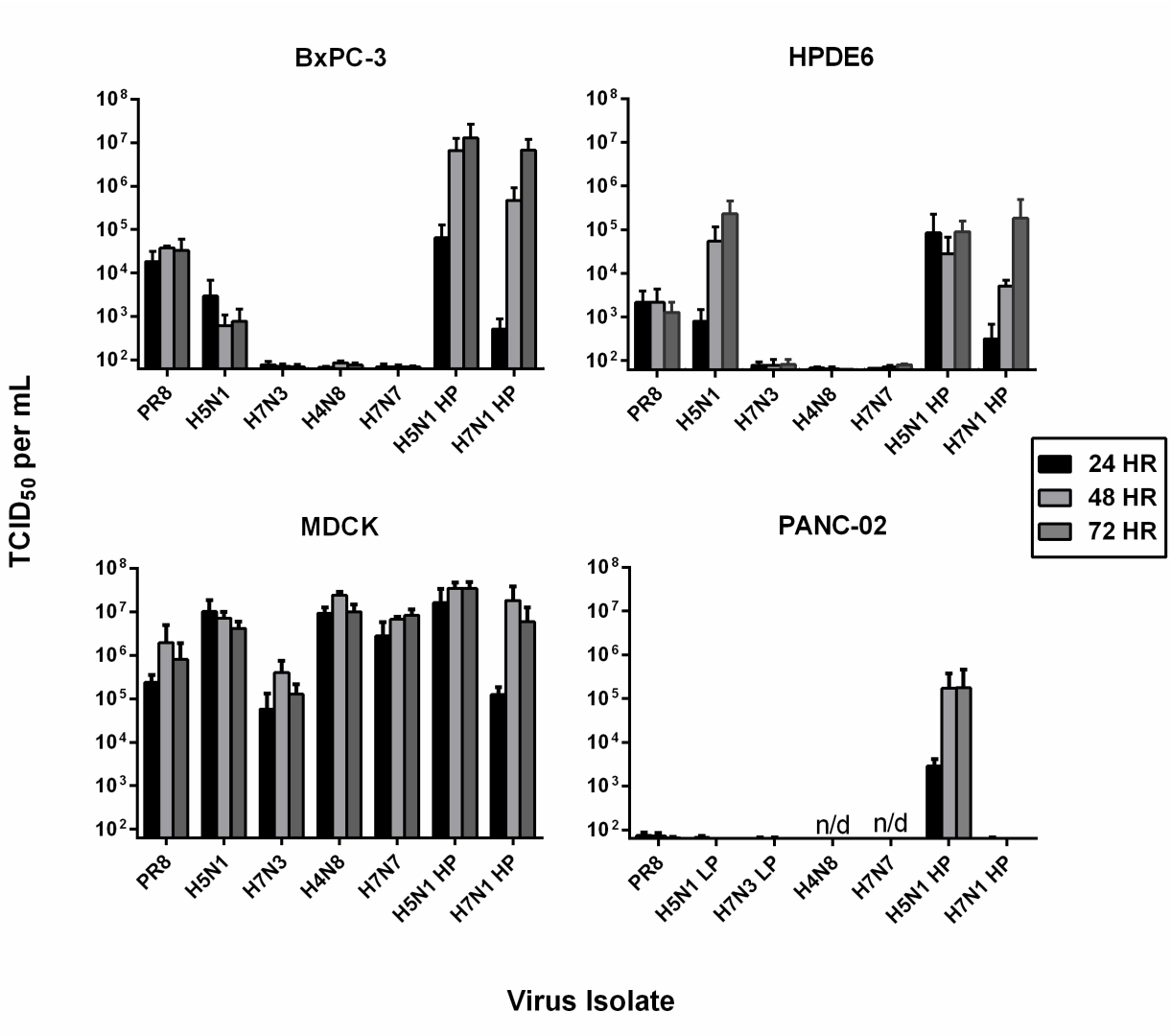

Figure 2. Replication Kinetics of influenza A viruses in BxPC-3, HPDE6, PANC-02 and MDCK. Cells were infected at an MOI of 0.001 pfu/cell and virus titres in infected supernatants were determined via the $TCID_{50}$ assay at 24 (black bars), 48 (light grey bars) and 72 (dark grey bars) hours post-infection. Results represent means plus standard deviation of three independent experiments of three replicate samples each. n/d = Not performed.

notable CPE at this MOI. Infection of BxPC-3 with PR/8 also led to productive infection as confirmed by virus isolation, though no CPE was observed and titres did not show a significant increase from 24 to 72 hours. In fact, this trend was observed for almost all trypsin-dependent viruses in all cell lines, where titres did not generally increase after 24 HPI, most likely due to the low TPCK-trypsin concentrations. Further testing of the H5N1 LP isolate, previously described as low pathogenic due to the absence of multi-basic residues in the HA cleavage site, showed an intermediate phenotype and ability to replicate to low levels even in the absence of exogenous trypsin (data not shown), thus explaining virus isolation results in the presence of low amounts of TPCK-trypsin. Results obtained in the non-transformed HPDE6 cell line were similar to those of BxPC-3, however for three of the four virus isolated titres were consistently lower (**Figure 2**). MDCK cells, which are considered the gold standard for *in vitro* replication of IAVs, supported the highest levels of replication compared to all cell lines tested. For all experiments, supernatants were also collected at 1 HPI and titrated. Values were used in growth curves to establish a baseline attributed to residual inoculum and were typically below or just at the limit of detection of the $TCID_{50}$ assay ($\leq 6.3 \times 10^1$). PANC-02, the murine PDA cell line, was the least permissive of all cell lines tested and thus was excluded from further studies.

4. Comparative Replication of influenza viruses at 33°C, 37°C, and 41°C.

To determine whether variations in virus titres observed between MDCKs and PDA cells could be attributable to sub-optimal temperatures for polymerase function, BxPC-3 and MDCKs were infected in parallel at three physiologically relevant temperatures for human and avian viruses; 33°C, 37°C and 41°C. A selection of 5 viruses representing HP and LP isolates were studied over a 72 hour time course. Replication kinetics of avian viruses followed the general trend of reaching higher titres at earlier time points when incubated at 41°C or 37°C compared to 33°C, in accordance with their host species of origin (**Figure 3**). Infection of MDCKs resulted in statistically significant differences in titres of H5N1 LP at 24 hours when comparing titres achieved with increasing temperatures ($p \leq 0.01$), and similarly with H7N1 HP at 48 hours ($p \leq 0.01$ for 37°C vs. 33°C), though in BxPC-3 there were no significant differences observed. This was also the case for the human PR/8 isolate, which showed an overall preference for 37°C, especially at 24 HPI, though differences were not statistically significant. Interestingly, all avian IAVs tested were able to efficiently replicate in the PDA cell line BxPC-3 even at 37°C, suggesting that their replication in human PDA cells might not be subjected to host-dependent temperature sensitivity. Therefore, considering overall good titres achieved at 37°C, it was deemed optimal for *in vitro* experiments with BxPC-3 and was used in all further studies.

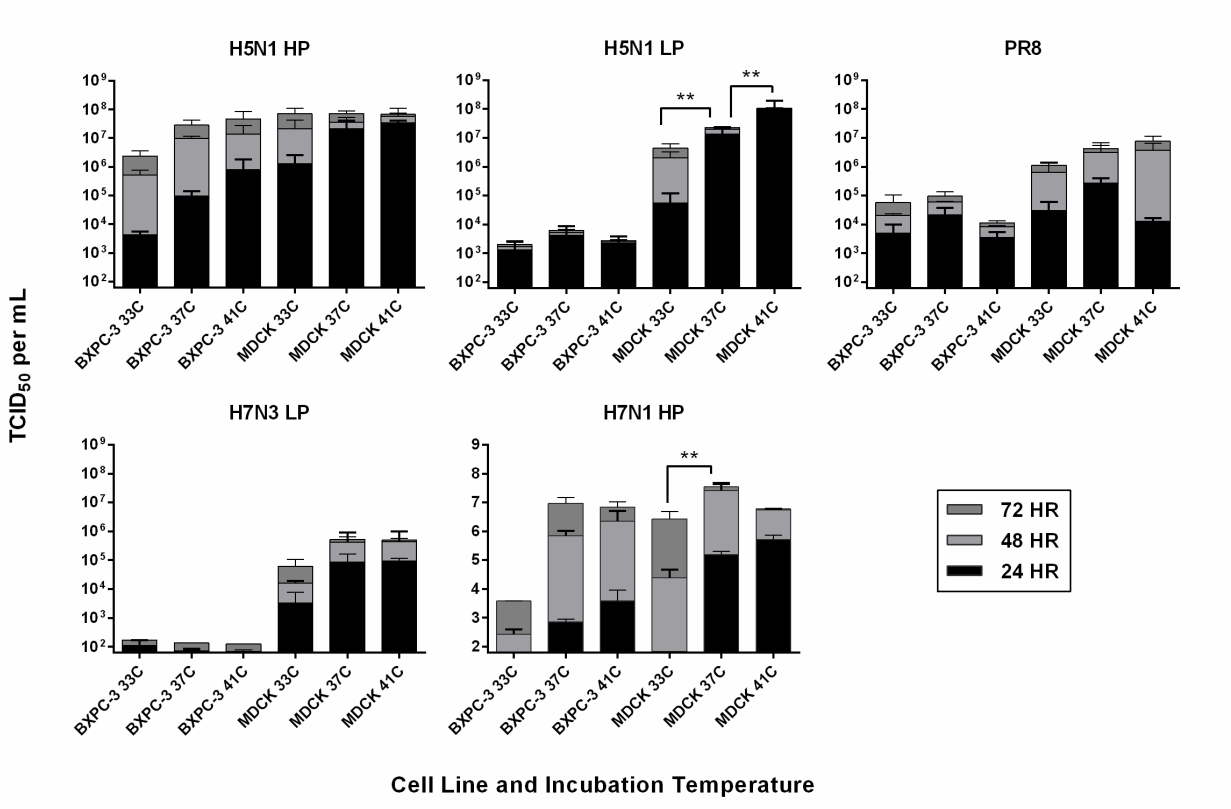

Figure 3. Comparative replication kinetics of influenza isolates at 33°C, 37°C and 41°C. BxPC-3 and MDCKs were infected at an MOI of 0.001 with the viruses indicated in the absence (for HP isolates) or presence of 0.05 μg/mL TPCK-Trypsin. At 24, 48 and 72 HPI supernatants from three independent wells were harvested and titrated via $TCID_{50}$ assay on MDCKs in the presence of 1 μg /ml TPCK-trypsin. Values shown are means and standard deviations from two independent experiments (**$p < 0.001$ at 24 HPI as determined by two-way ANOVA).

5. Viral RNA Replication Kinetics in PDA cells. Given the inability to isolate LP IAVs from PDA cells at a low MOI, we wanted to ensure that this was not due to a lack of effective genome replication. All cell lines were infected with the panel of LP isolates as well as PR/8 at a higher MOI of 0.1 in order to analyze replication kinetics over a 24 hours period. Active replication of viral RNA was noted for all viral isolates in all cell lines based on rRT-PCR results, in which CTs at 16 HPI were decreased compared to cultures sampled at 1 HPI **(Figure 4)**. The lack of changes in CT values from 16 to 24 HPI strongly suggests that replication was limited to a single cycle, most likely due to the low levels of TPCK-trypsin. When comparing different viruses, replication of the H7N3 isolate was overall highest in all of the cell lines tested while H4N8 generally presented lowest levels of replication. Similar trends were also observed for all isolates in MDCK cells, with no changes in CT between 16 and 24 HPI.

6. Assessment of cell proliferation post-infection. The MTT assay measures tetrazolium reduction by metabolically active and proliferating cells, and therefore is used as an indicator of cell viability (Riss *et al.*, 2013). Given the results of the experiments showing death of PDA cells infected with high concentrations of virus (**Table 2**), and the demonstration of active viral RNA replication in all PDA cell lines infected with LP IAVs (**Figure 4**), we were interested in examining the intensity of virus-induced cell death in the various PDA cell lines and possible variations between virus isolates. All pancreatic cell lines were infected with PR8 and the complete panel of LP avian IAVs used in previous experiments at MOI=1 to ensure all cells were infected upon analysis. MTT assay results showed a general agreement with observations from initial experiments on cell line sensitivity to the panel of virus isolates, with PANC-1 displaying highest levels of resistance whereas BxPC-3 and CFPAC-1 showed overall highest sensitivity to virus-induced cytotoxicity of the PDA cell lines (**Figure 5**). Furthermore, the H7N7 and H7N3 isolates, whose RNA replication rates were the highest among the viruses tested, consistently caused the greatest loss of cell viability across the panel of cell lines tested, with highly statistically significant differences compared to controls ($p<0.01$ - $p<0.0001$). The H7N3 isolate in particular showed the greatest innate affinity for the PDA cells, causing higher losses of cell proliferation in BxPC-3 and CFPAC-1 cells compared to the normal ductal HPDE6 cells ($p<0.0001$). Of note, absorbance values did not necessarily correlate with visible cell damage as H7N3 infection of CFPAC and BxPC-3 cells resulted in massive CPE and complete destruction of the monolayer yet results indicated that 30% of proliferative activity was retained (**Figure 5**).

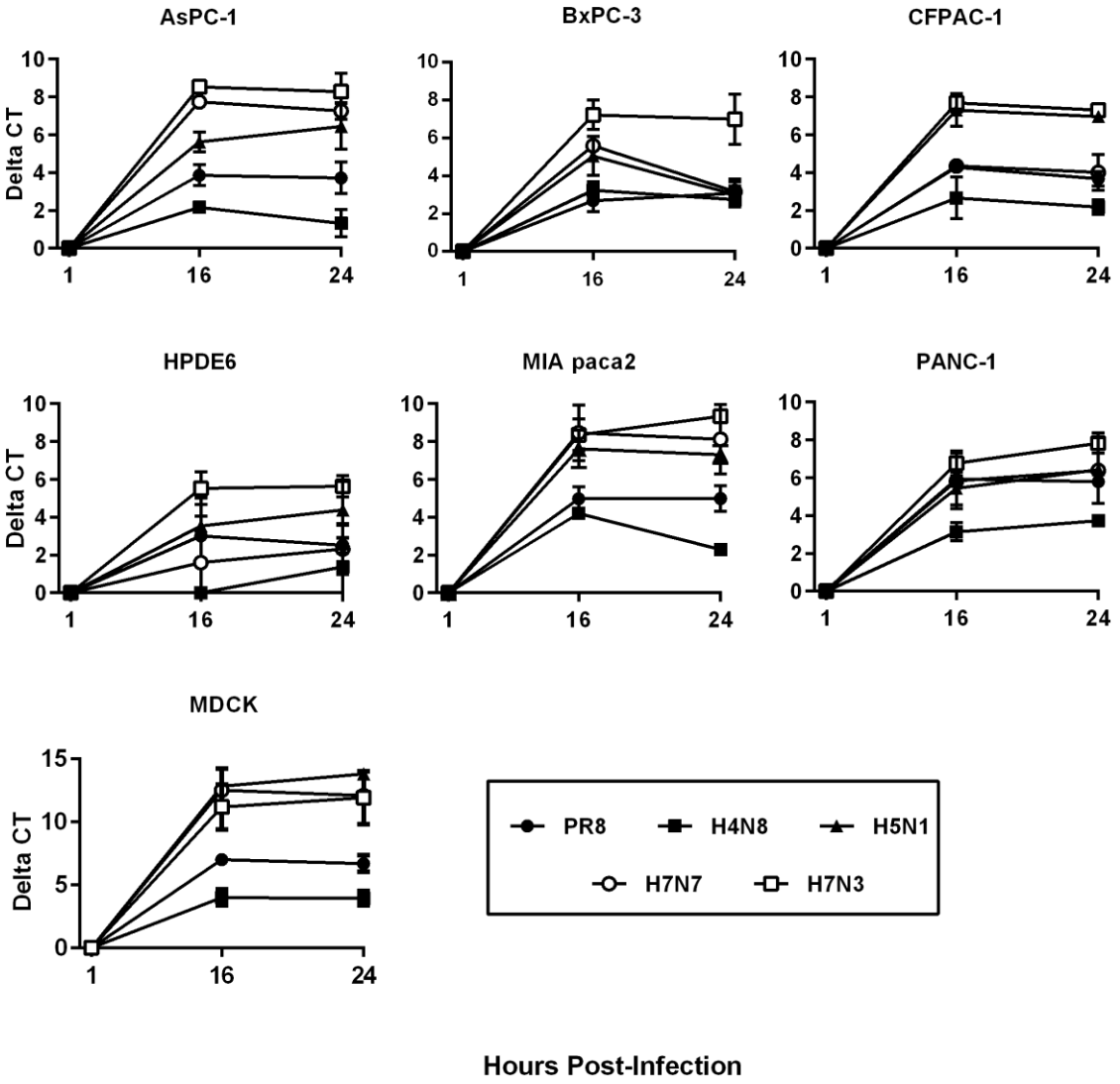

Figure 4. Viral RNA replication kinetics in infected PDA cells. AsPC-1, BxPC-3, CFPAC-1, MIA paca2, PANC-1, HPDE6 and MDCK cells were infected with a panel of low pathogenic influenza viruses at MOI = 0.1. Supernatants and cell pellets were harvested together at T=1, 16 and 24 HPI and extracted RNA was amplified using viral matrix gene-specific r RT-PCR. Data represent means plus standard deviation of triplicate samples indicating change in CT values from T=1 HPI.

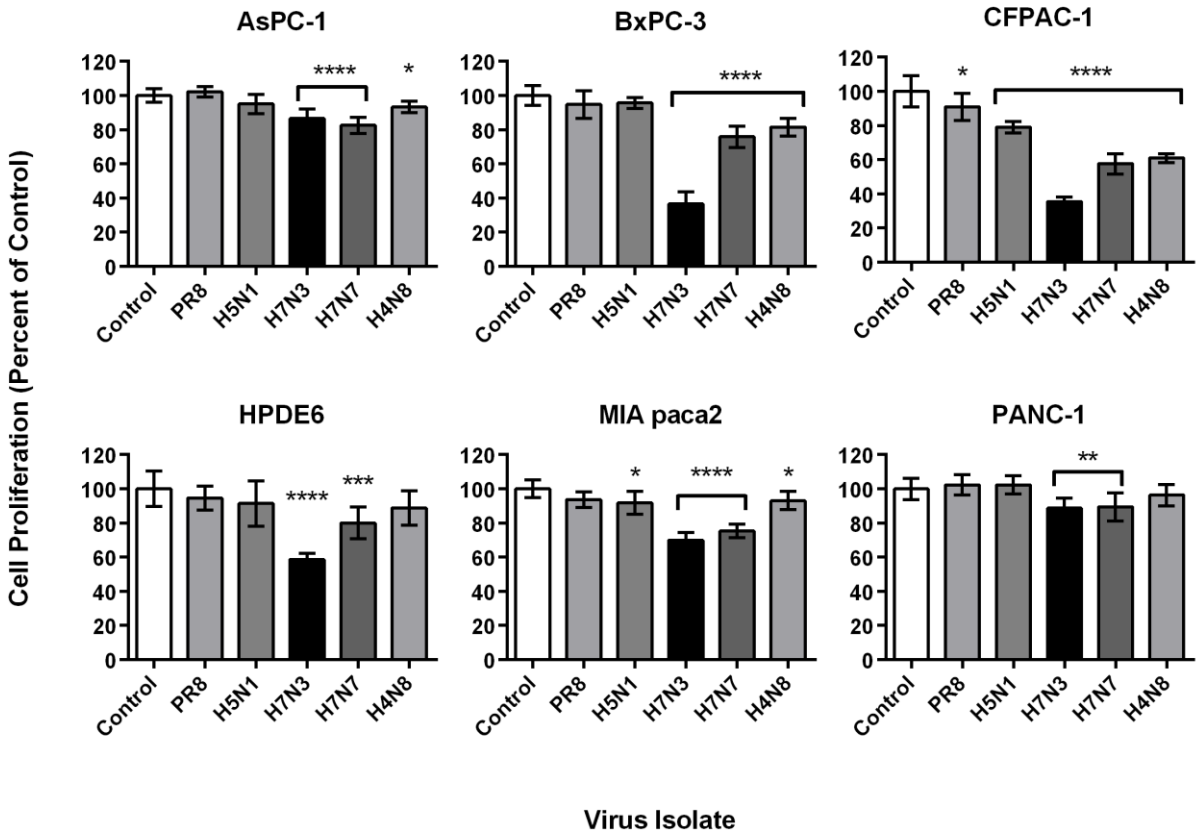

Figure 5. PDA cell proliferation following influenza A virus infection. AsPC-1, BxPC-3, CFPAC-1, MIA paca 2, PANC-1, and the non-transformed HPDE6 cells were infected with a panel of low pathogenic influenza viruses at an MOI of 1 and analyzed for cell proliferation at 24 HPI via MTT assay. Absorbance readings at 570 nm corrected for 690nm have been normalized to mock-infected controls. Results shown represent means plus standard deviation of two independent experiments of four replicates each, with statistical significances indicated for virus-infected cells from mock infected controls based on one-way ANOVA followed by Dunnett's post-hoc test (*$p < 0.05$, **$p < 0.01$,***$p < 0.001$, ****$p < 0.0001$).

7. Induction of Apoptosis following Influenza virus infection. To build on results observed in MTT assays and examine the mode of cell death induced, the ability of IAVs to induce apoptosis in PDA cells was assessed following infection at an MOI of 1. Engagement of the apoptotic program was assessed by Annexin V binding and flow cytometry at 16 and 24 HPI. As a positive control, cells were subject to a high concentration gemcitabine-cisplatin (gem+cisp) treatment, selected based the fact that gemcitabine is the standard therapy for PDA and cisplatin has been proposed for use in combination therapy. Levels of apoptosis were highly variable between cell lines and virus isolates, ranging from only 5% of H7N7-infected PANC-1 cells to over 60% of H7N3-infected BxPC-3 cells by 16HPI **(Figure 6)**. BxPC-3 were the most sensitive among the PDA cell lines to IAV-induced apoptosis, followed by AsPC-1, CFPAC-1, MIA paca 2 and PANC-1, which was the most resistant cell line. Interestingly, PR/8-induced far less apoptosis compared to LP avian IAVs, which often were more powerful than gem+cisp treatment. Consistent with results from MTT assays, the H7N3 isolate was by and large the most potent inducer of apoptosis in all of the PDA cell lines examined (**Figure 6**).

8. Influenza virus-induced caspase activation. Given that influenza may cause apoptosis via both intrinsic and extrinsic pathways (Lowry, 2003; Zamarin *et al.*, 2005), and that the disruption of both pathways has been documented in different cancers (Fulda & Debatin, 2006), it was important to test the mechanism of IAV-induced cell death in PDA. As BxPC-3 represented the most sensitive PDA cell line while HPDE6 were largely insensitive to virus-induced apoptosis, we investigated whether different apoptotic effector mechanisms were at play and were differently engaged by different virus isolates. Results of immunocytochemistry analyses showed a marked induction of caspase-3 in experimentally infected BxPC-3 cells, with a significantly higher level ($p \leq 0.0001$) induced by H7N3 infection (50.72% positive) when compared to PR/8 (10.14%) or gemcitabine & cipstlatin combination (8.92%) **(Figure 7)**. Consistent with the Annexin V results, infection of HPDE6 with influenza viruses resulted in much lower caspase 3 induction (13.52% with H7N3 and 6.12% with PR/8), which was lower than that induced by gemcitabine and cisplatin (17.32%, $p \leq 0.0001$). To differentiate between intrinsic and extrinsic pathways, cells were stained with anti-Caspase 8 and 9 antibodies, respectively. BxPC-3 infected with H7N3 showed activation of both caspases, however positivity for Caspase 9 was consistently higher than Caspase 8 (46.1 vs 21.7% at 16 HPI and 72.02 vs 38.1% at 24HPI), suggesting a stronger involvement of the intrinsic-mitochondrial pathway. With the PR/8 virus, however, twice as many cells were positive for Caspase 8 than caspase 9 at 16 HPI, suggesting that the extrinsic apoptotic pathway is was preferentially engaged by this virus.

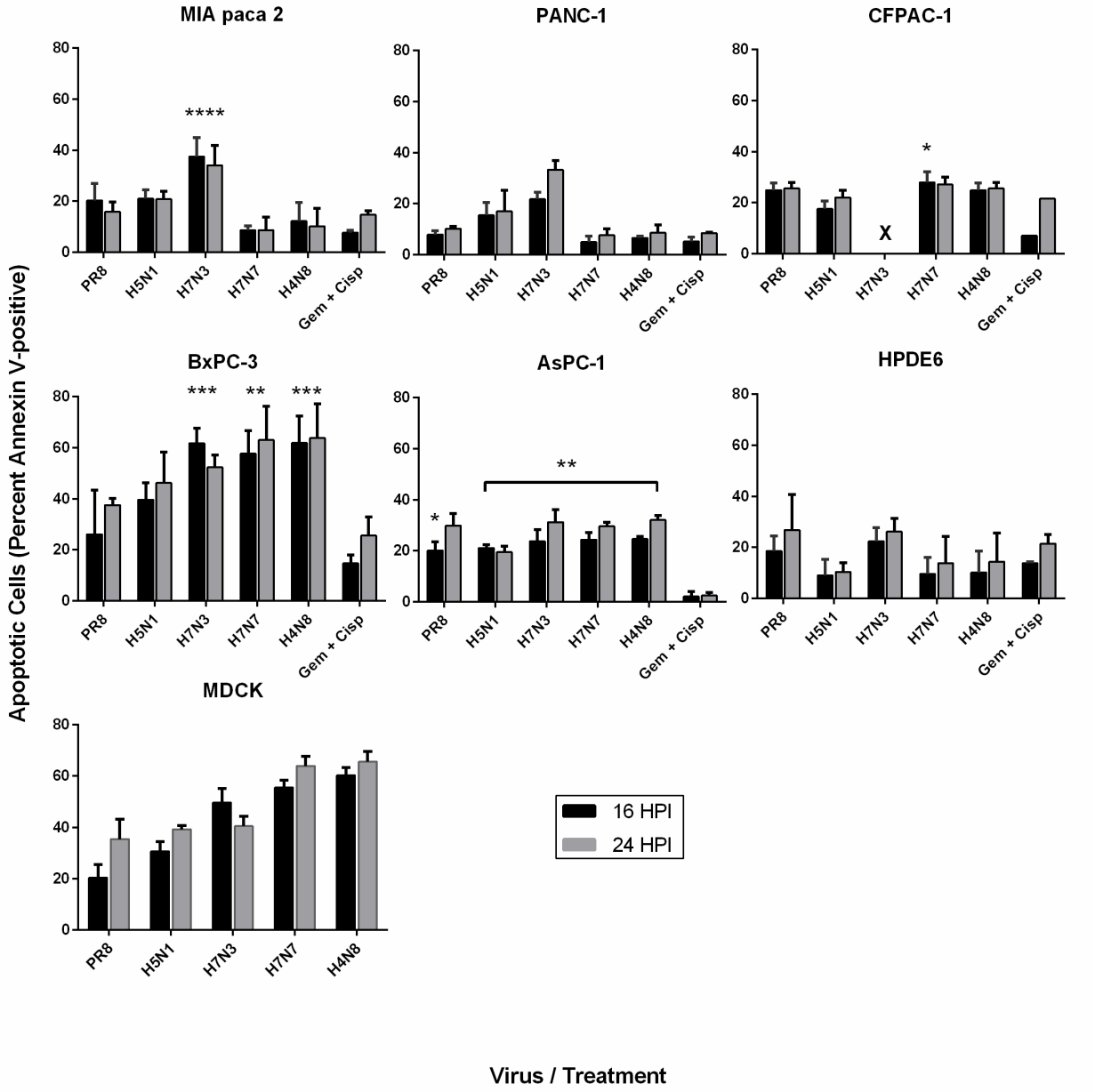

Figure 6. Comparative induction of apoptosis in PDA cells following infection with influenza A virus. Cells infected at MOI=1 with IAV or cultured with gemcitabine (2 mM) plus cisplatin (0.8μM) were assessed for induction of apoptosis at 16 HPI (black bars) and 24 HPI (grey bars) by Alexa Fluor 647-labelled Annexin V binding and flow cytometry. Results are normalized to uninfected controls and represent means plus standard deviation of two (Gem + Cisp treatment) or three (virus infections) independent experiments. Statistically significant differences between virus-induced and Gem + Cisp-induced apoptosis at 16 HPI are indicated (*$p < 0.05$, **$p < 0.01$,***$p < 0.001$, ****$p < 0.0001$). Note - Severe cell death induced in H7N3-infected CFPAC-1 cells (x) prevented proper Annexin V cell labeling at time points examined.

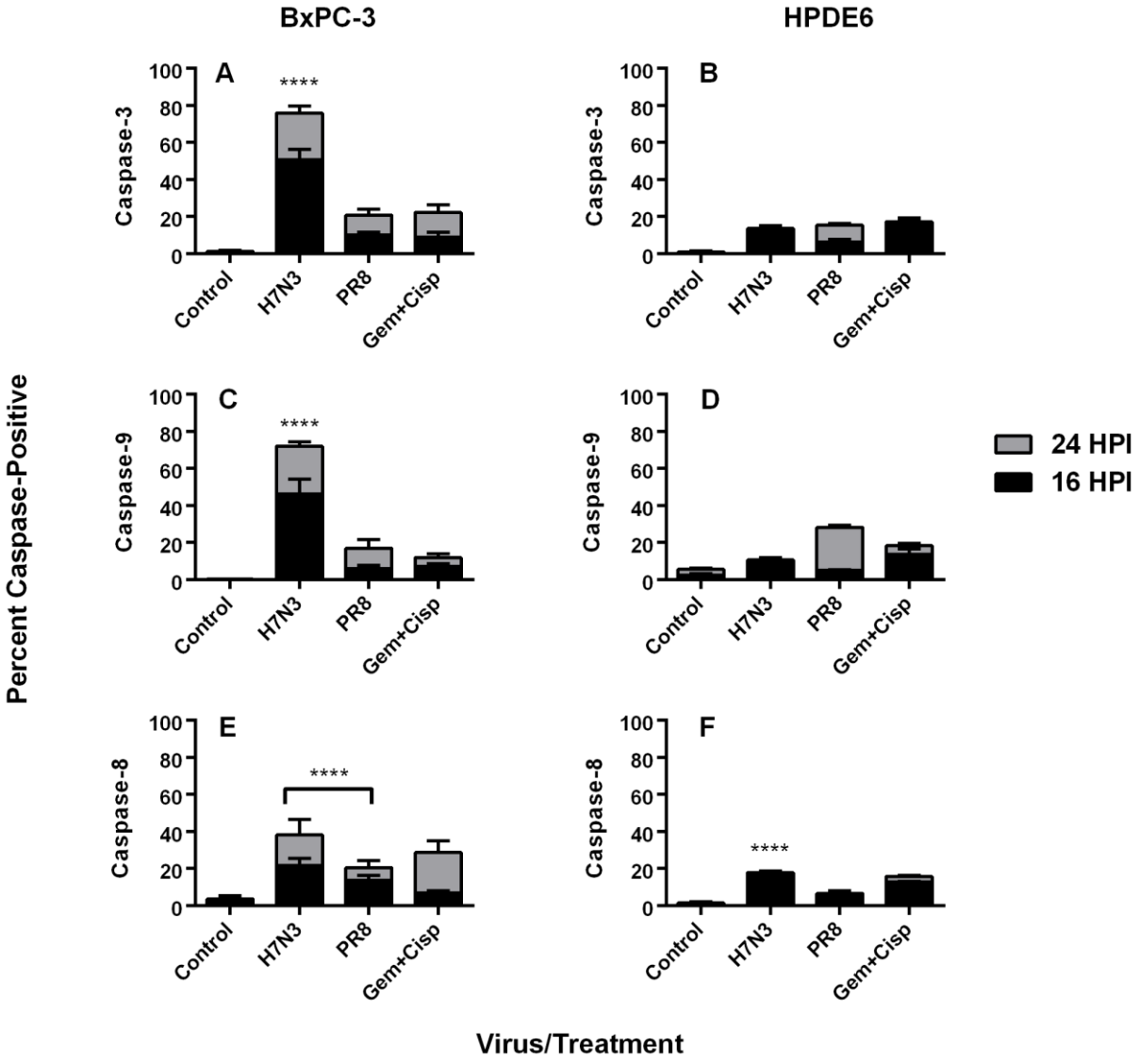

Figure 7. Caspase induction in influenza A virus infected cells. Semi-confluent monolayers of BxPC-3 and HPDE6 cells grown on glass chamber slides were infected with A/turkey/Italy/2602/2003 (H7N3) or A/PR/8/34 (H1N1) at an MOI of 1 and tested by immunocytochemistry for expression of cleaved caspase-3 (A + B), caspase-9 (C + D) and caspase-8 (E + F). Gemcitabine (2 mM) and cisplatin (0.8 μM) were included as positive controls. Results are means plus standard deviations for 10 repeat counts of 500 cells each, with significance shown for virus compared to gem+cisp at 16 HPI (**** $p<0.0001$).

9. Binding Affinities of Experimental Isolates to sialic acid glycoforms. To determine the overall binding affinities of experimental isolates to standard human or avian receptor glycoforms, direct binding to HRP-labeled fetuins expressing either α-2,3 (3-Fet-HRP) or α-2,6-linked sialic acids (6-Fet-HRP) was measured via solid phase binding assays. Three experimental isolates were selected for characterization based on high RNA replication rates and strong induction of apoptosis in PDA cell. Binding results from these assays showed that all three viruses bound with highest affinity to 3-Fet-HRP, in accordance with their avian origin (**Figure 8**). Surprisingly, the H7N7 isolate demonstrated the ability to bind alpha-2,6-linkages, suggesting possible interaction with human receptors.

To understand the receptor preferences of these viruses beyond the type of sialic acid linkage, binding assays were performed using synthetic polymers containing structural modifications to the glycan core, including sulfation, fucosylation, and alternative underlying sugars. Initially all experiments were repeated using both standard and high molecular weight polymers, and additionally, binding was assessed both directly and through an indirect (Fetuin binding inhibition, FBI) assay. Early results indicated that viruses had generally good binding affinities and therefore high molecular weight polymers were not required. When results from direct and indirect binding assays were compared, it was evident that direct binding assays produced highly variable results in that the H7 isolates did not appear to exhibit binding properties typical to that subtype and further the control viruses showed binding patterns different to previous published results (**Supplementary Figures 1-3**). Results from FBI assays using non-labelled polymers proved to be reproducible and produced results that fell in line with those from other publications. The H4N8 virus showed strongest binding to STF, a galactosamine-containing glycan with no additional sulfate or fucose residues to the glycan core. The virus had no particular predilection for sulfate, however the presence of fucose negatively impacted virus binding as seen by the difference in K_{ass} for 3'SLN and SLe^x (**Figure 9**). Both H7N7 and H7N3 displayed preferential binding to sulphated polymers, with association constants at least 3-fold higher when comparing Sulfated 3'SLN to its non-sulfated form and at least 5-fold higher to Su-Sle^x than Sle^x (**Figures10-11**). Both viruses also showed no appreciable preference or inhibition by fucosylated glycans, as association constants were quite similar for 3'SLN and Slex as well as Sle^c and Sle^a. Of note, unlike observations from direct binding assays, the H7N7 had no detectable interaction with the a-2,6-linked glycan (6'SLN) in the FBI assay.

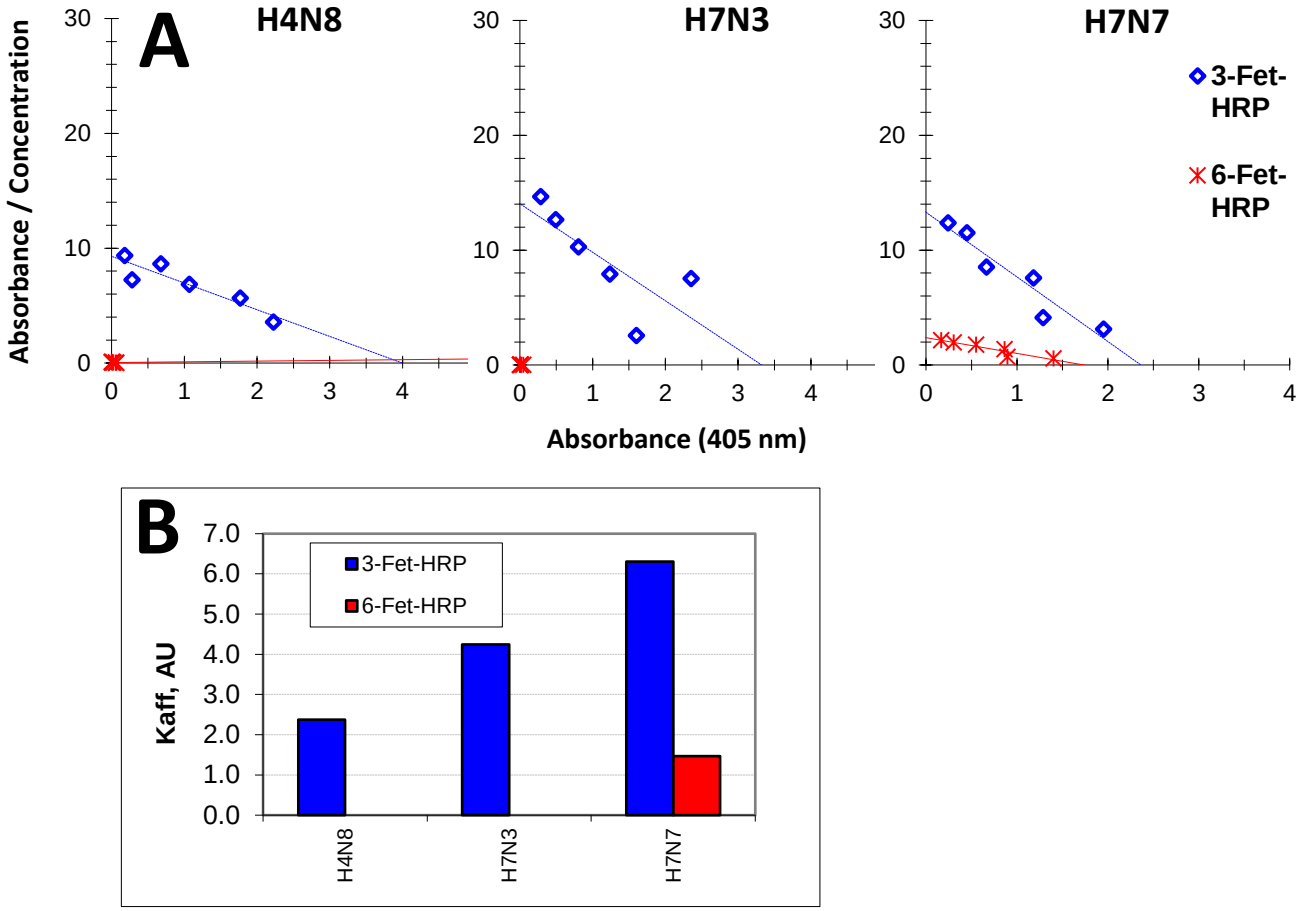

Figure 8. Binding affinities of A/turkey/Italy/2962/2003 (H7N3), A/cockatoo/England/72 (H4N8), A/macaw/England/626/80 (H7N7) to α-2,3 and α-2,6-linked sialic acids determined by direct binding assays. A) Scatchard plots for the binding of 3-Fet-HRP (a-2,6-linked) and 6-Fet-HRP (a-2,6-linked) to the experimental isolates and B) Virus binding affinity (Kaff, in arbitrary units) calclutated from Scatchard Plot data. Results are from one of three representative experiments.

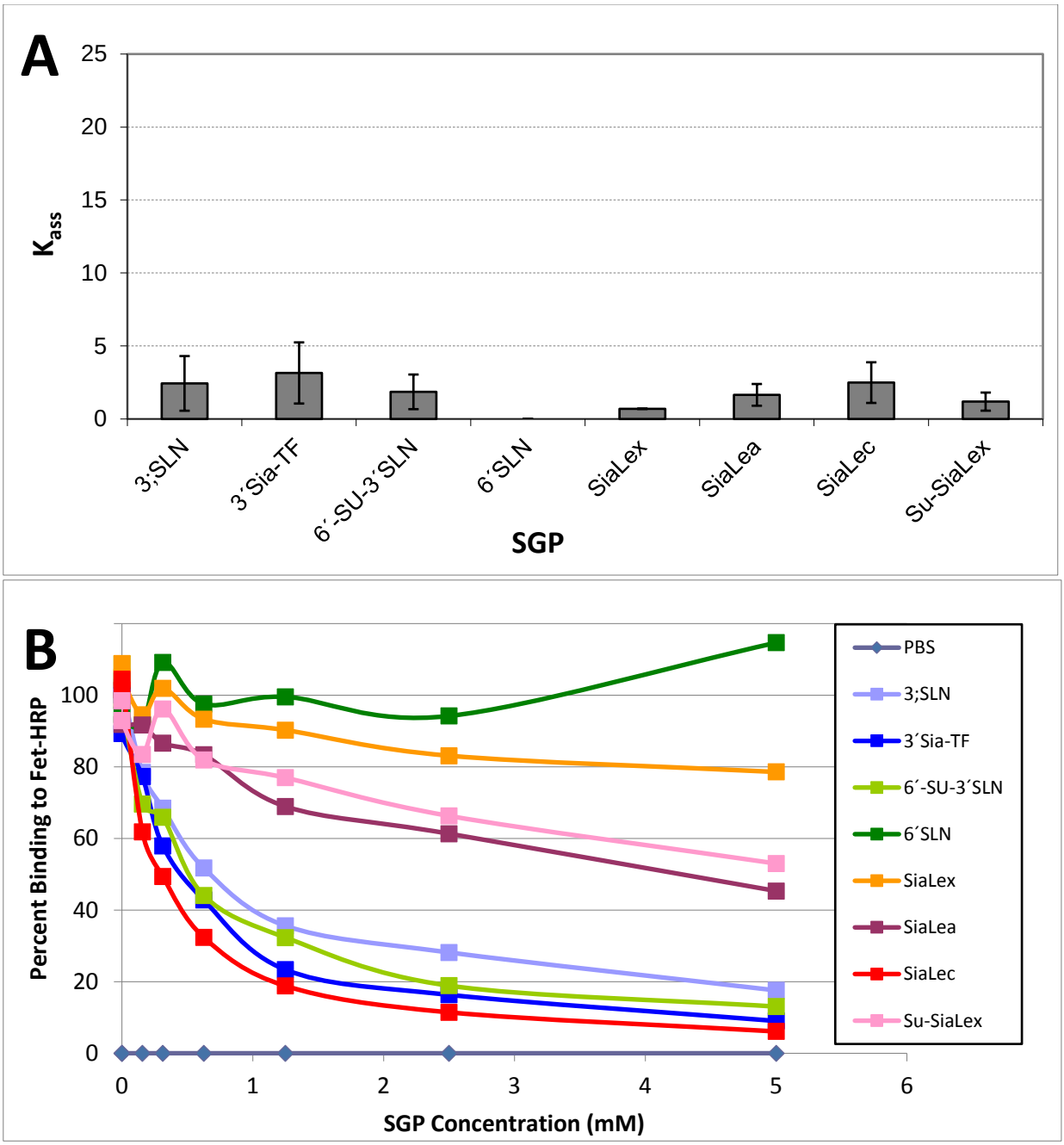

Figure 9. Binding affinity of A/cockatoo/England/72 (H4N8) to sialylglycopolymers. A)Association constants of bound virus with low molecular weight synthetic unlabelled sialylglycopolymers (SGPs) determined by Fetuin binding inhibition assay. Serial two-fold dilutions of unlabeled SGPs starting from 5 μM were prepared in a 1:1000 working dilution of standard Fet-HRP, with association constants (Kass) reflecting the ability of a particular SGP to inhibit binding to Fet-HRP. B) Graphical representation of virus binding to Fet-HRP in the presence of each SGP. Results shown are from one of three representative experiments.

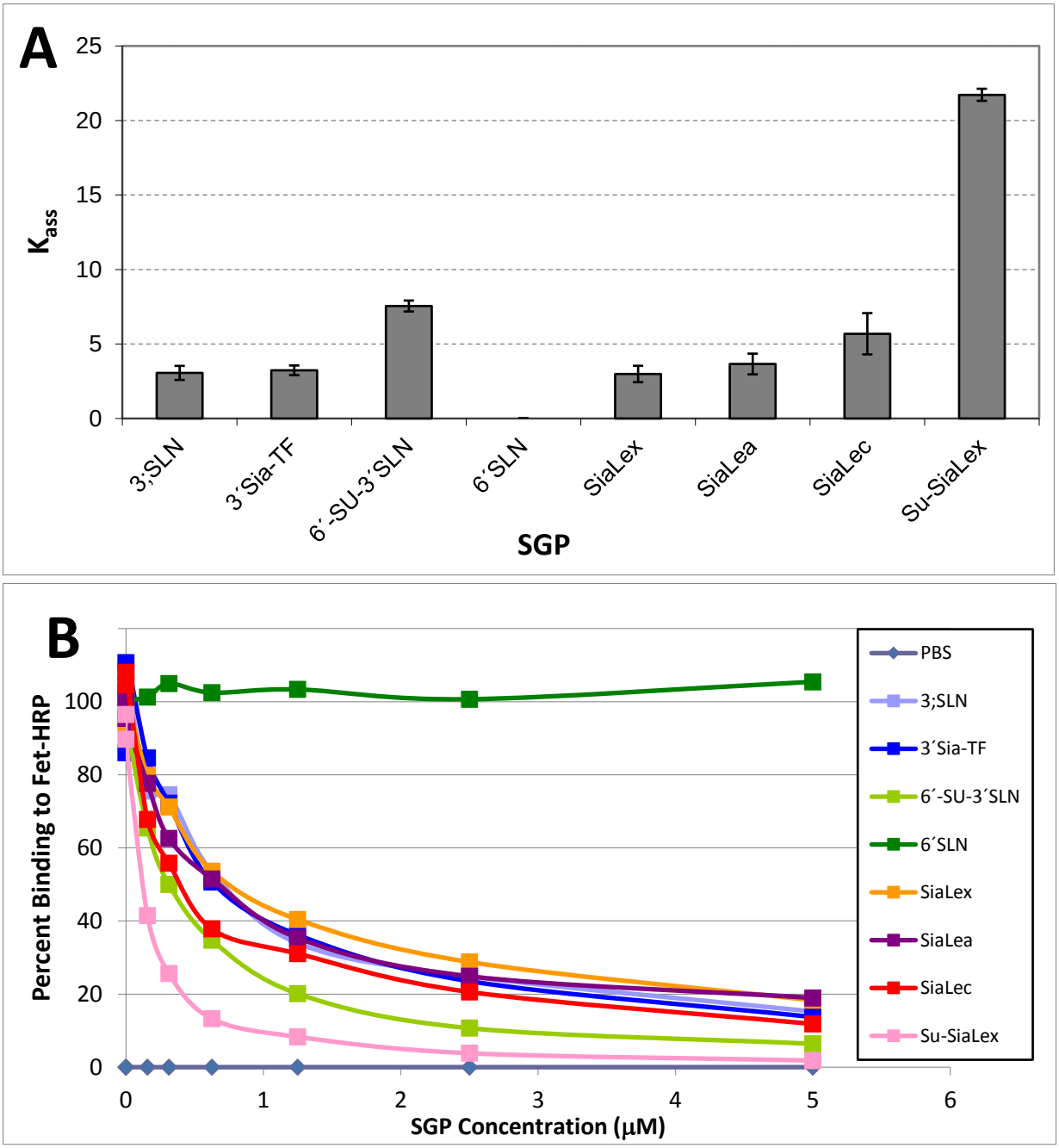

Figure 10. Binding affinity of A/macaw/England/626/80 (H7N7) to sialylglycopolymers. A)Association constants of bound virus with low molecular weight synthetic unlabelled sialylglycopolymers (SGPs) determined by Fetuin binding inhibition assay. Serial two-fold dilutions of unlabeled SGPs starting from 5 µM were prepared in a 1:1000 working dilution of standard Fet-HRP, with association constants (Kass) reflecting the ability of a particular SGP to inhibit binding to Fet-HRP. B) Graphical representation of virus binding to Fet-HRP in the presence of each SGP. Results shown are from one of three representative experiments.

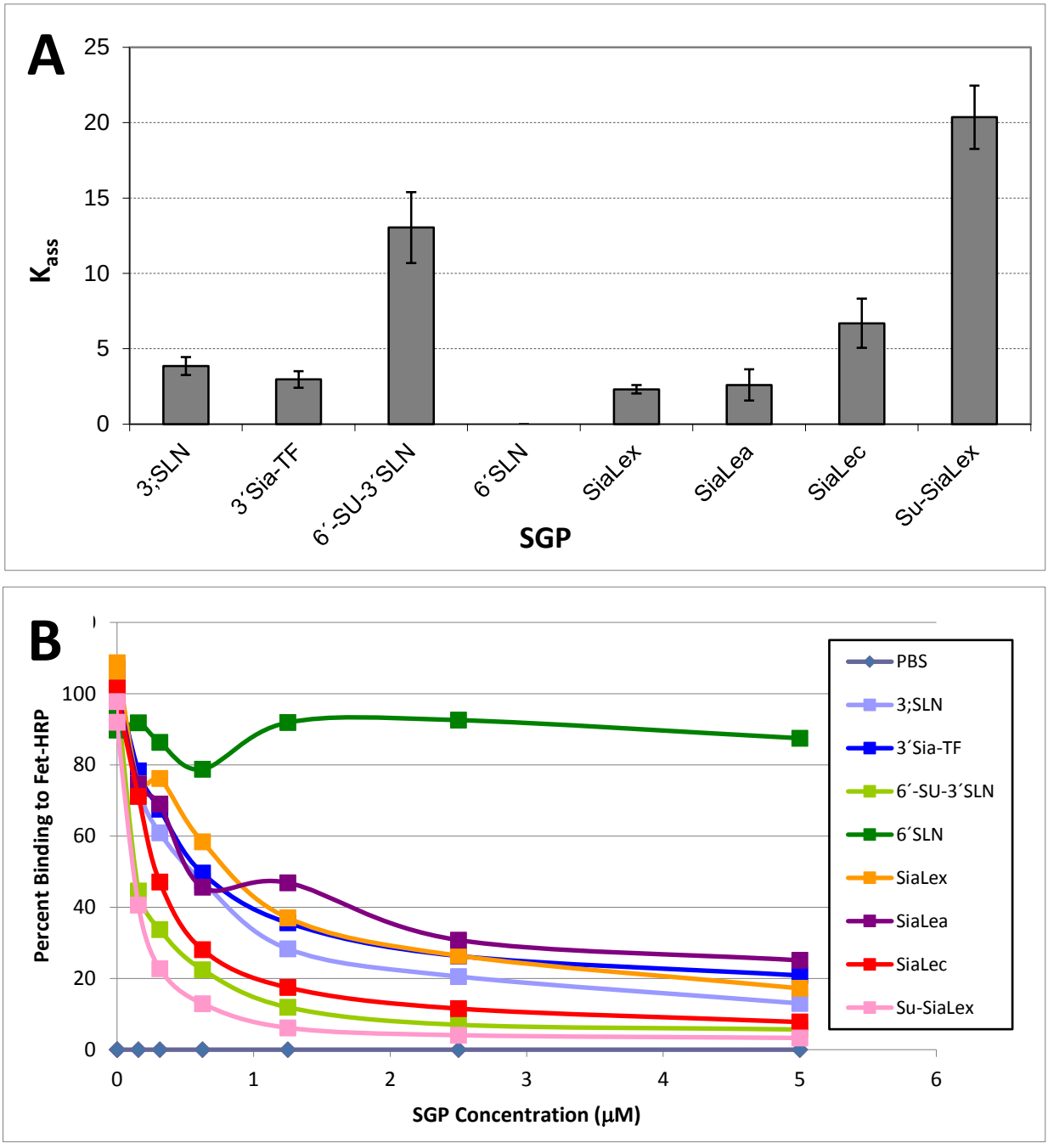

Figure 11. Binding affinity ofA/turkey/Italy/2962/2003 (H7N3) to sialylglycopolymers. A)Association constants of bound virus with low molecular weight synthetic unlabelled sialylglycopolymers (SGPs) determined by Fetuin binding inhibition assay. Serial two-fold dilutions of unlabeled SGPs starting from 5 µM were prepared in a 1:1000 working dilution of standard Fet-HRP, with association constants (Kass) reflecting the ability of a particular SGP to inhibit binding to Fet-HRP. B) Graphical representation of virus binding to Fet-HRP in the presence of each SGP. Results shown are from one of three representative experiments.

10. Glycan profiling of PDA cells by Mass Spectrometry. In an attempt to deduce the specific glycan profile of pancreatic cell lines used in the present research, cells underwent a rigorous series of treatments and purification steps to isolate *N*-glycans for MALDI-TOF profiling. *O*-glycans were similarly purified however poor sample quality made them unsuitable for analysis. MALDI-TOF was performed on the 35%, 50% and 75% acetonitrile fractions of permethylated *N*-glycans obtained from the final purification step, and fractions containing the highest concentration of glycans, typically the 35% or 50% fractions, were analyzed for specific structures using GlycoWorkbench software suite. For BxPC-3, HPDE6 and AsPC-1 cells, a good quality final product was obtained and Mass Spectrometry profiles revealed detailed glycan data with reads of up to m/z of approximately 3500 (Figure 12-14). Several sialylated structures were observed in all cell lines however these were not the predominant glycan species encountered, and further, very few appeared to have additional underlying fucose structures. MALDI-TOF profiling of CFPAC-1 and MIA paca2 revealed samples of lower quality with fewer detailed analysis of glycan structures obtainable (Figure 15-16). Finally, the permethylated N-glycans obtained from the PANC-1 cells proved to be of too poor quality and no usable MS data was obtained.

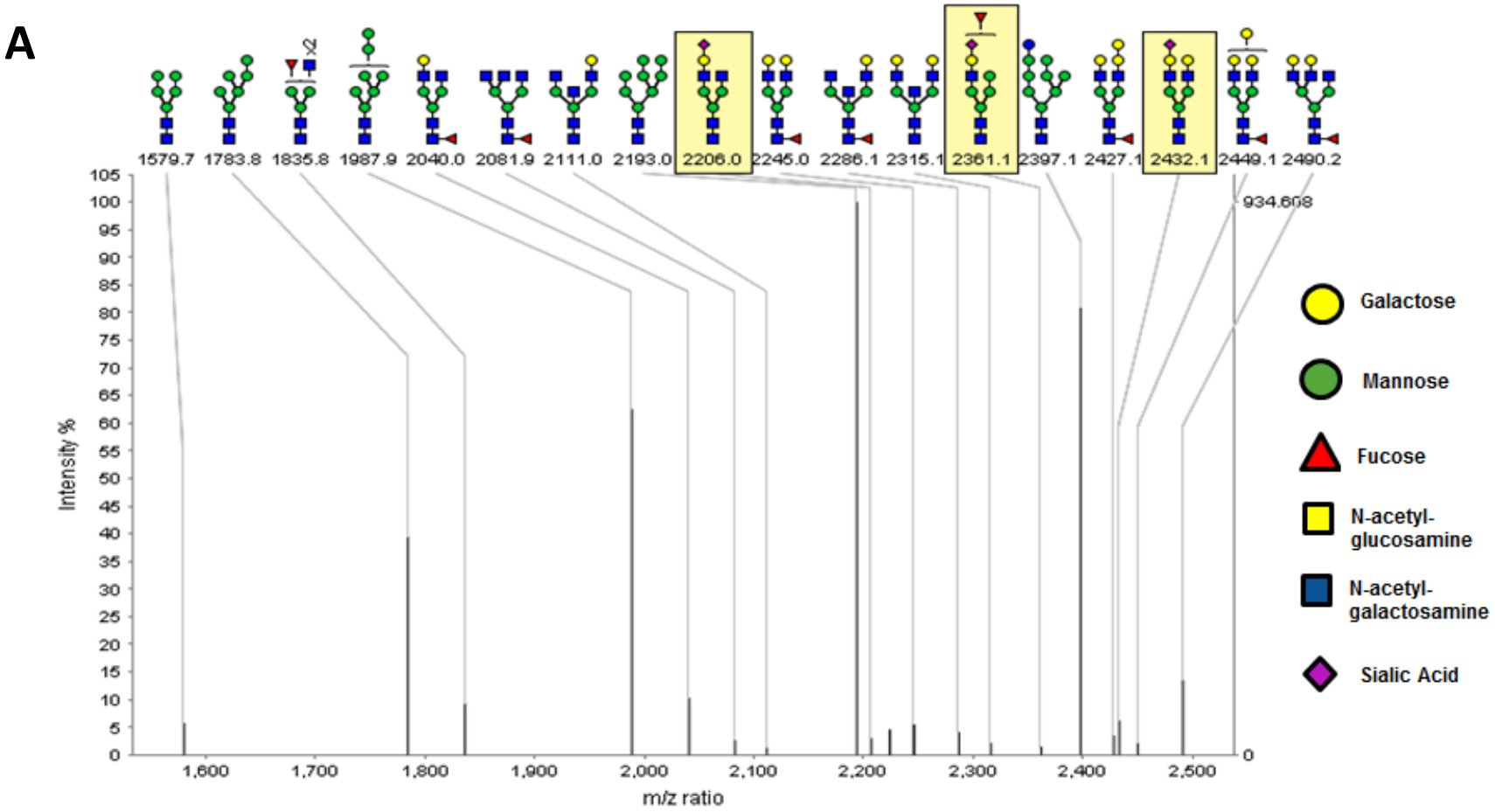

Figure 12. MALDI-TOF mass spectrometry profiles of the permethylated N-linked glycans derived from BxPC-3 cells. Results shown were obtained from the 50% acetonitrile fraction and peak annotations were generated using GlycoWorkbench Software, with sialic acid-containing structures highlighted in yellow. A) Peaks ranging from m/z = 1500-2500 B) Peaks ranging from m/z = 2500-3000 C) Peaks ranging from m/z = 2825–3600.

12.B

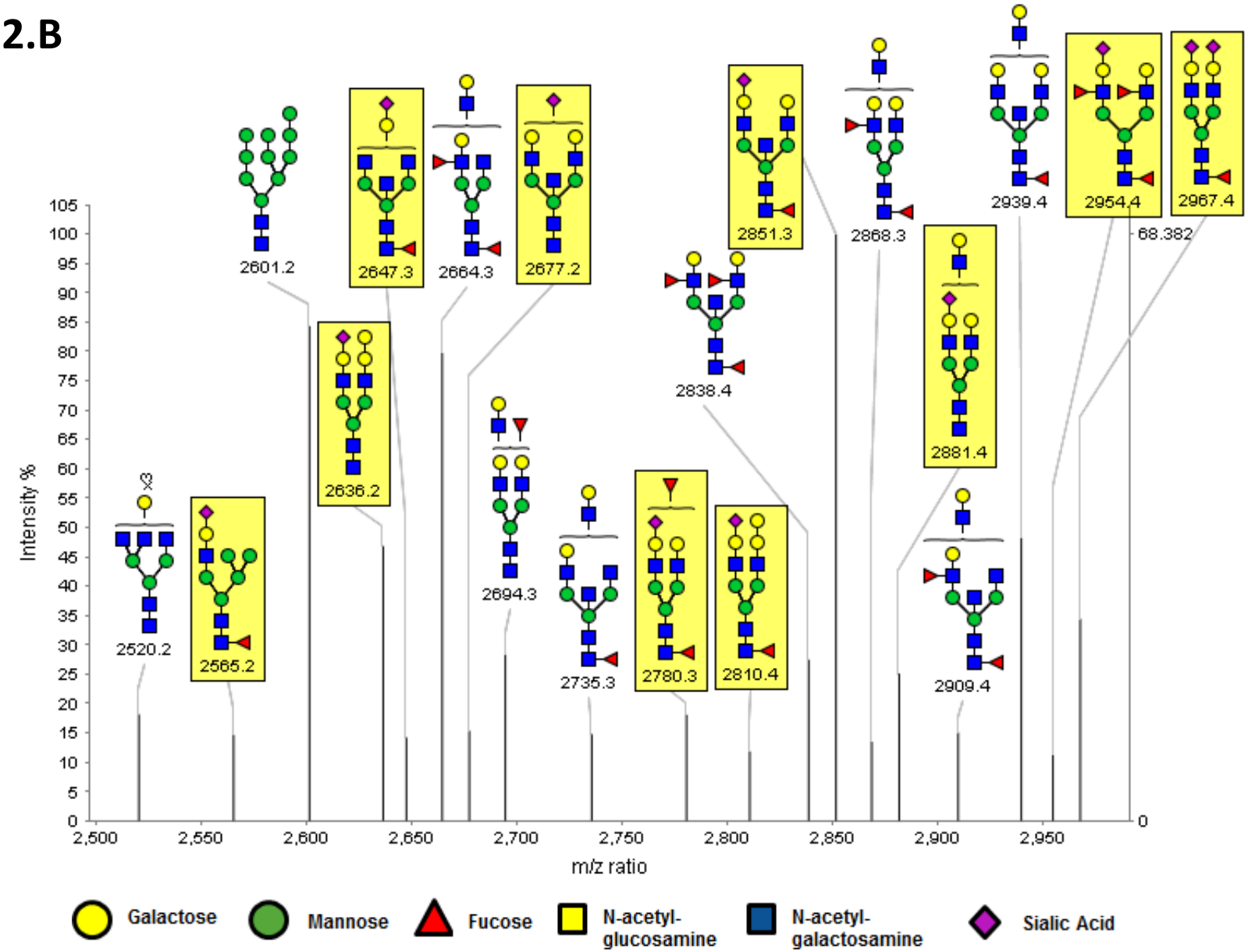
Intensity %
m/z ratio
2,500
2,550
2,600
2,650
2,700
2,750
2,800
2,850
2,900
2,950
0
5
10
15
20
25
30
35
40
45
50
55
60
65
70
75
80
85
90
95
100
105
×3
2520.2
2565.2
2601.2
2636.2
2647.3
2664.3
2677.2
2694.3
2735.3
2780.3
2810.4
2838.4
2851.3
2868.3
2881.4
2909.4
2939.4
2954.4
2967.4
68.382
Galactose
Mannose
Fucose
N-acetyl-glucosamine
N-acetyl-galactosamine
Sialic Acid

12.C

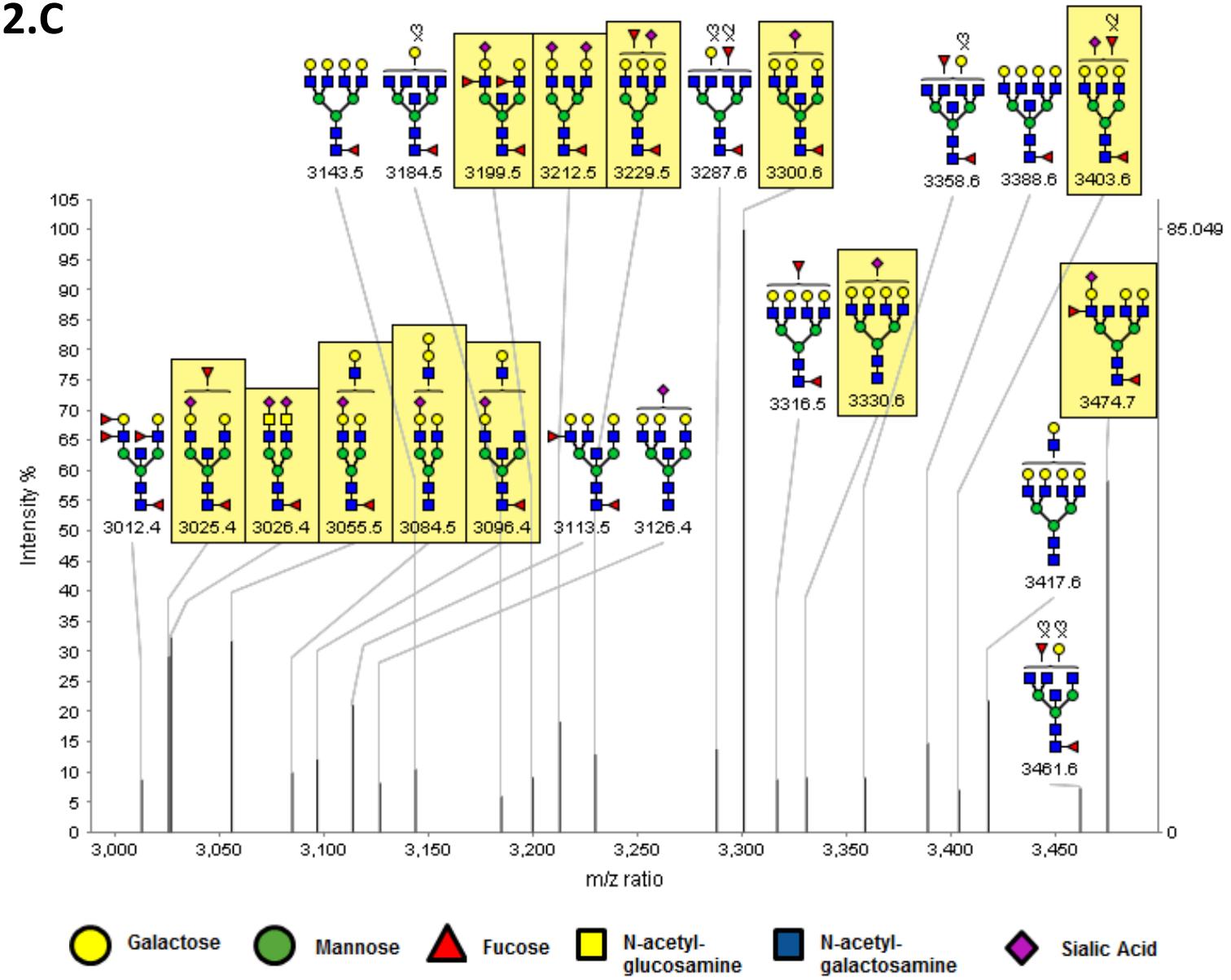
3143.5
3184.5
3199.5
3212.5
3229.5
3287.6
3300.6
3358.6
3388.6
3403.6
3012.4
3025.4
3026.4
3055.5
3084.5
3096.4
3113.5
3126.4
3316.5
3330.6
3474.7
3417.6
3461.6
85.049
0
Intensity %
m/z ratio
3,000
3,050
3,100
3,150
3,200
3,250
3,300
3,350
3,400
3,450
Galactose
Mannose
Fucose
N-acetyl-glucosamine
N-acetyl-galactosamine
Sialic Acid

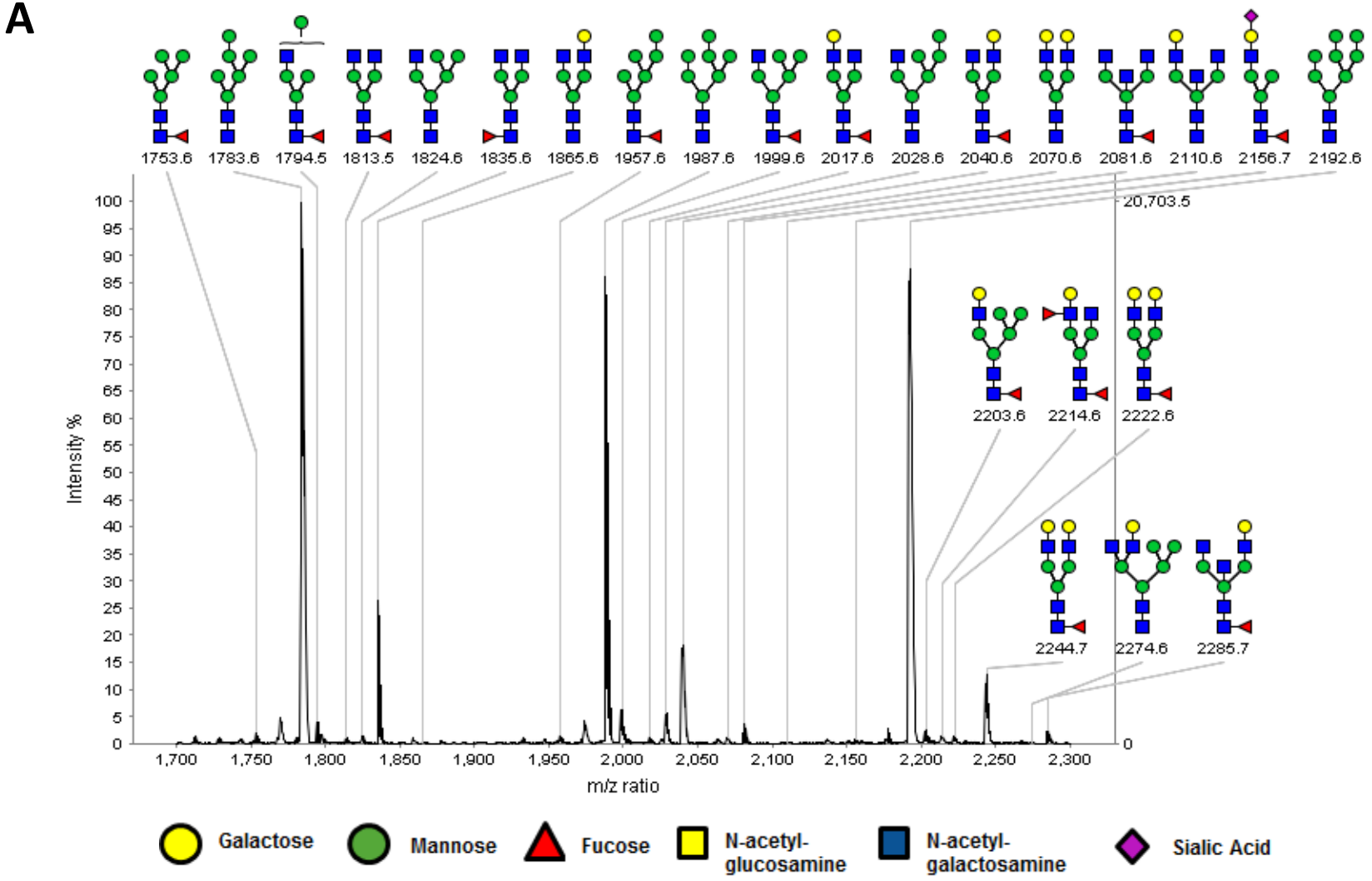

Figure 13. MALDI-TOF mass spectrometry profiles of the permethylated N-linked glycans derived from AsPC-1 cells. Results shown were obtained from the 50% acetonitrile fraction and peak annotations were generated using GlycoWorkbench Software. A) Peaks ranging from m/z = 1700-2300 B) Peaks ranging from m/z = 2300-2800 C) Peaks ranging from m/z = 2800–3500.

13.B

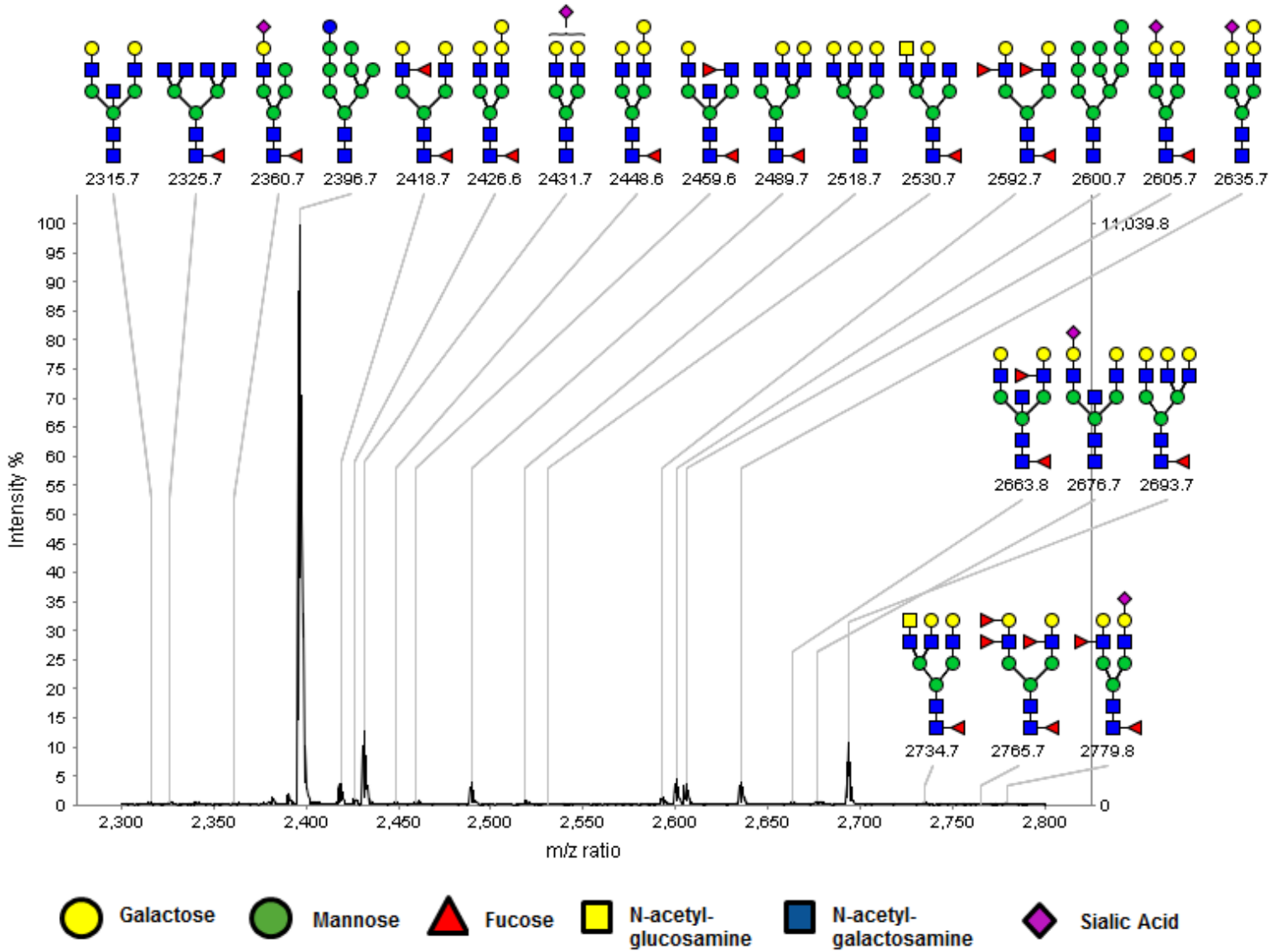
2315.7
2325.7
2360.7
2396.7
2418.7
2426.6
2431.7
2448.6
2459.6
2489.7
2518.7
2530.7
2592.7
2600.7
2605.7
2635.7
11,039.8
2663.8
2676.7
2693.7
2734.7
2765.7
2779.8
Intensity %
m/z ratio
Galactose
Mannose
Fucose
N-acetyl-glucosamine
N-acetyl-galactosamine
Sialic Acid

13.C

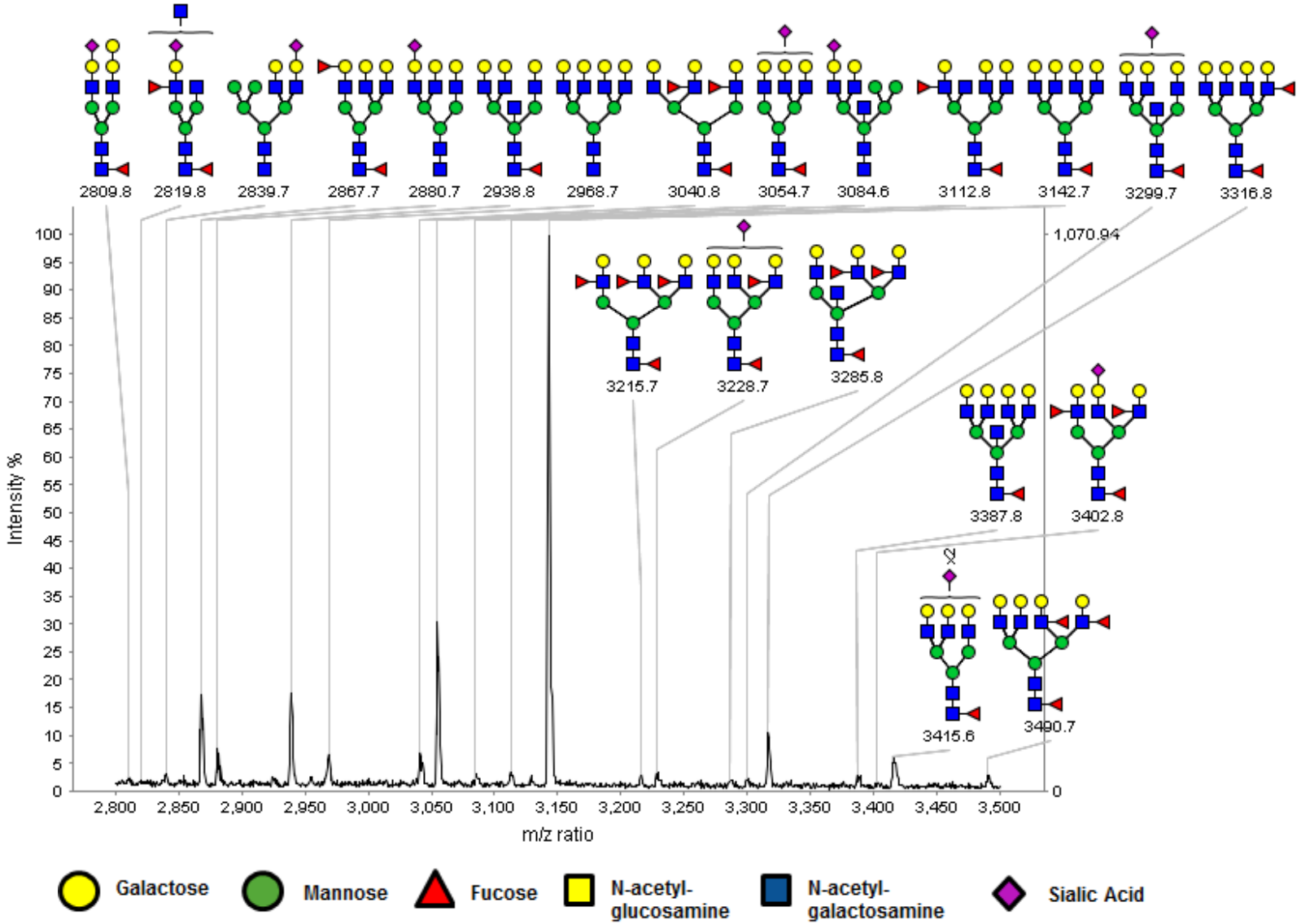
2809.8
2819.8
2839.7
2867.7
2880.7
2938.8
2968.7
3040.8
3054.7
3084.6
3112.8
3142.7
3299.7
3316.8
3215.7
3228.7
3285.8
3387.8
3402.8
3415.6
3490.7
1,070.94
Intensity %
m/z ratio
Galactose
Mannose
Fucose
N-acetyl-glucosamine
N-acetyl-galactosamine
Sialic Acid

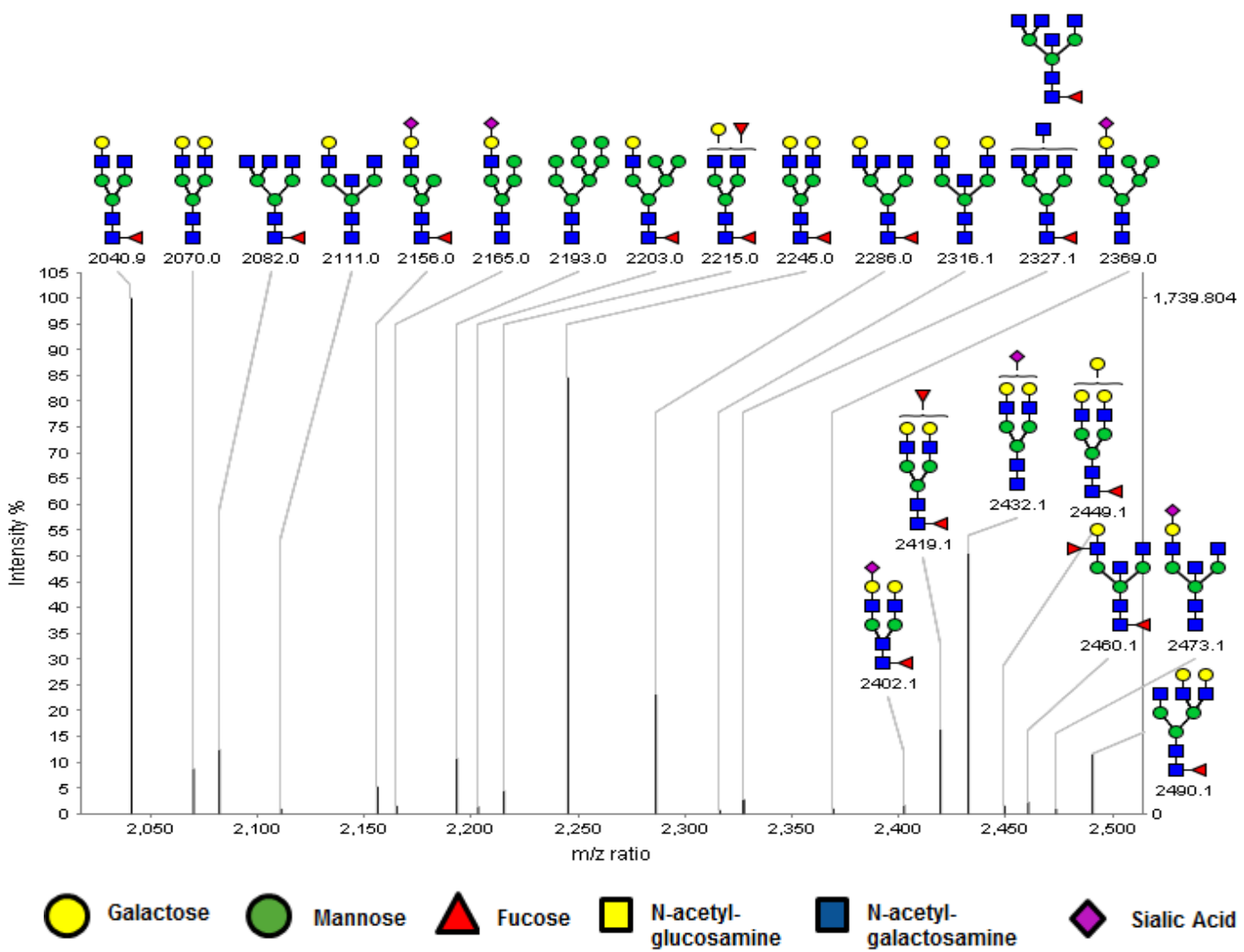

Figure 14. MALDI-TOF mass spectrometry profiles of the permethylated N-linked glycans derived from HPDE6 cells. Results shown were obtained from the 50% acetonitrile fraction and peak annotations were generated using GlycoWorkbench Software. A) Peaks ranging from m/z = 2000-2500 B) Peaks ranging from m/z = 2500-2825 C) Peaks ranging from m/z = 2825–3600.

14.B

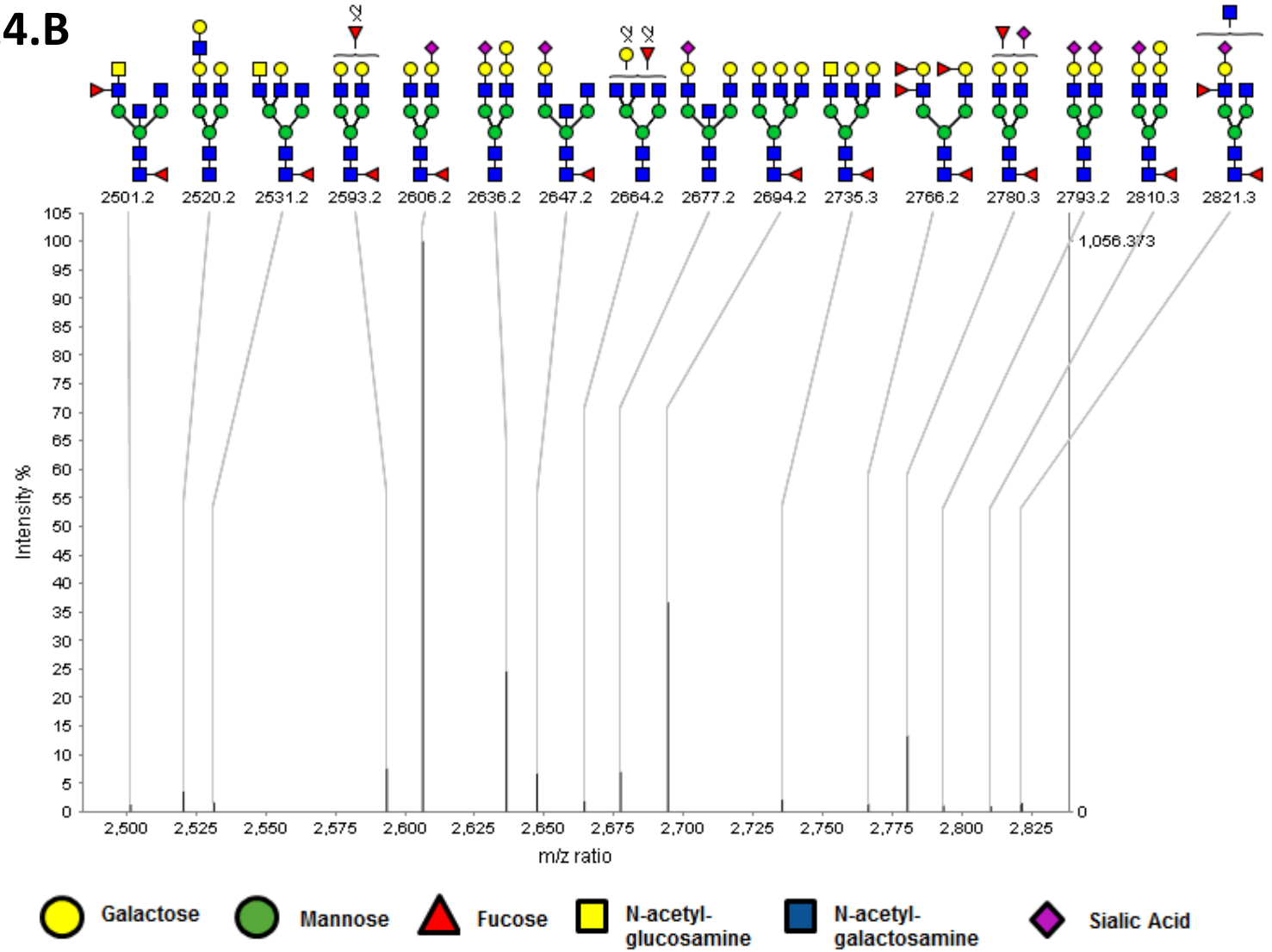
2501.2
2520.2
2531.2
2593.2
2606.2
2636.2
2647.2
2664.2
2677.2
2694.2
2735.3
2766.2
2780.3
2793.2
2810.3
2821.3
1,056.373
Intensity %
m/z ratio
Galactose
Mannose
Fucose
N-acetyl-glucosamine
N-acetyl-galactosamine
Sialic Acid

14.C

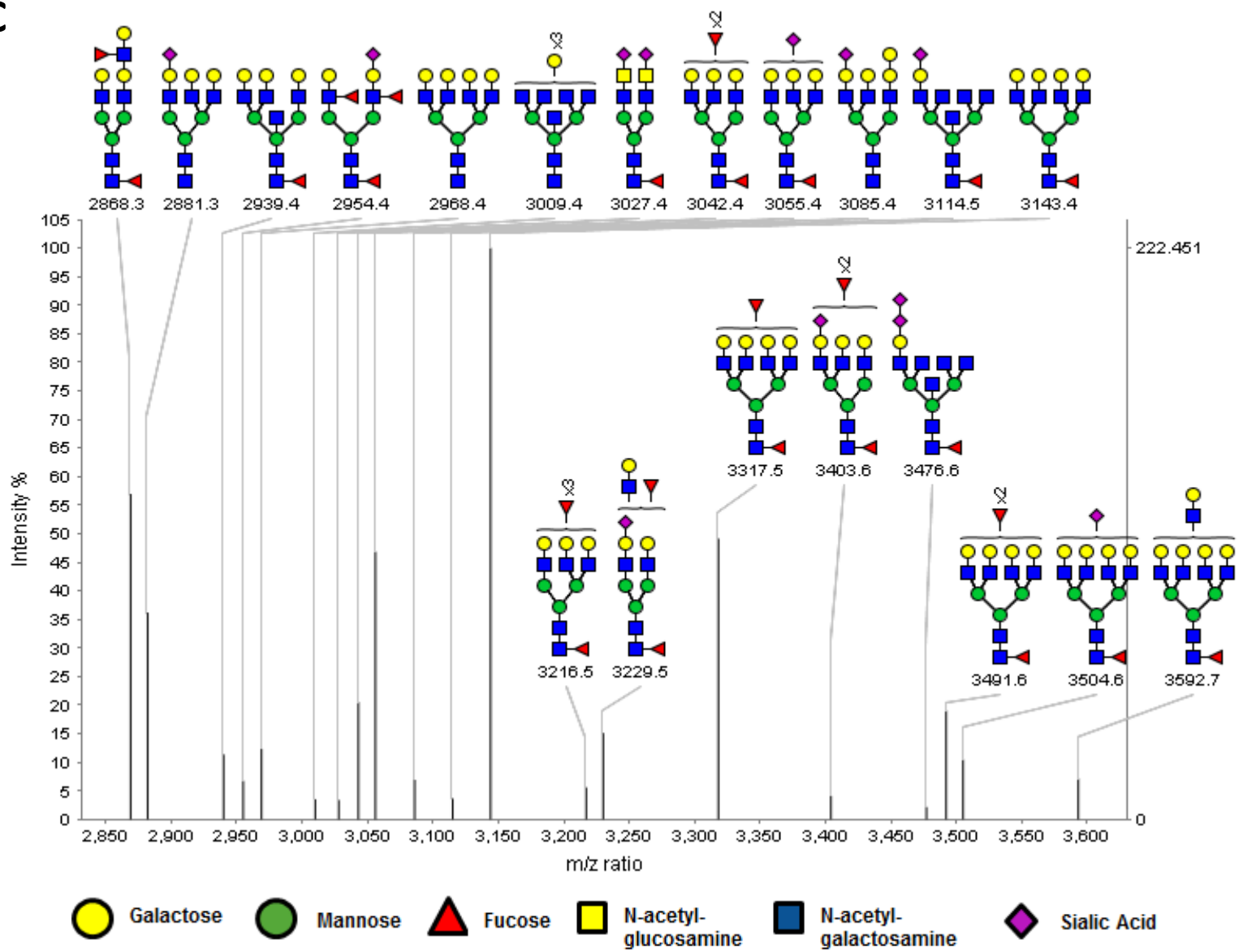
2868.3
2881.3
2939.4
2954.4
2968.4
3009.4
3027.4
3042.4
3055.4
3085.4
3114.5
3143.4
3216.5
3229.5
3317.5
3403.6
3476.6
3491.6
3504.6
3592.7
222.451
Intensity %
m/z ratio
Galactose
Mannose
Fucose
N-acetyl-glucosamine
N-acetyl-galactosamine
Sialic Acid

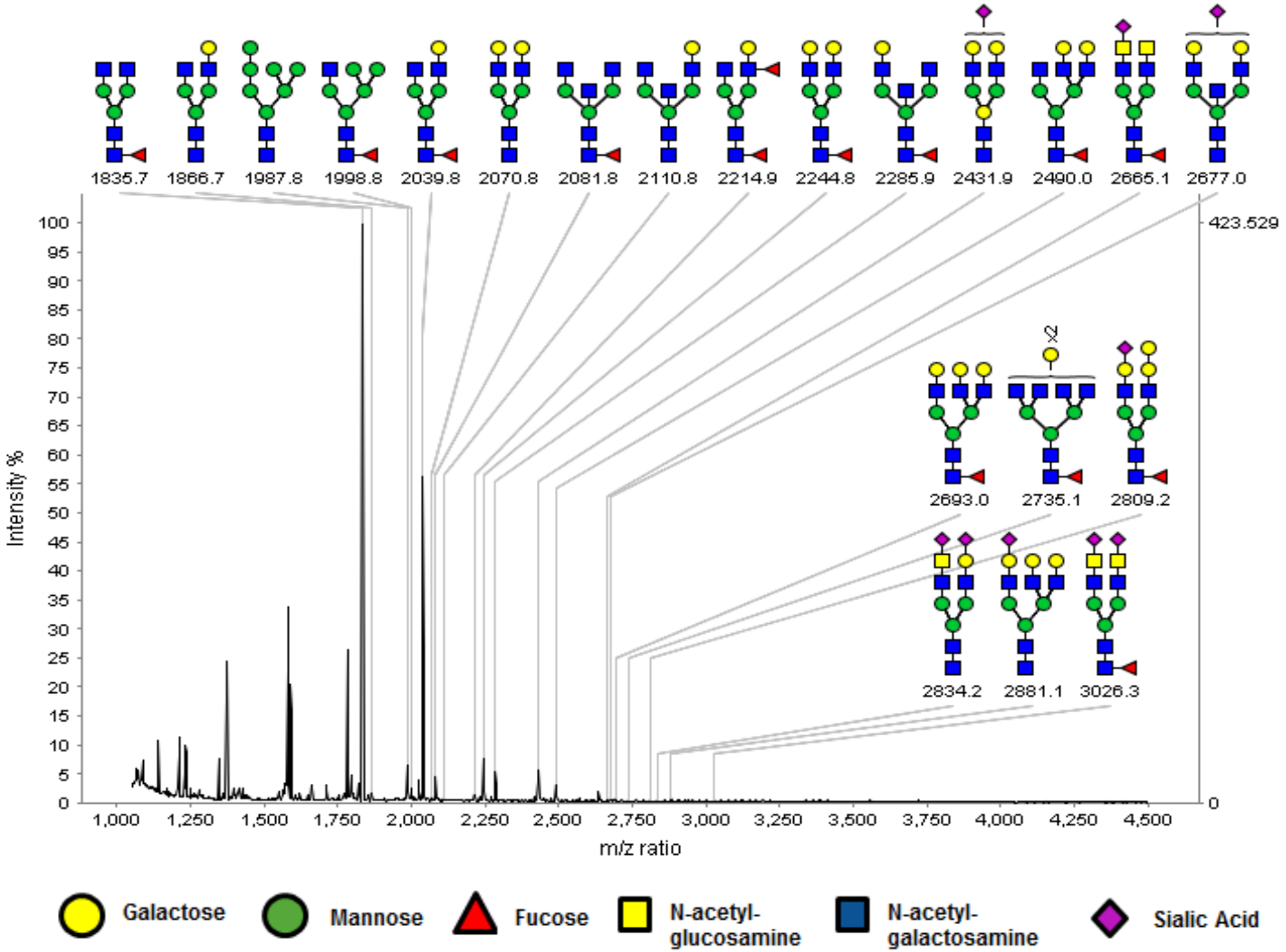

Figure 15. MALDI-TOF mass spectrometry profiles of the permethylated N-linked glycans derived from CFPAC-1 cells highlighting the major glycan structures. Results shown were obtained from the 35% acetonitrile fraction and peak annotations were generated using GlycoWorkbench Software.

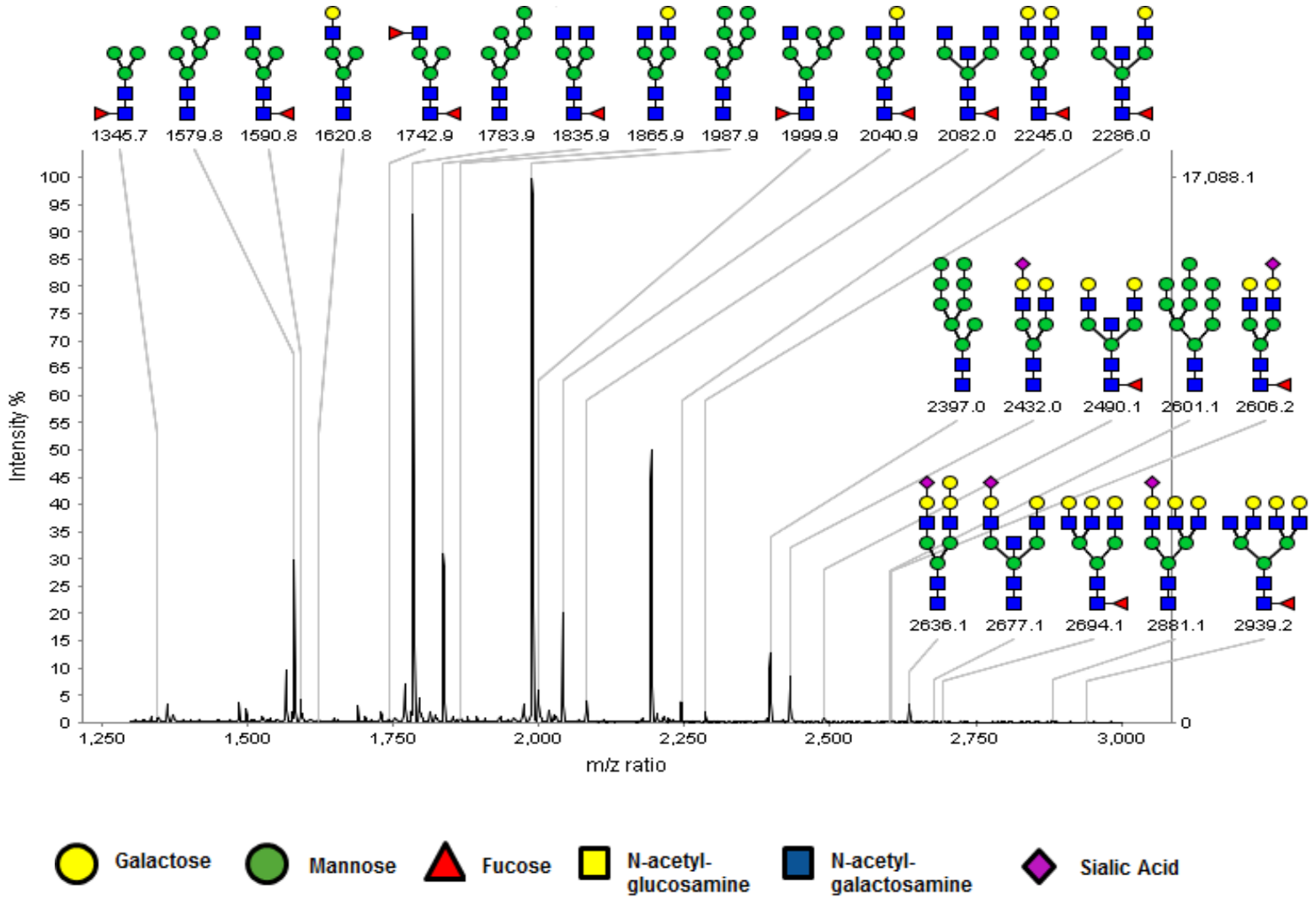

Figure 16. MALDI-TOF mass spectrometry profiles of the permethylated N-linked glycans derived from MIA paca2 cells highlighting the major glycan structures. Results shown were obtained from the 50% acetonitrile fraction and peak annotations were generated using GlycoWorkbench Software.

11. Oncolytic effects of LP IAV *in vivo*. The oncolytic ability of the H7N3 virus isolate was further examined *in vivo* in a SCID mouse tumour xenograft model. Following four successive virus inoculations into palpable BxPC-3 tumours over seven days, the oncolytic effect of IAV on tumour reduction was compared to a PBS control group. Overall, H7N3 treatment resulted in a significant reduction in tumour growth versus PBS alone ($p \leq 0.01$) **(Figure 17A)**, and all tumours collected from H7N3-treated mice sacrificed upon termination of the experiment, ten days after the last virus injection, resulted positive for IAV infection by rRT-PCR (**Figure 17B**).

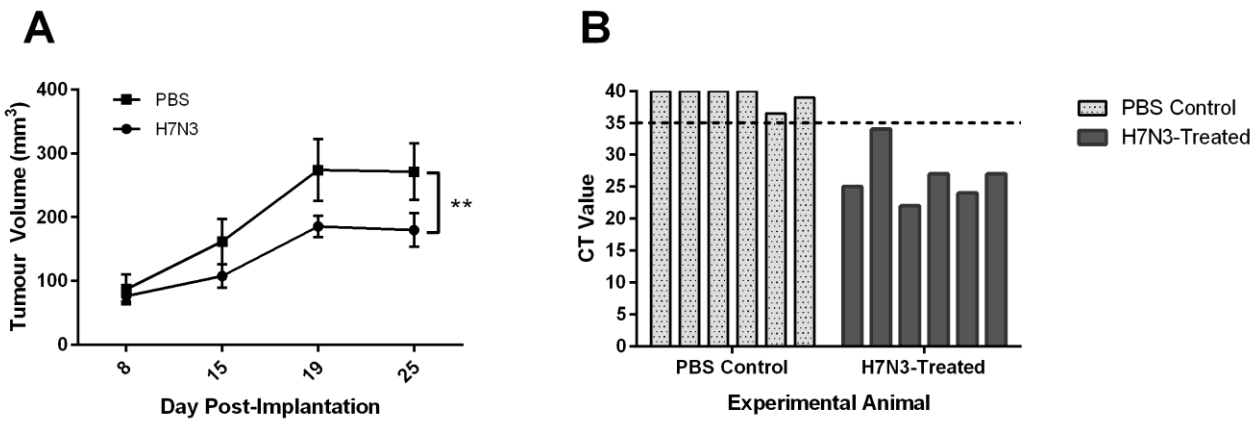

Figure 17. Oncolytic effect of a low pathogenic avian influenza A virus in an orthotopic SCID mouse model of pancreatic ductal adenocarcinoma. Six-week-old female SCID mice were subcutaneously implanted with 5×10^6 BxPC-3 cells in a volume of 100 µL into the right flank. At 8 days post-implantation palpable tumour became established, and mice were randomly divided in two groups (n=6 each), receiving either four intratumoural injections of 2.4×10^4 pfu of low pathogenic H7N3 virus (circles) between day 8 and day 15 or four injections of PBS (squares). A) Caliper measurements of tumour dimensions were taken on indicated days post-BxPC-3 implantation for calculation of tumour volumes. Data shown represent mean volume + SEM, with statistically significant differences between the two treatment groups determined by two-way ANOVA ($p < 0.01$). B) The presence of influenza viral RNA in tumours of experimental animals was assessed in each individual upon sacrifice by rRT-PCR, with samples resulting in CT values of less than 35 considered positive.

DISCUSSION

The present work provides the first description of influenza A virus infection of human pancreatic cancer cells, demonstrating its ability to replicate and induce apoptosis in several PDA cell lines. Results have shown that low pathogenic avian IAVs may present interesting candidates as oncolytic viruses given their enhanced activity in PDA cell lines compared to non-tumoural pancreatic ductal cells and demonstrated ability to reduce tumour size following intratumoural injection in a mouse xenograft model.

As the first step in IAV infection is binding with its sialic acid receptor, the first step of this study was to characterize the receptor profiles of a panel of human pancreatic adenocarcinoma cell lines. Of interest was the fact that these cells generally contained equal levels of both α-2,6 and α α-2,3 sialic acid linkages, making them susceptible to infection by both avian and mammalian viruses. While the upper respiratory tract is the primary site of infection for human influenza viruses as a result of high levels of α-2,6-linked sialic acids (SA), the expression of α-2,3-linked SA has been detected on other human tissues including endothelial cells of the heart, brain, intestines, and liver as well as non-ciliated cells in the lung (Yao *et al.*, 2008) Although all PDA cell lines expressed both types of SA receptors on their surfaces, differences in expression levels were noted. Such heterogeneity in levels of SA expression in different cell lines was not surprising, as altered expression levels of sialyltransferases and fucosyltransferases have been demonstrated in different types of tumours including pancreatic, breast, colon, gastric, cervical and renal cancers (Mas *et al.*, 1998; Pérez-Garay *et al.*, 2010). Similar results have also been observed in the case of melanoma cell lines, with heterogeneous distribution of surface receptors when different lines were compared (Pietra *et al.*, 2009).

The central concept to oncolytic virotherapy involves the use of a modified, targeted virus that can specifically kill tumour cells while leaving healthy somatic cells unharmed. Though the scope of this research was to assess the oncolytic abilities of avian influenza A viruses in their natural forms, an investigation into a particular targeting strategy was undertaken. Specifically, if the experimental isolates showed any inherent binding preference for PDA-associated glycans, or if this could have been artificially enhanced through genetic modification of the receptor binding site, then this may have been one possible strategy to increase cancer cell targeting. The receptor binding phenotypes of three experimental isolates was determined by assessing their binding affinity towards well characterized synthetic glycan polymers. Both of the H7 viruses, H7N3 and H7N7, showed high affinity for alpha-2,3-linked sialic acids containing sulfated and fucosylated glycan cores, binding with highest affinity to

sulfated sialyl Lewis X . These results correlated well with previous observations in literature, as H7 viruses isolated from land-based poultry have a tendency towards this phenotype, attributed to the presence of particular amino acids within their receptor binding sites that can accommodate bulky fucose residues and have strong ionic interactions with sulfate (Gambaryan *et al.*, 2008, 2012). A hallmark of cancer is changes in glycosylation, with altered sialylation particularly important (Fuster & Esko, 2005; Varki *et al.*, 2009). Immunohistochemical studies on human tissues comparing pancreatic tissues from normal pancreas, patients with chronic pancreatitis, and pancreatic adenocarcinoma demonstrated Lewis x-related antigens were found in the majority of pancreatic cancer tissues while absent from normal tissues, and were particularly highly expressed on cells of highly differentiated tumours (Kim *et al.*, 1988b; Mas *et al.*, 1998). Similarly, in the clinical setting, increased levels of SLe^x on pancreatic tumours cells are correlated with poor patient prognosis (Pérez-Garay *et al.*, 2010). The increased affinity for SLe^X-related structures by the two H7 viruses tested at first seemed like a promising result in terms of PDA affinity, however these results must be interpreted with caution for a number of reasons. First, though a good binding profile was obtained with fucosylated glycans SLe^X and Expression of Lewis antigens such as SLe^X and SLe^A, the viruses actually displayed the highest affinity for sulfated glycans (Su-SLeX and 6'Su-3'SLN), and sulfation of glycans is often downregulated in cancers (Varki *et al.*, 2009). Further, the binding of influenza A viruses to host receptor molecules is a low affinity, high avidity interaction, and therefore so long as a target cell is not glycosylated solely with sialylated glycans that cannot interact with the receptor binding site due to steric hindrance or severe ionic clashes, binding will likely still occur. As such, it would seem more effective to create a modified virus that is de-targeted towards a particular molecule, as a good interaction with one glycan does not rule out binding with others.

A number of in depth glycan analyses of various host species and particular physiological sites have been carried out in recent years to deduce important receptor molecules for IAV infection, or lack thereof (Bateman et al., 2010; Chan et al., 2013; Jayaraman et al., 2012; Walther et al., 2013). On the same note, an attempt to deduce the major *N*-glycan species on the PDA cells was made through mass spectrometric analysis. The lengthy and delicate nature of sample processing caused some of the cell lines to produce much poorer reads than others, though a significant number of structures were interpreted from BxPC-3, AsPC-1 and HPDE6 cells. However, the lack of MS/MS analyses to fully and accurately describe the structures deduced from MALDI-TOF spectra leaves the possibility of highly subjective interpretations in terms of whether large glycans were branched vs. long chains, and only used likelihood to determine whether modifications of the glycan chain, including fucose residues,

were located near the terminal sialic acid (producing the SLe^X structure) or were in fact at the base of the glycan. Though the usefulness of this particular type of study for the generation of a modified, PDA-targeted influenza virus is not very great due to reasons stated above, further analysis of the samples generated using MS/MS technologies would be of great interest to the field of pancreatic oncology with potential to reveal new markers not previously observed in PDA cells using standard immunological methods (Fuster & Esko, 2005).

The ability of IAV to replicate in different host systems is thought to be influenced by an optimal temperature at which viral polymerase functions and interacts with the host RNA replication machinery. Particular attention has been paid to residue 627 of the viral polymerase basic 2 (PB2) protein, which has been considered a major determinant of temperature sensitivity and mediates optimal RNA polymerase activity at the temperature of the natural host. The core temperature of the avian GI tract, the site of avian influenza virus infection, is approximately 41^{o}C, whereas temperatures in the human respiratory tract, the site of human influenza virus infection, range from 33^{o}C in the upper portion to 37^{o}C in the lower respiratory tract. Viruses of avian origin typically contain glutamic acid at this position, restricting growth in mammalian cells, whereas mammalian viruses carry a lysine, allowing for successful replication in mammalian systems (Labadie *et al.*, 2007; Subbarao *et al.*, 1993). This was demonstrated experimentally in MDCK cells, where titres of avian viruses were significantly decreased at 33^{o}C incubation temperature compared to 37^{o}C while human viruses reached similar titres at both temperatures (Massin *et al.*, 2001). Several investigators have since demonstrated its role by looking at whole virus replication or transcription/replication activity of *in vitro*-reconstituted RNP complexes in mammalian cell lines, including primary human cells of respiratory origin (Bradel-Tretheway *et al.*, 2008; Massin *et al.*, 2010). Based on such observations, we wanted to investigate whether viruses from diverse host backgrounds would have diverse optimal replication temperatures in the human PDA cell model. As such, we investigated whether low viral titres achieved with certain isolates in human pancreatic cells resulted from temperature sensitivity in this host system. Growth curves conducted at physiologically relevant temperatures for humans (33 and 37^{o}C) and birds (41^{o}C) did in fact indicate that the virus replicative fitness mimicked the host in which it was isolated, with lowest titres usually reached when incubated at temperatures least reflective of those in their natural hosts, as seen with PR/8 when incubated at 41^{o}C compared to 33^{o}C or 37^{o}C and the highly pathogenic H5N1 and H7N1 isolates when comparing titres at 33^{o}C to those at 37^{o}C or 41^{o}C. However, this trend was not observed for all virus isolates and further, differences were never found to be significant in

BxPC-3 cells, indicating that the avian isolates did not suffer from limited polymerase activity in these human PDA cells at temperatures reflective of the *in vivo* context.

Susceptibility of PDA cell lines to HP avian IAVs was greater than to LP avian IAVs as demonstrated by replication kinetic experiments. To confirm that this was not a result of the low TPCK-trypsin concentrations used in the experiments, parallel infections were performed in MDCKs using concentrations of 1 μg/mL or 0.05 μg/mL TPCK-trypsin, in which similar titres of virus were obtained under both conditions (results not shown). While these results suggest that low trypsin concentrations were not the limiting factor, multi-cycle replication of human IAVs, which typically require the addition of trypsin, has been observed in a number of cases (Noma *et al.,* 1998; Tumpey *et al.*, 2005). It is therefore probable that proteolytic activation of the LPAI viruses is likely sub-optimal under the present experimental conditions and this was confirmed experimentally when examining viral genome replication, as no increases were found between 16 and 24 HPI, indicating the absence of multicycle replication. While the pancreas is the site of trypsinogen production, this pro-enzyme is typically activated to trypsin in other organs of the digestive tract. On the other hand, in a diseased state, such as in acute pancreatitis, trypsin activation may occur within the pancreas, suggesting the possibility of supporting multiple rounds of influenza A virus replication *in vivo* (Sherwood *et al.*, 2007).

In a study of oncolytic properties of a modified human influenza A virus isolate in colorectal cancer cells, viruses were shown to undergo multicycle replication in vitro without the addition of exogenous trypsin, suggesting the production of trypsin or a trypsin-like enzyme by the cells examined (Sturlan *et al.*, 2010). The enhanced production of proteolytic enzymes is a hallmark of cancer cells as they aid in invasion and metastasis (Vartak & Gemeinhart, 2007), and altered expression of matrix metalloproteinase and their inhibitors have been particularly associated with progression of pancreatic cancer (Bramhall *et al.*, 1997; Jones *et al.*, 2004; Keleg *et al.*, 2003; Sato *et al.*, 2003; Yamamoto *et al.*, 2001) and exploitation of these proteases has been suggested as a mode of targeted cancer treatment (Vartak & Gemeinhart, 2007). In fact, MMP-targeting has been used as a strategy for tumours-specific targeting of oncolytic viruses in the case of measles virus (Mühlebach *et al.*, 2010; Springfeld *et al.*, 2006), retroviruses (Schneider *et al.*, 2003; Szécsi *et al.*, 2006) and sendai virus (Kinoh *et al.*, 2004), and modifications to the HA proteolytic cleavage site to render it MMP-specific are being planned to not only increase specificity of PDA-associated proteases but to allow for multicycle replication in the absence of exogenous trypsin.

Influenza viruses are known to induce apoptosis in a number of cell lines and tissues, while in others they induce death via necrosis (van Rikxoort *et al.*, 2012; Takizawa *et al.*, 1993; Zhirnov & Klenk, 2003). Based on MTT assay results showing that low pathogenic avian IAVs cause reduction in cell viability, we tested whether these viruses induced apoptotic cell death in PDA cells. Results of Annexin V cell staining indicated that LP avian IAVs viruses caused death by apoptosis in the panel of PDA cell lines tested, and generally correlated well with levels of cytotoxicity observed in the MTT assay. However, in a few instances there were notable discrepancies in which Annexin V staining showed greater induction of apoptosis compared to results from the MTT assay, and this was especially true for BxPC-3 infections. Differences in sensitivity levels of these two assays have been observed elsewhere (Wu *et al.*, 2013), confirming the notion that while metabolic assays may provide a good overall picture of cytotoxicity, the use of additional assays is favored in order to accurately deduce levels of cell death.

Similar to variations observed in RNA replication rates and sensitivity to infection, Annexin V staining demonstrated that IAV-induced apoptosis in PDA cells varied highly depending on virus isolate and cell line tested. Alterations in apoptotic signaling pathways are among the most frequent genetic changes observed in pancreatic cancers (Jones *et al.*, 2008; Westphal & Kalthoff, 2003), contributing to resistance against chemotherapeutic agents (Fulda & Debatin, 2006; Karikari *et al.*, 2007). BxPC-3 cells were the most sensitive and unlike the others contain a wild type K-RAS (Deer *et al.*, 2010). As a modulator of numerous cellular signal transduction pathways, K-RAS mutations are known to increase resistance to apoptosis (Moon *et al.*, 2012). The fact that BxPC-3 cells contain a wild-type K-RAS may thus partially explain the higher levels of apoptosis observed in this cell line, however the fact that the non-transformed HPDE6 cells also contain wild-type K-RAS (Ouyang *et al.*, 2000) and displayed a resistant phenotype suggests that other contributing factors were at play.

The interferon status of tumour cells has also been proven highly influential on the oncolytic activity of several viruses, IAV included (Efferson *et al.*, 2006; Elankumaran *et al.*, 2010; Sturlan *et al.*, 2010). A recent publication detailing the susceptibility of PDA cell lines to vesicular stomatitis virus found that the lack of Type 1 IFN production by AsPC-1, CFPAC-1, MIA paca 2, and Panc-1 cells largely correlated with sensitivity to infection, however both IFN-negative BxPC-3 cells and IFN-producing HPDE6 cells showed resistance (Murphy *et al.*, 2012). In the present study, however, the degree of PDA sensitivity to to IAV-induced apoptosis does not correlate to the cells' interferon status, as cells incapable of IFN production resulted as both highly sensitive (BxPC-3) or relatively resistant

(Panc-1) similar to a recent report on PDA cell line sensitivity to Newcastle disease virus (Buijs *et al.*, 2014).

PDAs are associated with a constellation of genetic alterations in oncogenes and tumour suppressor genes, the four most frequent being observed in *KRAS, TP53, SSMAD4/DPC4* and *CDKN2A/p16* (Deer *et al.*, 2010; Qian *et al.*, 2005). The status of these four genes has been previously described for all six pancreatic cell lines included in this study however no immediate associations can be made by comparing the individual cell genotypes with their phenotypes regarding sensitivity to influenza virus-induced apoptosis. It is likely that complex interactions between a multitude of genes controlling cell cycle, signal transduction pathways, apoptosis resistance and interferon status all determine the ability of influenza virus to induce apoptosis in PDA cells, and an understanding of the specific mechanisms at hand will be crucial for future development of modified oncolytic influenza viruses with potential in a clinical setting.

The lack of apoptotic induction following gemcitabine and cisplatin treatment observed in the present study is not entirely in agreement with other publications using the same PDA cell lines, but this is likely to result from differences in experimental conditions. Several reports documenting gemcitabine sensitivity of PDA cell lines show higher induction of apoptosis following treatment with chemotherapeutic agents, but these studies involve cells treated for 48-72 hours and seeded at densities ranging from five to fifteen times lower than in the present study (Cui *et al.*, 2012; Rathos *et al.*, 2012; Réjiba *et al.*, 2009). As the research presented was concerned with the ability of influenza virus to induce apoptosis following infection at a high MOI, a period of 24 hours was chosen to study the response; starting with confluent monolayers to monitor CPE following infection. It is likely that the higher cell density with increased cell-cell contact combined with the 24 hour observation window resulted in lower observed response rates to gemcitabine and cisplatin treatment in the present study despite the increased drug concentrations. Even more interesting than the differences observed between cell lines was the major differences observed between viral isolates in their ability to induce apoptosis in PDA cells. While several of the isolates tested showed significantly enhanced ability to induce apoptosis compared to treatment with gemcitabine and cisplatin, the H7N3 isolate repeatedly out-performed the others in terms of the rapidity and potency of cell death induced. Strain-specific variations in apoptotic induction have been previously documented in primary cultures and established cell lines in the case of human, avian and swine influenza viruses (Choi et al., 2006; Mok et al., 2007).

The particularity of the H7N3 isolate raised questions to be investigated further, examining the specific apoptotic pathway induced in a highly sensitive cell line (BxPC-3) compared to a resistant line

(HPDE6). Based on the expression of effector and executioner caspases in infected cells, H7N3-induced apoptosis appeared to result from activation of the intrinsic mitochondrial pathway in BxPC-3 cells, but this phenomenon was not observed in the HPDE6 cells. Induction of cell death via the intrinsic pathway is a characteristic of a number of oncolytic viruses, including Newcastle Disease Virus and Vesicular Stomatitis Virus (Gadaleta *et al.,* 2005; Mansour *et al.,* 2011; Tumilasci *et al.*, 2008). Though caspase-independent mechanisms of apoptosis cannot be ruled out, our results strongly suggest that the ability to induce the intrinsic pathway is a critical factor in the success of the H7N3 isolate at pancreatic cancer cell-killing. A constellation of viral proteins, including NS1, PB1-F2, NA, (Hale *et al.*, 2008; Xing *et al.*, 2011) have been demonstrated as regulators of the apoptotic response in infected cells, and the distinct genetic signatures of the H7N3 isolate are currently under study.

Building on results observed *in vitro,* an experiment using a SCID mouse xenograft model was performed to examine the oncosuppressive activity of the H7N3 virus in an *in vivo* setting. As reflected by *in vitro* sensitivity, BxPC-3-based tumours showed significantly reduced growth following H7N3 treatment compared to PBS alone. The presence of viral RNA in tumours of all H7N3-treated animals sacrificed one week following the final injection confirmed that all tumours were successfully infected with IAV although virus isolations were not performed to determine whether this represented live virus. Given the inability of the low pathogenic viruses to undergo multiple rounds of replication in PDA cells *in vitro,* most likely due to protease-limiting conditions, the H7N3 virus was not expected to undergo multiple rounds of infection in the BxPC-3 tumour cells. However, detection of viral RNA in treated tumours up to one week following the final injection opens the possibility that virus replication did occur within the tumour microenvironment. In any case, the overall positive results and lack of detrimental side effects observed in the *in vivo* trial are a promising sign for future studies with IAVs harboring appropriate PDA-specific modifications.

The fact that low pathogenic influenza viruses are able to induce levels of apoptosis in PDA cells that are significantly higher and targeted to the cancerous cells as compared to commonly employed chemotherapeutic agents indicates that these viruses have a higher tropism for the cancerous phenotype that may be further exploited. These observations were further confirmed in an *in vivo* xenograft model, where intratumoural inoculation with a low pathogenic H7N3 isolate decreased tumour growth as compared to the control. Taken together, our results indicate that PDA cells are sensitive to the oncolytic effects of influenza viruses and further studies are warranted to understand this phenomenon at the molecular level, leading to the generation of specific and targeted viruses with enhanced potential *in vivo* and ultimately in a clinical setting.

REFERENCES

Abbas, A. & Lichtman, A. (2003). *Cellular and Molecular Immunology*, 5th edn. Philadelphia: W B Saunders Co.

Abbas, S. (2013). Molecular biology of adenocarcinoma of the pancreatic duct, current state and future therapeutic avenues. *Surg Oncol* **22**, 69–76. Elsevier Ltd.

Ady JW, Heffner J, Klein E, F. Y. (2014). Oncolytic viral therapy for pancreatic cancer : current research and future directions. *Oncolytic Virotherapy* **3**, 35–46.

Alexander, D. J. (2007). An overview of the epidemiology of avian influenza. *Vaccine* **25**, 5637–5644.

Angelova, A. L., Grekova, S. P., Heller, A., Kuhlmann, O., Soyka, E., Giese, T., Aprahamian, M., Bour, G., Rüffer, S. & other authors. **(2014).** Complementary induction of immunogenic cell death by oncolytic parvovirus H-1PV and gemcitabine in pancreatic cancer. *J Virol* **88**, 5263–76.

Armstrong, L., Arrington, A., Han, J., Gavrikova, T., Brown, E., Yamamoto, M. & Vickers, S. M. (2012). Generation of a Novel, Cox2-Targeted, Interferon-Expressing, Conditionally-Replicative Adenovirus for Pancreatic Cancer Therapy Leonard. *Am J Surg* **204**, 741–750.

Auer, R. & Bell, J. C. (2012). Oncolytic viruses: smart therapeutics for smart cancers. *Future Oncol* **8**, 1–4.

Baran, B., Karaca, C., Soyer, O. M., Lacin, S., Demir, K., Besisik, F. & Boztas, G. (2012). Acute pancreatitis associated with H1N1 influenza during 2009 pandemic: a case report. *Clin Res Hepatol Gastroenterol* **36**, e69–70.

Barnes, D., Kunitomi, M. & Vignuzzi, M. (2008). Harnessing endogenous miRNAs to control virus tissue tropism as a strategy for developing attenuated virus vaccines. *Cell Host Microbe* **4**, 239–248.

Bartel, D. (2004). MicroRNAs: genomics, biogenesis, mechanism, and function. *Cell* **116**, 281–297.

Bateman, A. C., Karamanska, R., Busch, M. G., Dell, A., Olsen, C. W. & Haslam, S. M. (2010). Glycan analysis and influenza A virus infection of primary swine respiratory epithelial cells: The importance of NeuAc??2-6 glycans. *J Biol Chem* **285**, 34016–34026.

Bergmann, M., Romirer, I. & Sachet, M. (2001). A genetically engineered influenza A virus with ras-dependent oncolytic properties. *Cancer Res* 8188–8193.

Blackham, A. U., Northrup, S. a, Willingham, M., Sirintrapun, J., Russell, G. B., Lyles, D. S. & Stewart, J. H. (2014). Molecular determinants of susceptibility to oncolytic vesicular stomatitis virus in pancreatic adenocarcinoma. *J Surg Res* **187**, 412–26. Elsevier Inc.

Blum, A., Podvitzky, O., Shalabi, R. & Simsolo, C. (2010). Acute pancreatitis may be caused by H1N1 influenza A virus infection. *Isr Med Assoc J* **12**, 640–641.

Le Bœuf, F. & Bell, J. C. (2010). United virus: The oncolytic tag-team against cancer! *Cytokine Growth Factor Rev* **21**, 205–211. Elsevier Ltd.

Bradel-Tretheway, B. G., Kelley, Z., Chakraborty-Sett, S., Takimoto, T., Kim, B. & Dewhurst, S. (2008). The human H5N1 influenza A virus polymerase complex is active in vitro over a broad range of temperatures, in contrast to the WSN complex, and this property can be attributed to the PB2 subunit. *J Gen Virol* **89**, 2923–2932.

Bramhall, S. R., Neoptolemos, J. P., Stamp, G. W. H. & Lemoine, N. R. (1997). Imbalance of expression of matrix metalloproteinases (MMPs) and tissue inhibitors of the matrix metalloproteinases (TIMPs) in human pancreatic carcinoma. *J Pathol* **182**, 347–355.

Brojer, C., Agren, E. O., Uhlhorn, H., Bernodt, K., Morner, T., Jansson, S., Mattsson, R., Zohari, S., Thoren, P. & other authors. **(2009).** Pathology of Natural Highly Pathogenic Avian Influenza H5N1 Infection in Wild Tufted Ducks (Aythya Fuligula). *J Vet Diagnostic Investig* **21**, 579–587.

Buijs, P. R. a, van Eijck, C. H. J., Hofland, L. J., Fouchier, R. a M. & van den Hoogen, B. G. (2014). Different responses of human pancreatic adenocarcinoma cell lines to oncolytic Newcastle disease virus infection. *Cancer Gene Ther* **21**, 24–30. Nature Publishing Group.

Calore, E. E., Uip, D. E. & Perez, N. M. (2011). Pathology of the swine-origin influenza A (H1N1) flu. *Pathol Res Pract* **207**, 86–90. Elsevier GmbH.

Capua, I. & Alexander, D. J. (2008). Ecology, epidemiology and human health implications of avian influenza viruses: Why do we need to share genetic data? *Zoonoses Public Health* **55**, 2–15.

Capua, I., Mercalli, A., Pizzuto, M. S., Romero-Tejeda, A., Kasloff, S., De Battisti, C., Bonfante, F., Patrono, L. V, Vicenzi, E. & other authors. **(2013).** Influenza A viruses grow in human pancreatic cells and cause pancreatitis and diabetes in an animal model. *J Virol* **87**, 597–610.

Cassel, W. (1957). Multiplication of influenza virus in the Ehrlich ascites carcinoma. *Cancer Res* 618–622.

Cattaneo, R., Miest, T., Shashkova, E. V & Barry, M. a. **(2008).** Reprogrammed viruses as cancer therapeutics: targeted, armed and shielded. *Nat Rev Microbiol* **6**, 529–40.

Ceroni, A., Maass, K., Geyer, H., Geyer, R., Dell, A. & Haslam, S. M. (2008). GlycoWorkbench: A tool for the computer-assisted annotation of mass spectra of glycans. *J Proteome Res* **7**, 1650–1659.

Chan, R. W. Y., Karamanska, R., Van Poucke, S., Van Reeth, K., Chan, I. W. W., Chan, M. C. W., Dell, A., Peiris, J. S. M., Haslam, S. M. & other authors. **(2013).** Infection of swine ex vivo tissues with avian viruses including H7N9 and correlation with glycomic analysis. *Influenza Other Respi Viruses* **7**, 1269–1282.

Cheung, T. K. W. & Poon, L. L. M. (2007). Biology of influenza a virus. In *Ann N Y Acad Sci*, pp. 1–25.

Choi, Y. K., Kim, T.-K., Kim, C.-J., Lee, J.-S., Oh, S.-Y., Joo, H. S., Foster, D. N., Hong, K.-C., You, S. & Kim, H. (2006). Activation of the intrinsic mitochondrial apoptotic pathway in swine influenza virus-mediated cell death. *Exp Mol Med* **38**, 11–7.

Chu, Q. D., Sun, G., Pope, M., Luraguiz, N., Curiel, D. T., Kim, R., Li, B. D. L. & Mathis, J. M. (2012). Virotherapy using a novel chimeric oncolytic adenovirus prolongs survival in a human pancreatic cancer xenograft model. *Surgery* **152**, 441–8. Mosby, Inc.

Clavijo, a, Riva, J., Copps, J., Robinson, Y. & Zhou, E. M. (2001). Assessment of the pathogenicity of an emu-origin influenza A H5 virus in ostriches (Struthio camelus). *Avian Pathol* **30**, 83–9.

Clinicaltrials.gov. **(2015).** oncolytic | Open Studies.

Cox, N. J., Neumann, G., Donis, R. O. & Kawaoka, Y. (2010). Orthomyxoviruses: Influenza. In *Topley Wilson's Microbiol Microb Infect*, pp. 634–698. Edited by B. W. J. Mahy, V. ter Meulen, S. P. Borriello, P. R. Murray, G. Funke, S. H. E. Kaufmann, M. W. Steward, W. G. Merz, R. J. Hay, et al. Chichester, UK: John Wiley & Sons, Ltd.

Cui, Y., Brosnan, J. a, Blackford, A. L., Sur, S., Hruban, R. H., Kinzler, K. W., Vogelstein, B., Maitra, A., Diaz, L. a & other authors. **(2012).** Genetically defined subsets of human pancreatic cancer show unique in vitro chemosensitivity. *Clin Cancer Res* **18**, 6519–30.

Deer, E., González-Hernández, J. & Coursen, J. (2010). Phenotype and genotype of pancreatic cancer cell lines. *Pancreas* **39**, 425–435.

Deramaudt, T. & Rustgi, A. K. (2005). Mutant KRAS in the initiation of pancreatic cancer. *Biochim Biophys Acta* **1756**, 97–101.

Doly, J., Civas, A., Navarro, S. & Uze, G. (1998). Type I interferons: expression and signalization. *Cell Mol Life Sci C* **54**, 1109–1121.

Edge, R. E., Falls, T. J., Brown, C. W., Lichty, B. D., Atkins, H. & Bell, J. C. (2008). A let-7 MicroRNA-sensitive vesicular stomatitis virus demonstrates tumor-specific replication. *Mol Ther* **16**, 1437–43.

Efferson, C. L., Tsuda, N., Kawano, K., Nistal-villa, E., Sellappan, S., Yu, D., Murray, J. L., Garcı, A. & Ioannides, C. G. (2006). Prostate Tumor Cells Infected with a Recombinant Influenza Virus Expressing a Truncated NS1 Protein Activate Cytolytic CD8+ Cells To Recognize. *J Virol* **80**, 383–394.

Elankumaran, S., Chavan, V., Qiao, D., Shobana, R., Moorkanat, G., Biswas, M. & Samal, S. K. (2010). Type I interferon-sensitive recombinant newcastle disease virus for oncolytic virotherapy. *J Virol* **84**, 3835–3844.

Ferguson, M. S., Lemoine, N. R. & Wang, Y. (2012). Systemic delivery of oncolytic viruses: hopes and hurdles. *Adv Virol* **2012**, 1–14.

Fernandez-Sesma, A., Marukian, S., Ebersole, B. J., Kaminski, D., Park, M.-S., Yuen, T., Sealfon, S. C., García-Sastre, A. & Moran, T. M. (2006). Influenza virus evades innate and adaptive immunity via the NS1 protein. *J Virol* **80**, 6295–304.

Fodor, E. (2013). The RNA polymerase of influenza A virus : mechanisms of viral transcription and replication. *Acta Virol* 113–122.

Fodor, E., Devenish, L., Engelhardt, O., Palese, P., Brownlee, G. & García-Sastre, A. (1999). Rescue of influenza A virus from recombinant DNA. *J Virol* **73**, 9679–9682.

Fulda, S. & Debatin, K.-M. (2006). Extrinsic versus intrinsic apoptosis pathways in anticancer chemotherapy. *Oncogene* **25**, 4798–811.

Fuster, M. M. & Esko, J. D. (2005). The sweet and sour of cancer: glycans as novel therapeutic targets. *Nat Rev Cancer* **5**, 526–42.

Gadaleta, P., Perfetti, X., Mersich, S. & Coulombié, F. (2005). Early activation of the mitochondrial apoptotic pathway in Vesicular Stomatitis virus-infected cells. *Virus Res* **109**, 65–9.

Gambaryan, A. S., Tuzikov, A. B., Pazynina, G. V, Desheva, J. a, Bovin, N. V, Matrosovich, M. N. & Klimov, A. I. (2008). 6-sulfo sialyl Lewis X is the common receptor determinant recognized by H5, H6, H7 and H9 influenza viruses of terrestrial poultry. *Virol J* **5**, 1–14.

Gambaryan, A. S., Matrosovich, T. Y., Philipp, J., Munster, V. J., Fouchier, R. a M., Cattoli, G., Capua, I., Krauss, S. L., Webster, R. G. & other authors. (2012). Receptor-binding profiles of H7 subtype influenza viruses in different host species. *J Virol* **86**, 4370–9.

Ganly, I., Kirn, D. & Eckhardt, S. (2000). A phase I study of Onyx-015, an E1B attenuated adenovirus, administered intratumorally to patients with recurrent head and neck cancer. *Clin Cancer Res* **6**, 798–806.

Goldufsky, J., Sivendran, S., Harcharik, S., Pan, M., Bernardo, S., Stern, R., Friedlander, P., Ruby, C., Saenger, Y. & Kaufman, H. (2013). Oncolytic virus therapy for cancer. *Oncolytic Virotherapy* **2**, 31–46.

Grandi, P., Fernandez, J. & Szentirmai, O. (2010). Targeting HSV-1 virions for specific binding to epidermal growth factor receptor-vIII-bearing tumor cells. *Cancer Gene Ther* **17**, 655–663.

Grandi, P., Wang, S., Schuback, D., Krasnykh, V., Spear, M., Curiel, D. T., Manservigi, R. & Breakefield, X. O. (2004). HSV-1 virions engineered for specific binding to cell surface receptors. *Mol Ther* **9**, 419–27.

Hale, B. G., Randall, R. E., Ortín, J. & Jackson, D. (2008). The multifunctional NS1 protein of influenza A viruses. *J Gen Virol* **89**, 2359–76.

Harris, J. K., Mansour, R., Choucair, B., Olson, J., Nissen, C. & Bhatt, J. (2014). Health department use of social media to identify foodborne illness - chicago, illinois, 2013-2014. *MMWR Morb Mortal Wkly Rep* **63**, 681–5.

Hartl, I., Schneider, R. M., Sun, Y., Medvedovska, J., Chadwick, M. P., Russell, S. J., Cichutek, K. & Buchholz, C. J. (2005). Library-based selection of retroviruses selectively spreading through matrix metalloprotease-positive cells. *Gene Ther* **12**, 918–26.

Hernández-Alcoceba, R. (2011). Recent advances in oncolytic virus design. *Clin Transl Oncol* **13**, 229–39.

Hong, S.-M., Park, J. Y., Hruban, R. H. & Goggins, M. (2011). Molecular signatures of pancreatic cancer. *Arch Pathol Lab Med* **135**, 716–727.

Hughes, T., Coffin, R., Lilley, C., Ponce, R. & Kaufman, H. (2014). Critical analysis of an oncolytic herpesvirus encoding granulocyte-macrophage colony stimulating factor for the treatment of malignant melanoma. *Oncolytic Virotherapy* **3**, 11–20.

Hutchinson, E. C. & Fodor, E. (2013). Transport of the influenza virus genome from nucleus to nucleus. *Viruses* **5**, 2424–46.

Jayaraman, A., Chandrasekaran, A., Viswanathan, K., Raman, R., Fox, J. G. & Sasisekharan, R. (2012). Decoding the distribution of glycan receptors for human-adapted influenza A viruses in ferret respiratory tract. *PLoS One* **7**.

Jones, L. E., Humphreys, M. J., Campbell, F., Neoptolemos, J. P. & Boyd, M. T. (2004). Comprehensive analysis of matrix metalloproteinase and tissue inhibitor expression in pancreatic cancer: increased expression of matrix metalloproteinase-7 predicts poor survival. *Clin Cancer Res* **10**, 2832–2845.

Jones, S., Zhang, X., Parsons, D. & Lin, J. (2008). Core signaling pathways in human pancreatic cancers revealed by global genomic analyses. *Science (80-)* **321**, 1801–1806.

José, A., Rovira-Rigau, M., Luna, J., Giménez-Alejandre, M., Vaquero, E., García de la Torre, B., Andreu, D., Alemany, R. & Fillat, C. (2014). A genetic fiber modification to achieve matrix-metalloprotease-activated infectivity of oncolytic adenovirus. *J Control Release* **192**, 148–56.

Karikari, C. a, Roy, I., Tryggestad, E., Feldmann, G., Pinilla, C., Welsh, K., Reed, J. C., Armour, E. P., Wong, J. & other authors. **(2007).** Targeting the apoptotic machinery in pancreatic cancers using small-molecule antagonists of the X-linked inhibitor of apoptosis protein. *Mol Cancer Ther* **6**, 957–66.

Katz, J., Garg, S. & Sambhara, S. (2006). Influenza vaccines: current and future strategies. In *Influ Virol Curr Top*. Edited by Y. Kawaoka. Norfolk: Caister Academic Press.

Kaur, B., Cripe, T. & Chiocca, E. (2009). "Buy one get one free:" armed viruses for the treatment of cancer cells and their microenvironment. *Curr Gene Ther* **9**, 341–355.

Keawcharoen, J., Riel, D. Van, Amerongen, G. Van, Bestebroer, T. & Beyer, W. E. (2008). Wild Ducks as Long-Distance Vectors of Highly Pathogenic Avian In fl uenza Virus (H5N1). *Emerg Infect Dis* **14**, 600–607.

Keleg, S., Büchler, P., Ludwig, R., Büchler, M. W. & Friess, H. (2003). Invasion and metastasis in pancreatic cancer. *Mol Cancer* **2**, 1–7.

Kelly, E. & Russell, S. J. (2007). History of Oncolytic Viruses : Genesis to Genetic Engineering. *Mol Ther* **15**, 651–659.

Kelly, E. J. & Russell, S. J. (2009). MicroRNAs and the regulation of vector tropism. *Mol Ther* **17**, 409–16.

Khan, M. L., Halfdanarson, T. R. & Borad, M. J. (2014). Immunotherapeutic and oncolytic viral therapeutic strategies in pancreatic cancer. *Future Oncol* **10**, 1255–75.

Kim, Y. S., Itzkowitz, S. H., Yuan, M., Chung, Y., Satake, K., Umeyama, K. & Hakomori, S. (1988a). Lex and Ley antigen expression in human pancreatic cancer. *Cancer Res* **48**, 475–482.

Kim, Y. S., Itzkowitz, S. H., Yuan, M., Chung, Y., Satake, K., Umeyama, K. & Hakomori, S. (1988b). Lex and Ley antigen expression in human pancreatic cancer. *Cancer Res* **48**, 475–482.

Kinoh, H., Inoue, M., Washizawa, K., Yamamoto, T., Fujikawa, S., Tokusumi, Y., Iida, a, Nagai, Y. & Hasegawa, M. (2004). Generation of a recombinant Sendai virus that is selectively activated and lyses human tumor cells expressing matrix metalloproteinases. *Gene Ther* **11**, 1137–45.

Klein, A. P. (2013). Genetic Susceptibility to Pancreatic Cancer. *Mol Carcinog* **51**, 14–24.

Koblinski, J. E., Ahram, M. & Sloane, B. F. (2000). Unraveling the role of proteases in cancer. *Clin Chim Acta* **291**, 113–135.

Kueberuwa, G., Cawood, R., Tedcastle, A. & Seymour, L. W. (2014). Tissue-specific attenuation of oncolytic sindbis virus without compromised genetic stability. *Hum Gene Ther Methods* **25**, 154–65.

Kwon, Y. K., Thomas, C. & Swayne, D. E. (2010). Variability in pathobiology of South Korean H5N1 high-pathogenicity avian influenza virus infection for 5 species of migratory waterfowl. *Vet Pathol* **47**, 495–506.

Labadie, K., Dos Santos Afonso, E., Rameix-Welti, M. A., van der Werf, S. & Naffakh, N. (2007). Host-range determinants on the PB2 protein of influenza A viruses control the interaction between the viral polymerase and nucleoprotein in human cells. *Virology* **362**, 271–282.

Leber, M. F., Bossow, S., Leonard, V. H. J., Zaoui, K., Grossardt, C., Frenzke, M., Miest, T., Sawall, S., Cattaneo, R. & other authors. (2011). MicroRNA-sensitive oncolytic measles viruses for cancer-specific vector tropism. *Mol Ther* **19**, 1097–106. Nature Publishing Group.

Lipatov, A. S., Kwon, Y. K., Pantin-Jackwood, M. J. & Swayne, D. E. (2009). Pathogenesis of H5N1 influenza virus infections in mice and ferret models differs according to respiratory tract or digestive system exposure. *J Infect Dis* **199**, 717–25.

Lowry, R. (2003). Influenza virus induction of apoptosis by intrinsic and extrinsic mechanisms. *Int Rev Immunol* **22**, 425–49.

Lun, X., Alain, T., Zemp, F. J., Zhou, H., Rahman, M. M., Hamilton, M. G., McFadden, G., Bell, J., Senger, D. L. & Forsyth, P. a. (2010). Myxoma virus virotherapy for glioma in immunocompetent animal models: optimizing administration routes and synergy with rapamycin. *Cancer Res* **70**, 598–608.

Makohon-Moore, A., Brosnan, J. a & Iacobuzio-Donahue, C. a. (2013). Pancreatic cancer genomics: insights and opportunities for clinical translation. *Genome Med* **5**, 26.

Mansour, M., Palese, P. & Zamarin, D. (2011). Oncolytic specificity of Newcastle disease virus is mediated by selectivity for apoptosis-resistant cells. *J Virol* **85**, 6015–6023.

Mänz, B., Schwemmle, M. & Brunotte, L. (2013). Adaptation of avian influenza A virus polymerase in mammals to overcome the host species barrier. *J Virol* **87**, 7200–9.

Mas, E., Pasqualini, E., Caillol, N., El Battari, a, Crotte, C., Lombardo, D. & Sadoulet, M. O. (1998). Fucosyltransferase activities in human pancreatic tissue: comparative study between cancer tissues and established tumoral cell lines. *Glycobiology* **8**, 605–613.

Massin, P., van der Werf, S. & Naffakh, N. (2001). Residue 627 of PB2 is a determinant of cold sensitivity in RNA replication of avian influenza viruses. *J Virol* **75**, 5398–5404.

Massin, P., Kuntz-Simon, G., Barbezange, C., Deblanc, C., Oger, A., Marquet-Blouin, E., Bougeard, S., van der Werf, S. & Jestin, V. (2010). Temperature sensitivity on growth and/or replication of H1N1, H1N2 and H3N2 influenza A viruses isolated from pigs and birds in mammalian cells. *Vet Microbiol* **142**, 232–241.

Mathis, J. M., Stoff-Khalili, M. a & Curiel, D. T. (2005). Oncolytic adenoviruses - selective retargeting to tumor cells. *Oncogene* **24**, 7775–91.

Matrosovich, M. N. & Gambaryan, A. S. (2012). Sold-Phase Assays of Receptor-Binding Specificity. *book*, Methods in Molecular Biology **865** (Y. Kawaoka & G. Neumann, Eds.). Totowa, NJ: Humana Press.

Mendieta Zerón, H., García Flores, J. R. & Romero Prieto, M. L. (2009). Limitations in improving detection of pancreatic adenocarcinoma. *Future Oncol* **5**, 657–68.

Miyatake, S., Iyer, a, Martuza, R. L. & Rabkin, S. D. (1997). Transcriptional targeting of herpes simplex virus for cell-specific replication. *J Virol* **71**, 5124–5132.

Mok, C. K. P., Lee, D. C. W., Cheung, C. Y., Peiris, M. & Lau, A. S. Y. (2007). Differential onset of apoptosis in influenza A virus H5N1- and H1N1-infected human blood macrophages. *J Gen Virol* **88**, 1275–1280.

Moon, D.-O., Kim, B. Y., Jang, J. H., Kim, M.-O., Jayasooriya, R. G. P. T., Kang, C.-H., Choi, Y. H., Moon, S.-K., Kim, W.-J. & other authors. **(2012).** K-RAS transformation in prostate epithelial cell overcomes H2O2-induced apoptosis via upregulation of gamma-glutamyltransferase-2. *Toxicol In Vitro* **26**, 429–34. Elsevier Ltd.

Mühlebach, M. D., Schaser, T., Zimmermann, M., Armeanu, S., Hanschmann, K.-M. O., Cattaneo, R., Bitzer, M., Lauer, U. M., Cichutek, K. & Buchholz, C. J. (2010). Liver cancer protease activity profiles support therapeutic options with matrix metalloproteinase-activatable oncolytic measles virus. *Cancer Res* **70**, 7620–9.

Mullen, J. T. & Tanabe, K. T. (2002). Viral Oncolysis. *Oncologist* **7**, 106–119.

Muramoto, Y., Takada, A., Fujii, K., Noda, T., Iwatsuki-Horimoto, K., Watanabe, S., Horimoto, T., Kida, H. & Kawaoka, Y. (2006). Hierarchy among viral RNA (vRNA) segments in their role in vRNA incorporation into influenza A virions. *J Virol* **80**, 2318–2325.

Murphy, A. M., Besmer, D. M., Moerdyk-Schauwecker, M., Moestl, N., Ornelles, D. a, Mukherjee, P. & Grdzelishvili, V. Z. (2012). Vesicular stomatitis virus as an oncolytic agent against pancreatic ductal adenocarcinoma. *J Virol* **86**, 3073–87.

Muster, T., Rajtarova, J., Sachet, M., Unger, H., Fleischhacker, R., Romirer, I., Grassauer, A., Url, A., García-Sastre, A. & other authors. **(2004).** Interferon resistance promotes oncolysis by influenza virus NS1-deletion mutants. *Int J Cancer* **110**, 15–21.

Nayak, D. P., Hui, E. K. W. & Barman, S. (2004). Assembly and budding of influenza virus. *Virus Res* **106**, 147–165.

Neumann, G. & Kawaoka, Y. (2011). The first influenza pandemic of the new millennium. *Influ other Respir Viruses …* **5**, 157–166.

Neumann, G., Watanabe, T., Ito, H., Watanabe, S., Goto, H., Gao, P., Hughes, M., Perez, D., Donis, R. & other authors. **(1999).** Generation of influenza A viruses entirely from cloned cDNAs. *PNAS* **96**, 9345–9350.

Neumann, G. & Kawaoka, Y. (2006). Host range restriction and pathogenicity in the context of influenza pandemic. *Emerg Infect Dis* **12**, 881–886.

Nicholls, J. M. (2013). The battle between influenza and the innate immune response in the human respiratory tract. *Infect Chemother* **45**, 11–21.

Nicholls, J. M., Chan, R. W. Y., Russell, R. J., Air, G. M. & Peiris, J. S. M. (2008). Evolving complexities of influenza virus and its receptors. *Trends Microbiol* **16**, 149–157.

Noma, K., Kiyotani, K., Kouchi, H., Fujii, Y., Egi, Y., Tanaka, K. & Yoshida, T. (1998). Endogenous protease-dependent replication of human influenza viruses in two MDCK cell lines. *Arch Virol* **143**, 1893–1909.

Nüesch, J. P. F., Lacroix, J., Marchini, A. & Rommelaere, J. (2012). Molecular pathways: rodent parvoviruses--mechanisms of oncolysis and prospects for clinical cancer treatment. *Clin Cancer Res* **18**, 3516–23.

Ogbomo, H., Michaelis, M., Geiler, J., van Rikxoort, M., Muster, T., Egorov, A., Doerr, H. W. & Cinatl, J. (2010). Tumor cells infected with oncolytic influenza A virus prime natural killer cells for lysis of resistant tumor cells. *Med Microbiol Immunol* **199**, 93–101.

Ouyang, H., Mou, L., Luk, C., Liu, N., Karaskova, J., Squire, J. & Tsao, M. S. (2000). Immortal human pancreatic duct epithelial cell lines with near normal genotype and phenotype. *Am J Pathol* **157**, 1623–1631.

Palese, P. & Shaw, M. (2007). Orthomyxoviridae: The Viruses and Their Replication. In *Fields Virol*, 5th edn., pp. 1648–1692. Philadelphia: Wolters Kluwer Health/LippincottWilliams & Wilkins.

Pantin-Jackwood, M. & Swayne, D. E. (2009). Pathogenesis and pathobiology of avian influenza virus infection in birds Pathogenicity of avian influenza viruses. *Rev sci tech Off int Epiz* **28**, 113–136.

Parato, K. a, Senger, D., Forsyth, P. a J. & Bell, J. C. (2005). Recent progress in the battle between oncolytic viruses and tumours. *Nat Rev Cancer* **5**, 965–76.

Perez, J. T., Pham, A. M., Lorini, M. H., Chua, M. a, Steel, J. & tenOever, B. R. (2009). MicroRNA-mediated species-specific attenuation of influenza A virus. *Nat Biotechnol* **27**, 572–6.

Pérez-Garay, M., Arteta, B., Pagès, L., de Llorens, R., de Bolòs, C., Vidal-Vanaclocha, F. & Peracaula, R. (2010). alpha2,3-sialyltransferase ST3Gal III modulates pancreatic cancer cell motility and adhesion in vitro and enhances its metastatic potential in vivo. *PLoS One* **5**, 1–11.

Pietra, G., Manzini, C., Vitale, M., Balsamo, M., Ognio, E., Boitano, M., Queirolo, P., Moretta, L. & Mingari, M. C. (2009). Natural killer cells kill human melanoma cells with characteristics of cancer stem cells. *Int Immunol* **21**, 793–801.

Pol, J., Bloy, N., Obrist, F. & Eggermont, A. (2007). Trial Watch: Oncolytic viruses for cancer therapy. *Oncoimmunology* **3**, 1–13.

Pol, J., Rességuier, J. & Lichty, B. (2011). Oncolytic viruses: a step into cancer immunotherapy. *Virus Adapt Treat* **2**, 1–21.

Qian, J., Niu, J., Li, M., Chiao, P. J. & Tsao, M. (2005). In vitro Modeling of Human Pancreatic Duct Epithelial Cell Transformation Defines Gene Expression Changes Induced by K- ras Oncogenic Activation in Pancreatic Carcinogenesis. *Cancer Res* **65**, 5045–5053.

Rathos, M. J., Joshi, K., Khanwalkar, H., Manohar, S. M. & Joshi, K. S. (2012). Molecular evidence for increased antitumor activity of gemcitabine in combination with a cyclin-dependent kinase inhibitor, P276-00 in pancreatic cancers. *J Transl Med* **10**, 1–11.

Reed, L. & Muench, H. (1938). A SIMPLE METHOD OF ESTIMATING FIFTY PER CENT ENDPOINTS. *Am J Hygeine* **27**, 493–497.

Réjiba, S., Bigand, C., Parmentier, C. & Hajri, A. (2009). Gemcitabine-based chemogene therapy for pancreatic cancer using Ad-dCK::UMK GDEPT and TS/RR siRNA strategies. *Neoplasia* **11**, 637–650.

Reperant, L., Rimmelzwaan, G. F. & Kuiken, T. (2009). Avian influenza viruses in mammals. *Rev Sci Tech* **28**, 137–159.

Van Rikxoort, M., Michaelis, M., Wolschek, M., Muster, T., Egorov, A., Seipelt, J., Doerr, H. W. & Cinatl, J. (2012). Oncolytic effects of a novel influenza A virus expressing interleukin-15 from the NS reading frame. *PLoS One* **7**, e36506.

Riss, T., Moravec, R., Niles, A. & Benink, H. (2013). Cell Viability Assays. In *Assay Guid Man*, p. 21. Edited by P. G. Sitta Sittampalam, PhD, Editor-in-chief, Neely Gal-Edd, MS, Associate Managing Editor, Michelle Arkin, PhD, Douglas Auld, PhD, Chris Austin, MD, Bruce Bejcek, PhD, Marcie Glicksman, PhD, James Inglese, PhD, Vance Lemmon, PhD, Zhuyin Li, PhD, James McGe.

Rivera, F., López-Tarruella, S., Vega-Villegas, M. E. & Salcedo, M. (2009). Treatment of advanced pancreatic cancer: from gemcitabine single agent to combinations and targeted therapy. *Cancer Treat Rev* **35**, 335–9. Elsevier Ltd.

Rossman, J. & Lamb, R. (2011). Influenza virus assembly and budding. *Virology* **411**, 229–236.

Russell, S. J. (2002). RNA viruses as virotherapy agents. *Cancer Gene Ther* **9**, 961–6.

Russell, S. J., Peng, K.-W. & Bell, J. C. (2012). Oncolytic virotherapy. *Nat Biotechnol* **30**, 658–70. Nature Publishing Group.

Sato, N., Maehara, N., Su, G. H. & Goggins, M. (2003). Effects of 5-aza-2'-deoxycytidine on matrix metalloproteinase expression and pancreatic cancer cell invasiveness. *J Natl Cancer Inst* **95**, 327–330.

Schneider, R. M., Medvedovska, Y., Hartl, I., Voelker, B., Chadwick, M. P., Russell, S. J., Cichutek, K. & Buchholz, C. J. (2003). Directed evolution of retroviruses activatable by tumour-associated matrix metalloproteases. *Gene Ther* **10**, 1370–80.

Seladi-Schulman, J., Steel, J. & Lowen, A. C. (2013). Spherical influenza viruses have a fitness advantage in embryonated eggs, while filament-producing strains are selected in vivo. *J Virol* **87**, 13343–53.

Sherwood, M. W., Prior, I. A., Voronina, S. G., Barrow, S. L., Woodsmith, J. D., Gerasimenko, O. V, Petersen, O. H. & Tepikin, A. V. **(2007).** Activation of trypsinogen in large endocytic vacuoles of pancreatic acinar cells. *Proc Natl Acad Sci U S A* **104**, 5674–5679.

Shinya, K., Awakura, T., Shimada, a, Silvano, F. D., Umemura, T. & Otsuki, K. (1995). Pathogenesis of pancreatic atrophy by avian influenza a virus infection. *Avian Pathol* **24**, 623–32.

Shinya, K., Ebina, M., Yamada, S., Ono, M., Kasai, N. & Kawaoka, Y. (2006). Avian flu: influenza virus receptors in the human airway. *Nature* **440**, 435–436.

Springfeld, C., von Messling, V., Frenzke, M., Ungerechts, G., Buchholz, C. J. & Cattaneo, R. (2006). Oncolytic efficacy and enhanced safety of measles virus activated by tumor-secreted matrix metalloproteinases. *Cancer Res* **66**, 7694–700.

Stevens, J., Blixt, O., Paulson, J. C. & Wilson, I. A. (2006). Glycan microarray technologies: tools to survey host specificity of influenza viruses. *Nat Rev Microbiol* **4**, 857–864.

Sturlan, S., Stremitzer, S., Bauman, S., Sachet, M., Wolschek, M., Ruthsatz, T., Egorov, A. & Bergmann, M. (2010). Endogenous expression of proteases in colon cancer cells facilitate influenza A viruses mediated oncolysis. *Cancer Biol Ther* **10**, 592–599.

Subbarao, E. K., London, W. & Murphy, B. R. (1993). A single amino acid in the PB2 gene of influenza A virus is a determinant of host range. *J Virol* **67**, 1761–1764.

Szécsi, J., Drury, R., Josserand, V., Grange, M.-P., Boson, B., Hartl, I., Schneider, R., Buchholz, C. J., Coll, J.-L. & other authors. **(2006).** Targeted retroviral vectors displaying a cleavage site-engineered hemagglutinin (HA) through HA-protease interactions. *Mol Ther* **14**, 735–44.

Takizawa, T., Matsukawa, S., Higuchi, Y., Nakamura, S., Nakanishi, Y. & Fukuda, R. (1993). Induction of programmed cell death (apoptosis) by influenza virus infection in tissue culture cells. *J Gen Virol* **74**, 2347–2355.

Tarendeau, F., Crepin, T., Guilligay, D., Ruigrok, R. W. H., Cusack, S. & Hart, D. J. (2008). Host determinant residue lysine 627 lies on the surface of a discrete, folded domain of influenza virus polymerase PB2 subunit. *PLoS Pathog* **4**, 1–8.

Taubenberger, J. (1998). Influenza virus hemagglutinin cleavage into HA1, HA2: No laughing matter. *Proc Natl Acad Sci U S A* **95**, 9713–9715.

Thomas, D., Patera, A., Graham, C. & Smith, C. (1998). Antibody-Mediated Immunity. In *Textb Influ*. Edited by K. Nicholson, R. Webster & A. Hay. Oxford: Blackwell Science Ltd.

Tong, S., Zhu, X., Li, Y., Shi, M., Zhang, J., Bourgeois, M., Yang, H., Chen, X., Recuenco, S. & other authors. **(2013).** New world bats harbor diverse influenza A viruses. *PLoS Pathog* **9**, e1003657.

Tumilasci, V. F., Olière, S., Nguyên, T. L.-A., Shamy, A., Bell, J. & Hiscott, J. (2008). Targeting the apoptotic pathway with BCL-2 inhibitors sensitizes primary chronic lymphocytic leukemia cells to vesicular stomatitis virus-induced oncolysis. *J Virol* **82**, 8487–8499.

Tumpey, T. M., Basler, C. F., Aguilar, P. V, Zeng, H., Solórzano, A., Swayne, D. E., Cox, N. J., Katz, J. M., Taubenberger, J. K. & other authors. (2005). Characterization of the reconstructed 1918 Spanish influenza pandemic virus. *Science* **310**, 77–80.

Varga, Z. & Palese, P. (2011). The influenza A virus protein PB1-F2: killing two birds with one stone? *Virulence* **2**, 542–546.

Varki, A., Kannagi, R. & Toole, B. (2009). Glycosylation Changes in Cancer. In *Essentials Glycobiol*, 2nd editio. Edited by A. Varki, R. Cummings, J. Esko & et al. Cold Spring Harbor: Cold Spring Harbor Laboratory Press.

Vartak, D. G. & Gemeinhart, R. a. (2007). Matrix metalloproteases: underutilized targets for drug delivery. *J Drug Target* **15**, 1–20.

Vasin, a V, Temkina, O. a, Egorov, V. V, Klotchenko, S. a, Plotnikova, M. a & Kiselev, O. I. (2014). Molecular mechanisms enhancing the proteome of influenza A viruses: an overview of recently discovered proteins. *Virus Res* **185**, 53–63. Elsevier B.V.

Vincent, A., Herman, J., Schulick, R., Hruban, R. H. & Goggins, M. (2011). Pancreatic cancer. *Lancet* **378**, 607–20. Elsevier Ltd.

Wagner, R. (1954). Influenza Virus Infection of Transplanted Tumors I. Multiplication of a "Neurotropic" Strain and Its Effect on Solid Neoplasms. *Cancer Res* 377–385.

Walther, T., Karamanska, R., Chan, R. W. Y., Chan, M. C. W., Jia, N., Air, G., Hopton, C., Wong, M. P., Dell, A. & other authors. (2013). Glycomic Analysis of Human Respiratory Tract Tissues and Correlation with Influenza Virus Infection. *PLoS Pathog* **9**.

Webster, R. G. (2006). H5 Influenza Viruses. In *Influ Virol Curr Top*. Edited by Y. Kawaoka. Norfolk: Caister Academic Press.

Webster, R. G. & Govorkova, E. a. (2014). Continuing challenges in influenza. *Ann N Y Acad Sci* **1323**, 115–39.

Wennier, S., Li, S. & McFadden, G. (2011). Oncolytic virotherapy for pancreatic cancer. *Expert Rev Mol Med* **13**, 1–22.

Wennier, S. T., Liu, J., Li, S., Rahman, M. M., Mona, M. & McFadden, G. (2012). Myxoma virus sensitizes cancer cells to gemcitabine and is an effective oncolytic virotherapeutic in models of disseminated pancreatic cancer. *Mol Ther* **20**, 759–68.

Westphal, S. & Kalthoff, H. (2003). Apoptosis : Targets in Pancreatic Cancer Apoptosis. *Mol Cancer* **2**, 1–14.

Wolfgang, C., Herman, J., Laheru, D., Klein, A., Erdek, M. A., Fishman, E. K. & Hruban, R. H. (2014). Recent Progress in Pancreatic Cancer. *CA Cancer J Clin* **63**, 318–348.

Wright, P., Neumann, G. & Kawaoka, Y. (2006). Orthomyxoviruses. In *Field's Virol 5th Ed*, 5ith edn., pp. 1691–740. Edited by D. Knipe, P. Howley, D. Griffin, R. Lamb, M. Martin, B. Roizman & S. Straus. Philadelphia: Lippincott Williams & Wilkins.

Wu, S., Liu, B., Zhang, Q., Liu, J., Zhou, W., Wang, C., Li, M., Bao, S. & Zhu, R. (2013). Dihydromyricetin reduced bcl-2 expression via p53 in human hepatoma HepG2 cells. *PLoS One* **8**.

Xing, Z., Harper, R., Anunciacion, J., Yang, Z., Gao, W., Qu, B., Guan, Y. & Cardona, C. J. (2011). Host immune and apoptotic responses to avian influenza virus H9N2 in human tracheobronchial epithelial cells. *Am J Respir Cell Mol Biol* **44**, 24–33.

Xu, C., Li, H., Su, C. & Li, Z. (2013). Viral therapy for pancreatic cancer: tackle the bad guys with poison. *Cancer Lett* **333**, 1–8. Elsevier Ireland Ltd.

Yamamoto, H., Itoh, F., Iku, S., Adachi, Y., Fukushima, H., Sasaki, S., Mukaiya, M., Hirata, K. & Imai, K. (2001). Expression of matrix metalloproteinases and tissue inhibitors of metalloproteinases in human pancreatic adenocarcinomas: Clinicopathologic and prognostic significance of matrilysin expression. *J Clin Oncol* **19**, 1118–1127.

Yamamoto, Y., Hiraoka, N., Goto, N., Rin, Y., Miura, K., Narumi, K., Uchida, H., Tagawa, M. & Aoki, K. (2014). A targeting ligand enhances infectivity and cytotoxicity of an oncolytic adenovirus in human pancreatic cancer tissues. *J Control Release* **192**, 284–93. Elsevier B.V.

Yao, L., Korteweg, C., Hsueh, W. & Gu, J. (2008). Avian influenza receptor expression in H5N1-infected and noninfected human tissues. *FASEB J* **22**, 733–740.

Ylösmäki, E., Lavilla-Alonso, S., Jäämaa, S., Vähä-Koskela, M., af Hällström, T., Hemminki, A., Arola, J., Mäkisalo, H. & Saksela, K. (2013a). MicroRNA-mediated suppression of oncolytic adenovirus replication in human liver. *PLoS One* **8**, e54506.

Ylösmäki, E., Martikainen, M., Hinkkanen, A. & Saksela, K. (2013b). Attenuation of Semliki Forest virus neurovirulence by microRNA-mediated detargeting. *J Virol* **87**, 335–44.

York, A. & Fodor, E. (2013). Biogenesis, assembly, and export of viral messenger ribonucleoproteins in the influenza A virus infected cell. *RNA Biol* **10**, 1274–82.

Yu, X., Tsibane, T., McGraw, P. A., House, F. S., Keefer, C. J., Hicar, M. D., Tumpey, T. M., Pappas, C., Perrone, L. A. & other authors. **(2008).** Neutralizing antibodies derived from the B cells of 1918 influenza pandemic survivors. *Nature* **455**, 532–536.

Zakharova, O. P., Karmazanovsky, G. G. & Egorov, V. I. (2012). Pancreatic adenocarcinoma: Outstanding problems. *World J Gastrointest Surg* **4**, 104–13.

Zamarin, D., García-Sastre, A., Xiao, X., Wang, R. & Palese, P. (2005). Influenza virus PB1-F2 protein induces cell death through mitochondrial ANT3 and VDAC1. *PLoS Pathog* **1**, 0040–0054.

Zheng, W. & Tao, Y. J. (2013). Structure and assembly of the influenza A virus ribonucleoprotein complex. *FEBS Lett* **587**, 1206–14. Federation of European Biochemical Societies.

Zhirnov, O. & Klenk, H.-D. (2003). Human influenza A viruses are proteolytically activated and do not induce apoptosis in CACO-2 cells. *Virology* **313**, 198–212.

Appendix I. Titration of Fetuin-HRP Preparations for FBI Assays and Determination of Alpha.

Plates coated with a single working dilution of each respective virus were incubated with two-fold serial dilutions of standard ("2.2") and high molecular weight ("39") Fetuin-HRP preparations with starting dilutions of 1:250 for 2.2 and 1:1000 for 39 added to the lowest row of wells. Raw data were collected following 30 minutes incubation with ABTS substrate and read on a standard plate reader at both 416nm and 405 nm.

	H4N8		H7N3		H7N7		
	39	2.2	39	2.2	39	2.2	
A	0.554	0.131	0.544	0.13	0.481	0.12	Read 1:416
	0.563	0.137	0.579	0.14	0.482	0.118	Read 2:405
B	1.007	0.195	1.159	0.188	0.695	0.169	Read 1:416
	1.054	0.206	1.153	0.199	0.838	0.167	Read 2:405
C	1.351	0.42	1.786	0.359	1.804	0.33	Read 1:416
	1.429	0.465	1.733	0.418	1.794	0.303	Read 2:405
D	2.453	0.701	2.419	0.607	1.666	0.527	Read 1:416
	2.723	0.717	2.782	0.665	1.979	0.625	Read 2:405
E	2.805	1.29	2.632	0.956	2.498	0.865	Read 1:416
	2.998	1.336	2.971	1.03	2.621	0.879	Read 2:405
F	3.392	1.992	2.689	1.285	2.63	1.132	Read 1:416
	3.431	1.977	3.084	1.329	2.852	1.289	Read 2:405
G	3.28	2.014	3.001	1.79	2.645	1.47	Read 1:416
	3.337	2.088	3.135	1.842	2.836	1.724	Read 2:405
H	3.363	2.677	3.35	2.473	2.894	2.145	Read 1:416
	3.571	2.777	3.554	2.626	3.07	2.231	Read 2:405

A single read (405nm) was selected and data was retabulated into two tables based on Fet-HRP. For simplicity, each Fet-HRP was assigned to a starting concentration of 1 arbitrary unit (AU) for graphical determination of Kaff. Note that a PBS blank was not included in the current exaple.

Fet-HRP 39 Absorbency report (Asample-Ablank)

Initial Fet-HRP dilution = 1:1000 Dilution factor---> **2.0**

	C, AU	H4N8	H7N3	H7N7
A	0.01	0.563	0.579	0.482
B	0.02	1.054	1.153	0.838
C	0.03	1.429	1.733	1.794
D	0.06	2.723	2.782	1.979
E	0.13	2.998	2.971	2.621
F	0.25	3.431	3.084	2.852
G	0.50	3.337	3.135	2.836
H	1.00	3.571	3.554	3.07

Fet-HRP 2.2 Absorbency report (Asample-Ablank)

Initial Fet-HRP dilution = 1:250 Dilution factor---> **2.0**

	C, AU	H4N8	H7N3	H7N7
A	0.01	0.137	0.14	0.118
B	0.02	0.206	0.199	0.167
C	0.03	0.465	0.418	0.303
D	0.06	0.717	0.665	0.625
E	0.13	1.336	1.03	0.879
F	0.25	1.977	1.329	1.289
G	0.50	2.088	1.842	1.724
H	1.00	2.777	2.626	2.231

Scatchard Plots were generated based on calculations of absorbance at 405nm / concentration vs. absorbance and trendlines were generated to deduce Amax for each Fet-HRP. Dilutions of each Fet-HRP giving approximately half Amax values (shown with arrows) for all viruses were selected and alpha values for each virus isolate were determined. Dilutions resulting in alpha values of close to 0.5 for all viruses is most desirable for subsequent binding inhibition assays.

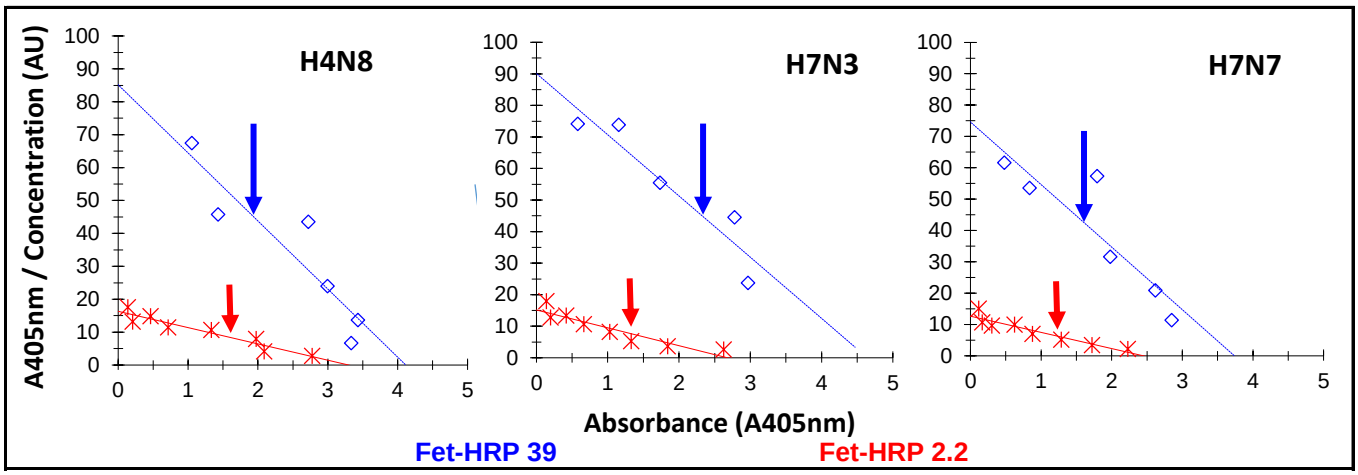

Sample Calculations for Alpha values of Fet-HRP 2.2:

H4N8

A_{405nm}	Dilution
0.137	1:32000
0.206	1:16000
0.465	1:8000
0.717	1:4000
1.336	1:2000
1.977	1:1000
2.088	1:500
2.777	1:250

Amax (from trendline) = 3.2
Half A max = 1.6
Fetuin dilutions in Half Amax range: 1:1000, 1:2000

H7N3

A_{405nm}	Dilution
0.14	1:32000
0.199	1:16000
0.418	1:8000
0.665	1:4000
1.03	1:2000
1.329	1:1000
1.842	1:500
2.626	1:250

Amax (from trendline) = 2.6
Half A max = 1.8
Fetuin dilutions in Half Amax range: 1:500, 1:1000

H7N7

A_{405nm}	Dilution	A_{405nm}	Dilution
0.118	1:32000	0.879	1:2000
0.167	1:16000	1.289	1:1000
0.303	1:8000	1.724	1:500
0.625	1:4000	2.231	1:250

Amax (from trendline) = 2.4
Half A max = 1.2
Fetuin dilutions in Half Amax range: 1:1000, 1:2000

Since the 1:1000 dilution of Fet-HRP 2.2 falls in the half Amax range for all viruses, it will be the working concentration used for FBI assays. Alpha vaues for each virus must be calculated for later determination of binding association constants in FBI assays. Calculations are as follows:

Alpha = (Amax - A405nm) / Amax

H4N8	**H7N3**	**H7N7**
A_{405nm} = 1.977	A_{405nm} = 1.329	A_{405nm} = 1.289
Amax = 3.2	Amax = 2.6	Amax = 2.4
alpha = (3.2 - 1.977) / 3.2	alpha = (2.6 - 1.329) / 2.6	alpha = (2.4 - 1.289) / 2.4
α 1:1000 = 0.382	**α 1:1000 = 0.489**	**α 1:1000 = 0.463**

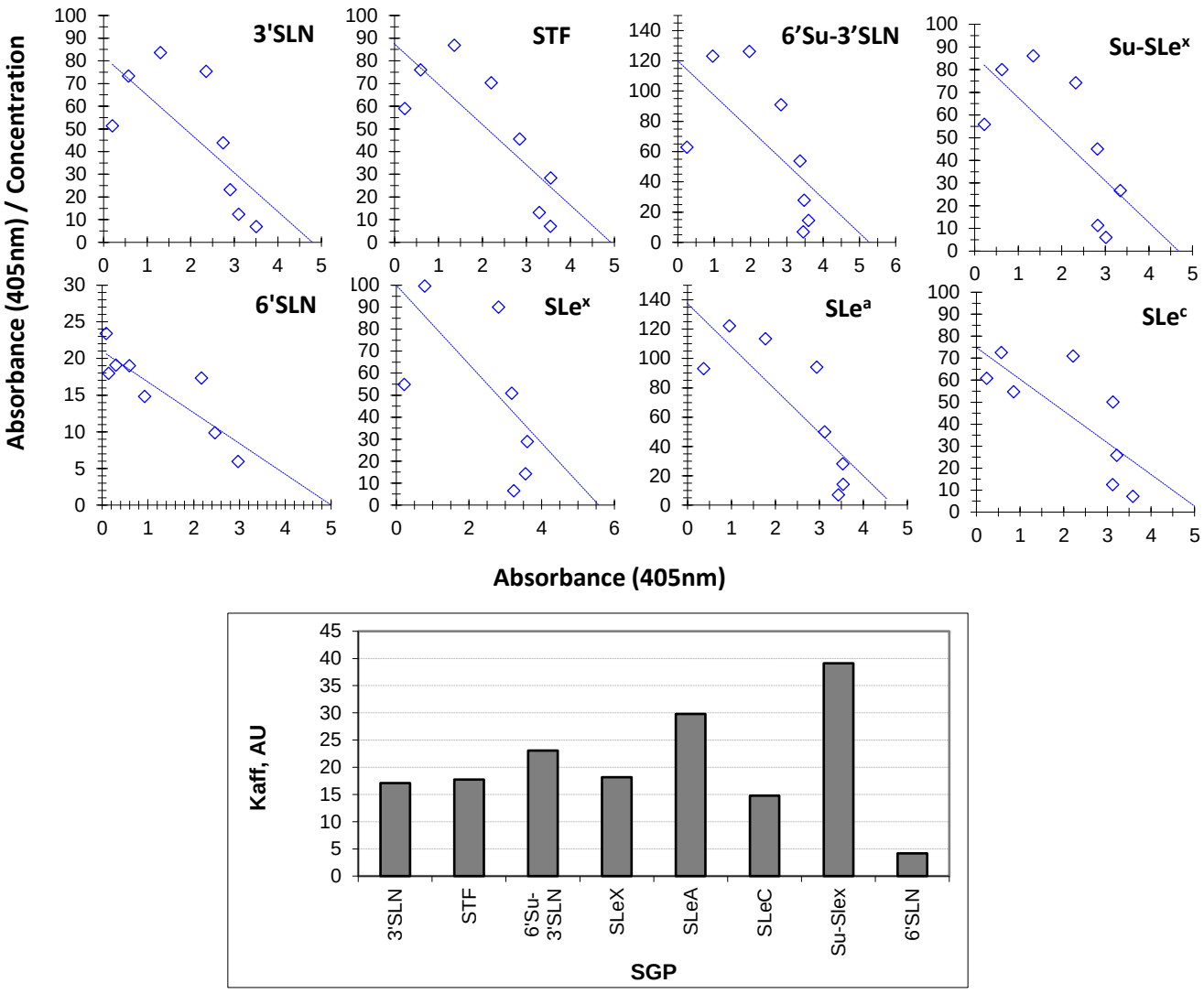

Figure S1. Binding affinity of A/turkey/Italy/2962/2003 (H7N3) to sialylglycopolymers by direct binding assay. Affinity constants (Kaff) were determined following incubation of virus-coated plates with biotinylated SGPs and results were read following 30 minutes of development with ABTS substrate. Results shown are absorbance-corrected values and represent one of two repeat experiments.

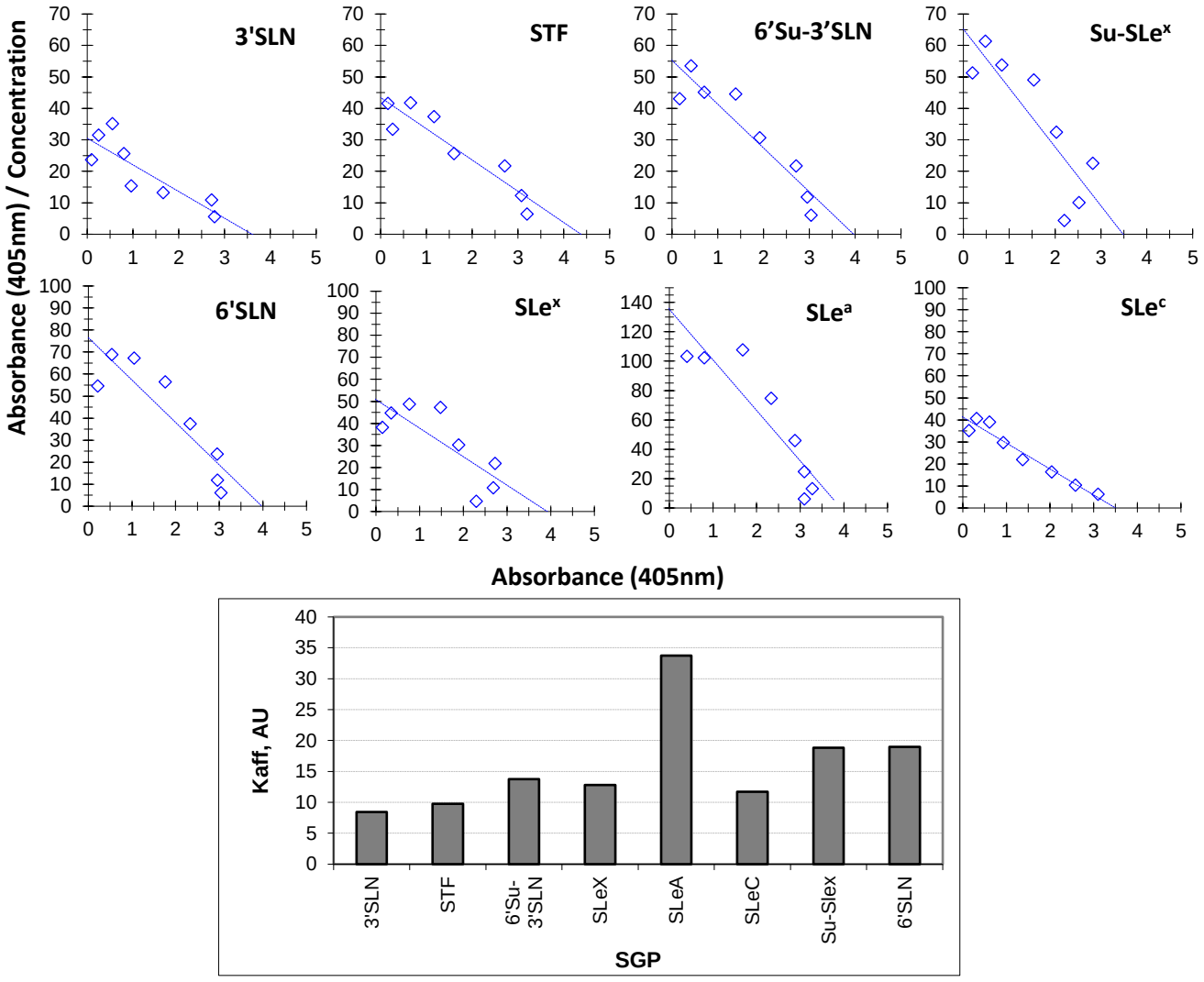

Figure S2. Binding affinity of A/macaw/England/626/80 (H7N7) to sialylglycopolymers by direct binding assay. Affinity constants (Kaff) were determined following incubation of virus-coated plates with biotinylated SGPs and results were read following 30 minutes of development with ABTS substrate. Results shown are absorbance-corrected values and represent one of two repeat experiments.

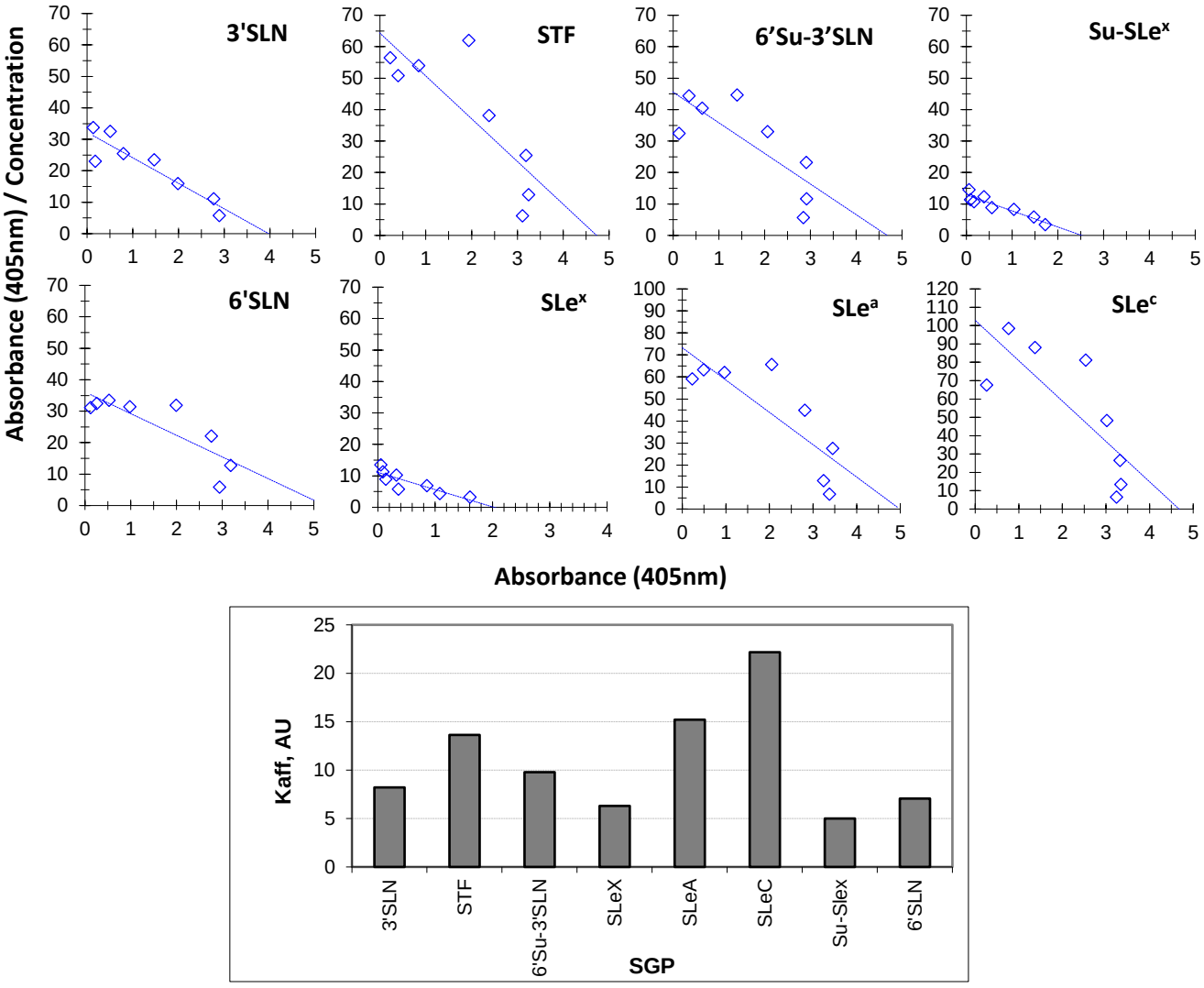

Figure S3. Binding affinity of A/cockatoo/England/72 (H4N8) to sialylglycopolymers by direct binding assay. Affinity constants (Kaff) were determined following incubation of virus-coated plates with biotinylated SGPs and results were read following 30 minutes of development with ABTS substrate. Results shown are absorbance-corrected values and represent one of two repeat experiments.